NUREG/CR-3704
LA-10039-MS

Los Alamos National Laboratory is operated by the University of California for the United States Department of Energy under contract W-7405-ENG-36.

Three-Dimensional Calculations of Transient Fluid-Thermal Mixing in the Downcomer of the Calvert Cliffs-1 Plant Using SOLA-PTS

Los Alamos National Laboratory
Los Alamos, New Mexico 87545

Prepared by Adrienne Hayes, Group T-3

NUREG/CR-3704
LA-10039-MS

R4

Three-Dimensional Calculations of Transient Fluid-Thermal Mixing in the Downcomer of the Calvert Cliffs-1 Plant Using SOLA-PTS

Bart J. Daly

Manuscript submitted: February 1984
Date published: April 1984

Prepared for
Division of Accident Evaluation
Office of Nuclear Regulatory Research
US Nuclear Regulatory Commission
Washington, DC 20555

NRC FIN No. A7306

Los Alamos National Laboratory
Los Alamos, New Mexico 87545

THREE-DIMENSIONAL CALCULATIONS OF TRANSIENT FLUID-THERMAL MIXING IN THE DOWNCOMER OF THE CALVERT CLIFFS-1 PLANT USING SOLA-PTS

by

Bart J. Daly

ABSTRACT

The SOLA-PTS code has been used to analyze transient fluid-thermal mixing in a 180° sector of the downcomer and a cold leg of the Calvert Cliffs-1 plant for three assumed accident scenarios. The inlet boundary conditions for these calculations were obtained from mass flow rates and temperatures that were computed in systems code studies. The results of the three-dimensional SOLA-PTS calculations indicated that a pressurized thermal shock risk was mitigated for these accident scenarios as the result of the particular circulation patterns that developed in the downcomer.

I. INTRODUCTION

This report describes the application of the transient, three-dimensional SOLA-PTS code[1] to the study of certain pressurized thermal shock (PTS) transients in a Combustion Engineering-designed pressurized water reactor. The term pressurized thermal shock refers to the potential for crack propagation through reactor vessel plates or weldments as the result of a severe overcooling of the vessel wall coincident with or followed by a repressurization of the reactor. The PTS risk is believed to increase with the age of the reactor as the result of prolonged neutron irradiation of the materials in the reactor vessel wall.

The TRAC code[2] has been used to analyze a series of 13 assumed accident transients[3] in the Calvert Cliffs Unit 1 nuclear power plant, which is operated by Baltimore Gas and Electric Company. Portions of three of these transients were analyzed with the SOLA-PTS code to examine detailed fluid-thermal mixing in the cold leg and downcomer regions. The results of the TRAC calculations[3] were used to determine whether the transients should be analyzed. A SOLA-PTS study was performed if the TRAC results indicated that there was:

(1) significant cooling of the downcomer fluid,

(2) repressurization of the reactor, and

(3) loop flow stagnation in some of the cold legs at a time when safety injection (SI) flow was activated.

Transients 1, 2, and 9 satisfied these criteria and were analyzed with SOLA-PTS. Transient 3 also satisfied these criteria but the period of flow stagnation was so brief (about 150 seconds) in that case that it was not felt that this was a real PTS threat.

Section II contains a description of the prescribed conditions and the procedures used in the SOLA-PTS calculations. In Sec. III we discuss some of the flow conditions in the downcomer that result from varying flow and thermal conditions in the broken and intact loop cold legs. The results of the calculations are presented and discussed in Sec. IV, and Sec. V provides a summary of the results and conclusions of this study.

II. THE SOLA-PTS CALCULATION

SOLA-PTS is a transient, three-dimensional computer program for calculating the turbulent mixing of fluids of different temperatures in complex geometries. The capability of including wall heat transfer effects, by coupling the solution of a fluid thermal transport equation with a wall thermal diffusion equation, is also present in the code. But this capability has not been utilized in the present application where the walls have been treated adiabatically. Reference 1 provides a complete description of the SOLA-PTS code.

In the calculations of this study we resolve a 180° sector of the unwrapped downcomer and assume symmetric boundary conditions at the azimuthal edges of the flow region. Some calculations were performed in a 90° sector of the downcomer,[4] but these will not be reported here because subsequent studies have demonstrated the necessity of including the effects of interactions between adjacent cold leg flows. The present studies resolve the unwrapped downcomer, the lower plenum, and part of the reactor core in a Cartesian coordinate system. An intact loop cold leg is also resolved together with its safety injection and charging flow inlets. This cold leg is treated as a square duct of the same cross-sectional area as the circular cold leg pipe. In the broken loop cold leg, where loop flow is maintained in all of the transients considered here, we assume thorough mixing of the safety injection and loop flows and inject this mixed fluid directly into the downcomer through an inlet region with the cross-sectional area of the cold leg.

The SOLA-PTS calculations are performed in a transient mode using data from the TRAC calculation to provide the time-varying inlet boundary conditions. These data include the mass flow rates and temperatures of the safety injection, charging, and broken loop cold leg flows. Generally the TRAC curves are fitted with a fourth degree polynomial using Newton's Formula for Forward Interpolation,[5] but constant values are used for the temperature of the safety injection flow and for the flow rate and temperature of the charging flow.

In order to make the SOLA-PTS calculations more efficient the time scale of the TRAC plots used to prescribe the SOLA-PTS inlet data are compressed, so that the ramp times are reduced. For example, we use the TRAC Transient 1 data, Figs. 1-3, to prescribe the inlet boundary conditions for the time interval t=300-1000 seconds. However, we have compressed this 700-second time interval by a factor of five so that the SOLA-PTS calculations cover a time interval of only 140 seconds. The factor of five was chosen so that the total computation time would be approximately ten times greater than the time it took for fluid to flow from the safety injection region to the downcomer, which was about 15 seconds for Transient 1. With this order of magnitude difference between total computation time and cold leg flushing time it was felt that no essential information was lost as a result of compressing the input data curves. For plotting purposes the SOLA-PTS time scale for Transient 1 is expanded by a factor of five so that the results presented below cover the interval t=300-1000 seconds. A factor of five was also used when compressing the input data for Transient 2, but a factor of two was used for Transient 9 because the total computation time was shorter in that study.

In addition to using the TRAC data to prescribe the time-varying input for these problems, we also used the TRAC fluid temperatures to set the initial temperature distribution in the cold leg and downcomer. It is important to account for the initial downcomer temperature distribution because it affects the buoyancy potential of the incoming cold leg flows. Transient 1 was first run with a uniform initial temperature in the downcomer, corresponding to the temperature of the broken loop flow. This loop flow was therefore neutrally buoyant, so a cold leg plume did not develop below this inlet. When this transient was rerun with the appropriate initial temperature distribution in the downcomer, a cold leg plume did develop below the broken loop inlet and a different circulation pattern was established in the downcomer. This circulation pattern had an important effect on downcomer temperatures, as will be discussed below.

The SOLA-PTS calculations were initiated by injecting safety injection and charging flows into the intact loop cold leg at the initial safety injection flow rate, the charging flow rate being constant in time. The loop flow and safety injection flow in the broken loop were set to zero during this initial phase. (We assume that there is no charging flow in the broken loop cold leg.) Once stratified flow has been established in the intact loop cold leg and the cold fluid layer has reached the downcomer, the broken loop flows are turned on and all inlet flow rates and temperatures are allowed to vary transiently according to the TRAC data. These calculations were terminated at a time when the TRAC results indicated that the stagnant flow conditions in the intact loop cold leg had ended (Transient 9) or when the SOLA-PTS calculations indicated increasing temperature conditions throughout the downcomer (Transients 1 and 2).

The Table lists the component information that was used to construct the SOLA-PTS finite difference mesh, as well as the inlet temperatures for the safety injection and charging flows and the charging flow rate. Since the charging fluid flows into two of the four cold legs, we have conservatively assumed that in the 180° sector considered in this study this flow exists in the intact loop cold leg but not in the broken loop cold leg.

The hot legs are treated as internal obstacles in the downcomer region. Since the azimuthal planes of symmetry pass through the centers of the hot legs, only half of these obstacles are resolved in the calculations. Although the core barrel wall has different thicknesses at different elevations in the vessel, these small variations could not be accounted for in the calculations, so a uniform thickness of 6.4 cm was used. The geometry of the cold leg bend is not resolved in the calculations, since the intact loop cold leg is treated as a straight square duct. Instead, an axial flow resistance is included in the cold leg at the position of the bend.

Figure 4 shows the locations of the reactor vessel welds[12] for the 180° downcomer sector considered here. Also shown in the figure are the centers of the hot and cold legs and the locations at which transient temperature measurements were made in the SOLA-PTS calculations. The broken and intact loop cold legs are centered at 60° and 120° azimuthal locations, respectively. Figures 5 and 6 show the locations at which the temperatures were recorded on the core barrel wall and on the centerline of the intact loop cold leg.

The computation mesh used in this study consisted of 12530 calculation cells, of which 7325 were fluid cells and the rest boundary cells. These

TABLE

INPUT DATA FOR CALVERT CLIFFS-1 PLANT

Item	Dimension	Ref.
Hot leg, o.d.	48.125 in. = 122.24 cm	6,7
Cold leg, i.d.	30.0 in. = 76.2 cm	6
Vessel, i.d.	172.0 in. = 436.88 cm	6
Core, i.d	148.0 in. = 375.92 cm	6
Height of UCSP above cold leg centerline	78.0 in. = 198.12 cm	6
Height of cold leg centerline above bottom of vessel	329.0 in. = 835.66 cm	6
Thickness of core barrel wall (upper plenum)	2.5 in. = 6.35 cm	7,8
Thickness of core barrel wall (core region)	1.75 in. = 4.44 cm	7,8
Thickness of core barrel wall (lower plenum)	2.25 in. = 5.72 cm	7,8
Distance of safety injection nozzle from vessel wall	137.19 in. = 348.46 cm[a]	7,9
Safety injection pipe, i.d.	10.126 in. = 25.72 cm	7
Orientation of safety injection pipe	60°, top	10
Distance of charging flow nozzle from vessel wall	144.38 in. = 366.73 cm	7,9
Charging flow pipe, i.d.	1.689 in. = 4.29 cm	7
Orientation of charging flow pipe	horizontal	11
Cold leg bends	60°F, horizontal[b]	9
Safety injection inlet temperature	55°F = 285.9K	8
Charging flow inlet temperature	85°F = 302.6K	8
Charging flow rate, divided between two cold legs	8.3 kg/s	8

[a] 144.38 in. = 366.73 cm in cold legs with charging flow.

[b] 30° horizontal in cold legs with charging flow.

calculations ran at about 100 times real time; when the computation times were compressed by a factor of five, the running time was reduced to about 20 times real time for Transients 1 and 2.

III. FLOW DISTRIBUTION IN THE DOWNCOMER

For an incompressible fluid, the total outflow from a system must equal the total inflow. In the present study, the outflow from the core region exactly balances the sum of the fluid flows entering through the safety injection pipes, the charging flow pipe, and the broken loop cold leg. There cannot be a net acceleration in the interior of the system. Thus, if cold fluid enters the downcomer from the cold legs and is accelerated downward due to buoyant forces, there must be corresponding upward accelerations in other parts of the downcomer. The resulting motions bring warm water from the lower part of the downcomer and from the lower plenum up to the cold leg regions to mix with the cold inlet fluid.

In none of the transients considered by the TRAC analysts is there flow stagnation in all cold legs at the same time. When stagnation occurs in one loop there is flow in the other loop, and this loop flow is generally large compared to the combined safety injection and charging flow into the stagnant loop. If this incoming loop flow (into which safety injection fluid has mixed) is cool compared to the downcomer fluid, then the predominant downward flow in the downcomer will occur beneath this loop flow inlet. This will lead to upward accelerations beneath the stagnated cold leg outlet. The trajectory of the cold fluid that exits from the stagnated cold leg will depend on the relative magnitudes of the upward convective force and the downward buoyant force. If the upward force exceeds the downward force then this fluid will be transported upward and azimuthally toward the cold leg in which the loop flow is maintained. We refer to this as loop flow dominated circulation. It results in considerable warming of the stratified cold fluid exiting from the stagnant cold leg and thereby reduces the thermal shock risk.

A different type of circulation occurs if the loop flow is warm so that it is, say, neutrally buoyant compared to the downcomer fluid. As this fluid impacts on the core barrel wall, it will tend to spread in all directions. The effect of this flow on the stratified cold water exiting from the stagnant loop is to mix with it and warm it and also to convect it azimuthally in a direction away from the cold leg with loop flow. The warming effect is enhanced by the fact that the loop flow water is entrained into the counter flowing warm layer at the

top of the stagnated cold leg and mixes with the cold layer in that pipe. Again, the effect of this warming is to reduce the thermal shock risk. We refer to this situation as stagnant loop dominated circulation. It appears as downward flow beneath the stagnant loop cold leg exit and upward flow beneath the cold leg in which the loop flow is maintained.

It would appear that the most serious flow situation from a PTS point of view would be one that began as a loop flow dominated circulation, but with a weak thermal potential. Then the downward buoyant force beneath the stagnant loop cold leg could exceed the upward convective force so that the cold water from the stratified layer could penetrate to the vessel weld regions. This falling cold fluid could set up a local circulation region beneath the stagnant loop cold leg, confined there by the larger loop flow dominated circulation pattern. This local circulation would not entrain as much warm water as the larger circulation so that the warming effect in the countercurrent stagnant loop cold leg flow would be reduced. A tendency toward this type of flow development occurs in one of the transients considered below, but it occurs at a time when the safety injection flow is small so the effect on the vessel temperatures is not great.

IV. RESULTS OF THE CALCULATIONS

Flow velocity and fluid temperature data are presented in this section for Transients 1, 2, and 9. In each case we show the transient TRAC data that was used to provide the input boundary conditions for the study. We also present some typical velocity vectors plots and a temperature contour plot for each transient showing the flow development in the intact loop cold leg and downcomer and the temperature distribution in the fluid adjacent to the vessel wall in the downcomer. Finally, we present plots showing the transient temperature variation at several locations on the vessel wall, on the core barrel wall, and in the intact loop cold leg. The vessel wall plots show the coldest temperatures at the various horizontal and vertical weld segments shown in Fig. 4. For the horizontal weld segments we also plot the TRAC downcomer fluid temperature measurement[3] at that axial level and azimuthal value.

A. Transient 1

Figures 1-3 show the TRAC measurements[3] of the broken loop cold leg mass flow rate and temperature and the total safety injection and charging mass flow rate that are used to specify the inlet boundary conditions for the SOLA-PTS calculation of Transient 1 in the time interval t=300-1000s. Note that the cold leg

temperature is roughly constant or increasing after t=1000s and that the safety injection flow has terminated after this time (the charging flow continues to the end of the TRAC transient). Thus the downcomer temperatures should increase after t=1000s.

The initial downcomer temperature distribution for the SOLA-PTS calculation is shown in Fig. 7. It was obtained from the TRAC calculation of Transient 1 at t=300s.

Figures 8-12 show velocity vector plots in various two-dimensional cuts through the intact loop cold leg and the downcomer at a time of 650s. Figure 8, which is in a vertical plane through the centerline of the cold leg, shows safety injection flow into the cold leg and the countercurrent flow development between the downcomer and the safety injection region. The charging flow inlet does not show on this plot. In the downcomer the fluid is carried upward by the strong loop flow dominated circulation pattern. This circulation pattern can be seen in Figs. 9 and 10, which are velocity vector plots in planes adjacent to the core barrel and vessel walls. These show strong downward flow below the broken loop cold leg on the left and upward flow beneath the intact loop cold leg on the right. This upward convective force is greater than the downward buoyant force acting on the cold water entering the downcomer from the intact loop cold leg so that fluid is carried upward and azimuthally to mix with the downward flow below the broken loop cold leg. The net effect is to maintain warmer temperatures than TRAC on the intact loop side and slightly cooler temperatures at some locations on the broken loop side.

Another view of the flow circulation in the downcomer is given in Figs. 11 and 12, which show velocity vector plots in horizontal planes through the bottom and top of the cold legs. At the bottom of the intact loop cold leg, the exiting cold water is entrained by the circulating flow in the downcomer and carried azimuthally toward the broken loop side. Because of the strong circulating flow, the cold water is confined to the vessel wall region. Consequently, the vertical weld section between the cold legs is colder at this time in the transient than the horizontal weld below the intact loop cold leg. The entrainment of the circulating flow into the top of the cold leg is very asymmetric, as shown in Fig. 12. One contribution to this asymmetry that does not appear in the figure is that the charging flow is injected on the right side of the cold leg.

Figure 13 is a temperature contour plot in a vertical plane adjacent to the vessel wall. The region of cold fluid below the broken loop cold leg is a

relatively narrow band extending to the lower plenum region. The coldest fluid is at the bottom of the intact loop cold leg inlet but this cold fluid is transported azimuthally toward the broken loop side. The fluid near the top of the downcomer remains warm and relatively stagnant throughout the transient.

The strong, loop flow dominated flow circulation in the downcomer begins to weaken after about t=750s when the broken loop cold leg temperature, Fig. 2, is near its minimum. As a result, the cold stream from the bottom of the intact loop cold leg is able to penetrate downward in the downcomer for a brief period before the safety injection flow, Fig. 3, ceases. The flow distribution and temperature fields that result are shown in Figs. 14-19.

Figure 14 shows that the cold fluid is penetrating into the downcomer below the centerline of the cold leg. The chilling effect on the vessel wall is emphasized by the fact that the flow from the cold leg does not impact on the core barrel wall but hugs the vessel wall for about two cold leg diameters below the junction. The flow distribution in the downcomer can be seen in Figs. 15 and 16. The downward flow beneath the broken loop cold leg is much less pronounced than in Figs. 9 and 10, and the downward penetrating flow beneath the intact loop cold leg is apparent. Figure 16 shows that in the vicinity of the vessel wall, this cold downflow is confined to a narrow stream by local recirculating flows. This downward flow does not penetrate to the bottom of the downcomer. As a result the local recirculations, which carry the water that will be entrained into the counterflowing stream at the top of the intact loop cold leg, remain relatively cool and this helps to maintain the cool temperature in the cold leg.

Figures 17 and 18 show the flow in the horizontal planes at the bottom and top of the cold legs. In Fig. 17 it is seen that the momentum of the circulating flow in the downcomer is insufficient to divert the cold layer at the bottom of the intact loop cold leg in the azimuthal direction. When this cold fluid reaches the downcomer, it falls vertically along the vessel wall as seen in Fig. 14. The flow field in the horizontal plane at the top of the cold legs, Fig. 18, looks very much like Fig. 12, with circulating flow being entrained into the counterflowing layer at the top of the cold leg.

The temperature contour plot in a vertical plane adjacent to the vessel wall shown in Fig. 19 looks much different from that of Fig. 13. A narrow cold stream is falling below the intact loop cold leg, and this narrow stream is surrounded by a wider cool region that shows the outline of the local recirculating flow. Below the broken loop cold leg the narrow cold stream seen in Fig. 13 has been

replaced in Fig. 19 by a thoroughly mixed cool region, and this relatively homogeneous temperature field reduces the thermal potential of the broken loop flow.

Transient temperature plots at locations adjacent to the vessel wall are shown in Figs. 20-30. The location shown on the ordinate title of these figures refers to the locations listed on Fig. 4. For example, location 2 on Fig. 20 is situated at the junction of the downcomer and the bottom of the intact loop cold leg at the centerline.

After the initial sharp drop the temperature at location 2 decreases at a fairly uniform rate until t≈750s, after which the temperature remains approximately constant until t≈900s when it begins to rise. This rise and those shown below for positions in the cold leg indicate that the coldest part of the transient is over. The small-scale oscillations (1-2°F) seen on the temperature plot in Fig. 20 result from slight dispersion errors in the high-order numerical scheme used in SOLA-PTS;[1] they have no physical significance.

The plots in Figs. 21-30 give the temperature variation at the coldest location on each of the horizontal and vertical weld segments shown in Fig. 4. On the horizontal weld segments, we also show the TRAC downcomer temperature[3] at approximately the same axial height and at TRAC azimuthal positions THETA-1 or THETA-6. THETA-1 corresponds to positions on the broken loop cold leg side and THETA-6 to those on the intact loop side. Referring to Figs. 21 and 23, one can see that the TRAC and SOLA-PTS temperatures are in good agreement on the broken loop side. This is consistent with the fact that this transient is dominated by the loop flow from the broken loop cold leg. The SOLA-PTS temperature in Fig. 25 is warmer than the TRAC temperature because this location is not in the cold stream below the broken loop cold leg (see Figs. 13 and 19). On the intact loop side, the SOLA-PTS temperatures are usually higher than the TRAC temperatures because throughout most of the transient the momentum force from the loop flow dominated circulation exceeded the cold fluid buoyant force at the intact loop cold leg. As a result, this cold fluid was carried upward and azimuthally toward the broken loop side. When the cold water does penetrate, as in Fig. 22 at around 800s, the SOLA-PTS temperature is colder than the TRAC temperature because TRAC can not account for thermal stratification in the cold leg. The minimum temperature in Fig. 22 is about 220°F, while on the broken loop side the minimum temperature in Fig. 21 is about 250°F. Notice that throughout most of the transient the temperature at location 35 (Fig. 28), which is located on the vertical weld

segment between the cold legs, is lower than that at location 13 below the intact loop cold leg (Fig. 22).

Figures 31-33 are temperature plots on the core barrel wall across from locations 6, 12, and 24, respectively on the vessel side. Location 42, Fig. 31, is just below the area of impact of the broken loop cold leg flow on the core barrel wall. Therefore the temperature here closely follows the TRAC broken loop inlet temperature, Fig. 2. It is generally cooler than the temperature at the corresponding location on the vessel side (Fig. 21) and does not exhibit the temperature oscillations seen there. The temperature profiles in Figs. 32 and 33 are very similar to the corresponding ones on the vessel side (Figs. 22 and 24) throughout most of the transient because the flow on the intact loop side is dominated by the loop flow generated circulation. However, Fig. 32 does not show the sharp drop in temperature seen in Fig. 22 around t=800s because, as we saw earlier, the cold water penetration occurred primarily on the vessel wall side.

Some temperature transients in the intact loop cold leg are displayed in Figs. 34-39. Figures 34-36 show the temperature variation with height under the safety injection inlet. At location 55, Fig. 36, directly under the inlet there has been some warming of the water, which was injected at 55°F, as a result of mixing with the counterflowing warm stream at the top of the cold leg. There is additional warming as the cold water jet entrains surrounding water, as shown in Figs. 34 and 35. The very rapid warming that occurs after t=900s, and is particularly apparent in Fig. 36, results from the exhaustion of safety injection fluid (see Fig. 3).

The warming trend that develops along the bottom of cold leg is shown in Figs. 34, 37-39. Most of this warming takes place between locations 53 and 56, i.e., in the immediate vicinity of the safety injection inlet. Very little warming takes place between the inlet region and the downcomer, indicating that there was little energy exchanged between the counterflowing hot and cold layers in the cold leg. Similar results were observed in previous zero loop flow SOLA-PTS calculations[4] that were shown to be in good agreement with Creare experimental data.[13] Figures 37-39 show that the minimum temperature at the bottom of the cold leg was reached at about 600 or 700s.

B. Transient 2

The mass flow rate and the temperature of the broken loop cold leg flow, and 1/4 of the total safety injection and charging flows from the TRAC calculation of

Transient 2, are shown in Figs. 40-42. The initial downcomer temperature distribution, which was obtained from the TRAC calculation at t=300s, is given in Fig. 43. Note that both the transient broken loop cold leg temperature, Fig. 41, and the initial downcomer temperature, Fig. 43, are cooler in Transient 2 than their counterparts in Transient 1, Figs. 2 and 7. The initial intact loop cold leg temperature (not shown) is also cooler in Transient 2. As a result of these cooler temperatures, the transient flow and temperature distributions in the downcomer are different in Transient 2 than in Transient 1. Because of the cooler initial temperature in the intact loop cold leg, the buoyant force in this region is sufficiently large to overcome the upward convective force that results from the loop flow dominated circulation. Thus the cold water penetrates to the weld regions on the intact loop side early in the transient. Eventually, however, the upward convective force overwhelms the buoyant force so the cold water that exits from the intact loop cold leg is carried upward and azimuthally toward the broken loop side as in Transient 1. Unlike Transient 1, this flow pattern, once established, is not altered later in the SOLA-PTS transient.

Figure 44 shows the flow field in a vertical plane through the intact loop cold leg centerline at t=800s. The cold fluid exiting from the bottom of the cold leg is turned vertically upward as it reaches the downcomer by the strong circulating flow that is shown in Figs. 45 and 46. The upward flow on the intact loop side is confined to a relatively narrow region below the hot leg. It turns in an azimuthal direction at the cold leg elevation and diverts the flow from the intact loop cold leg toward the broken loop side. The fluid below the intact loop cold leg is relatively stagnant.

Figures 47 and 48 show another view of this circulating flow, this time in horizontal planes through the bottom and top of the cold legs. The cold fluid exiting from the cold leg is carried azimuthally toward the broken loop side. This azimuthal flow is so strong that the cold leg flow does not impact on the core barrel wall on the intact loop side. At the top of the cold legs, Fig. 48, some of the circulating fluid is entrained into the intact loop cold leg.

As a result of the circulating flow in the downcomer, the temperatures at the weld locations on the intact loop side are warmer than the TRAC prediction throughout most of the transient. The temperature distribution in the downcomer near the vessel wall is shown in Fig. 49 at t=800s. It shows a very small cold fluid region at the intact loop cold leg and a narrow cold spike below the broken

loop cold leg that extends to the lower downcomer region. Most of the downcomer region is quite cool at this time, with temperatures in the range 235-275°F.

Transient temperature plots on the vessel wall are shown in Figs. 50-60. At location 2, Fig. 50, which is at the junction of the bottom of the intact loop cold leg and the downcomer, the temperature is relatively steady after about t=550s. This reflects the approximate constancy of temperatures in the cold leg that persists from about t=500s until the safety injection flow terminates. At location 5, Fig. 51, which is on the first horizontal weld below the cold leg on the broken loop side, the temperature decreases at about 5°F per 100s after t=500s reaching a minimum of 225°F at the termination of the calculation. The temperature transient calculated with SOLA-PTS is in good agreement with the TRAC downcomer temperature[3] at azimuthal location THETA-1 and axial level 8, which is shown by the dashed line on the plot. Similar good agreement with TRAC is shown at location 18, Fig. 53, at the second horizontal weld below the broken loop cold leg. At the lowest horizontal weld on that side, Fig. 55, the SOLA-PTS temperatures are generally higher than TRAC because location 28 is not situated at the coldest position on that side, which is on the narrow spike shown in Fig. 49.

On the intact loop side, the temperatures are usually higher than the TRAC downcomer temperatures,[3] which are from azimuthal angle THETA-6. Early in the SOLA-PTS transient, however, the cold flow from the bottom of the intact loop cold leg did penetrate to the first weld, and in that local region the SOLA-PTS temperatures were colder than TRAC. With time the location of the coldest region on this weld was transferred to the left by the upward circulating flow. This cold temperature persisted longest at location 10, shown in Fig. 52. The minimum SOLA-PTS temperature there was about 225°F, but the duration of this low temperature was less than 200 seconds. These low temperature plumes did not extend to the beltline weld as shown in Fig. 54. Thus the temperatures at the lower welds, Figs. 54 and 56, are higher than the TRAC temperatures by about 40°F. The transient temperatures on the vertical weld segments are shown in Figs. 57-60.

The temperature at location 42 on the core barrel wall is shown in Fig. 61. This temperature is cooler and fluctuates less than the corresponding temperature on the vessel wall at location 5, Fig. 51. However, on the intact loop side the temperature at location 44, Fig. 62, shows some of the same oscillations seen at location 10, Fig. 52, on the vessel wall. This indicates that when the cold water penetrates to the welds below the intact loop cold leg this cold water fills the downcomer gap at least part of the time.

Temperature transients in the intact loop cold leg are shown in Figs. 63-68. Locations 53, 54, and 55, Figs. 63-65, show the temperature variation with height directly under the safety injection inlet. The temperatures in this region are about 30°F cooler than in Transient 1, reflecting the greater safety injection flow rate as well as the cooler downcomer temperatures entrained into the cold leg. These temperatures reach a quasi-constant value very early in the transient, and this persists until shortly after 800s when the temperatures increase as the safety injection mass flow rate begins to fall off more rapidly and the broken loop temperature bottoms out.

The temperature variation along the cold leg can be seen by comparing the plots at locations 53, 56, 61, and 63, Figs. 63, 66-68. As we saw in Transient 1, the principal temperature rise takes place between locations 53 and 56, i.e., in the immediate vicinity of the inlet. These temperatures are relatively constant in the time period t=550-850s.

C. Transient 9

Transient 9 differs from Transients 1 and 2 both in the assumed originating accident [it was caused by a stuck-open main feedwater regulating valve (MFRV) while they resulted from main steamline breaks] and in the TRAC thermal history[3] that forms the boundary conditions for the SOLA-PTS calculation. Figures 69-71 show the mass flow rate and temperature in the broken loop cold leg and the safety injection mass flow rate. We calculate this transient for the time interval t=400-600s, the time when there is simultaneously flow stagnation in the intact loop cold leg and safety injection flow into the cold legs. Figure 72 shows the TRAC downcomer temperature[3] at t=400s that provides the initial downcomer temperature for the SOLA-PTS calculation.

The principal difference between Transient 9 and Transients 1 and 2 is the high temperature of the broken loop cold leg flow as shown in Fig. 70. Because of this high temperature, the fluid flowing from the broken leg is often warmer than the downcomer fluid or neutrally buoyant. Consequently, a thermal plume does not form below the broken loop cold leg; the flow from that cold leg spreads azimuthally and mixes with the cold plume that forms below the intact loop cold leg. The downcomer flow in this transient is therefore a stagnant loop dominated circulation with downward flow on the intact loop side and upward flow on the broken loop side. The strength of this circulation is much smaller than in the previous transients because the volume of downcomer water that is buoyantly accelerated is much reduced.

Figures 73-78 demonstrate this flow development. As indicated in Fig. 73, the flow that exits from the intact loop cold leg into the downcomer is not carried upward as in the previous transients. Instead, there is a strong downward flow on the intact loop side as shown in Figs. 74 and 75. When the flow from the broken loop cold leg impacts on the core barrel wall, it spreads uniformly as seen in Fig. 74, but much of it is entrained in the downward flow on the right. This spreading on the core barrel wall diverts the cold water from the intact loop cold leg in a direction away from the broken loop cold leg as shown in Figs. 74 and 75 and confines that cold water more closely to the vessel wall as seen in Figs. 75 and 76. This tends to increase the thermal shock threat, but a compensating factor is that a large volume of warm water from the broken loop flow is entrained into the intact loop cold leg, as shown in Fig. 77, where it mixes with the safety injection and charging fluids, so that the fluid that exits from the cold leg is much warmer than in the previous transients. The temperature distribution on the vessel wall that results from these processes is shown in Fig. 78. The only significant temperature variation occurs in the immediate vicinity of the intact loop cold leg outflow and in a narrow channel that extends for a few cold leg diameters downstream from the exit.

The transient temperature variations at locations on the vessel wall are shown in Figs. 79-83. The temperature at location 2, Fig. 79, which is at the junction of the bottom of the intact loop cold leg and the downcomer, is about 135°F warmer than that of Transient 2, reflecting the warming of the intact loop cold leg by water entrained from the broken loop cold leg. Notice that the upper limit on the vertical scale on these Transient 9 plots is 450°F, not 400°F as in Transients 1 and 2.

The temperatures at the weld locations on the broken loop side remain high and almost constant throughout the transient as shown in Fig. 80, at location 6. On the intact loop side there is a significant temperature drop at the first horizontal weld below the cold leg as shown at location 14, Fig. 81. The SOLA-PTS temperature here is about 50°F colder than the TRAC temperature, as result of allowing for flow stratification in the cold leg rather than requiring total mixing. This temperature difference diminishes with depth in the downcomer as indicated by the plots at locations 27 and 31, Figs. 82 and 83, on the lower welds.

Figure 84 shows the temperature variation at location 46 on the core barrel wall. Comparing this plot with that at location 14, Fig. 81, demonstrates that there is less temperature variation on the core barrel wall than on the vessel

wall. As indicated above, this is because the flow from the broken loop cold leg spreads along the core barrel wall and tends to confine the cold fluid from the intact loop cold leg to the vessel side.

The strong warming effect of entrained broken loop flow is very evident in Figs. 35-87, which show the temperature transients at locations 53-55 below the safety injection inlet in the intact loop cold leg. Notice in particular the increase in temperature, about 75°F, from location 55 to location 54, which is located in the middle of the cold leg. The temperature variation along the cold leg at location 53, 56, 61, and 63 is shown in Figs. 85, 88-90. As observed in the previous transients, the principal warming takes place between locations 53 and 56 near the safety injection inlet.

V. SUMMARY AND CONCLUSION

The three transients analyzed in this study display two fundamentally different flow developments: a stagnant loop dominated downcomer circulation as in Transient 9, in which there is downward flow on the stagnant loop side and a weak upward flow on the loop flow side, and a loop flow dominated circulation, such as that seen in Transients 1 and 2, where there are strong convective motions under the two cold legs. The effect of both of these flow circulations is to mitigate the thermal shock risk at the vessel welds, by thorough mixing of warm water with the safety injection fluid in the stagnant flow dominated case and by preventing the penetration of the cold fluid from the stratified cold leg flow to the weld regions in the loop flow dominated case.

There is a partial penetration of cold fluid to the weld area in Transient 1, but this occurs late in the transient when the safety injection flow has almost ceased. However, this event suggests a more serious transient condition. If the flow conditions in the cold leg with loop flow were such that a weak loop-flow-dominated circulation developed in the downcomer, so that the upward convective force under the stagnant flow cold leg was not great enough to overcome the downward buoyant force on that side, then cold fluid could penetrate to the weld regions over a longer period of the transient than occurred in Transient 1. In this case, the flows from the two cold legs become essentially divorced from one another.

This is the flow situation that was assumed to exist in all of the preliminary studies, numerical and experimental, in the pressurized thermal shock program. These studies only addressed flow in a 90° sector of the downcomer, with

the tacit assumption that similar conditions existed in the remaining sectors. However, the TRAC studies[3] of the Calvert Cliffs transient scenarios have shown that asymmetric conditions in adjacent cold legs are the norm. Thus, these preliminary studies, while useful for code validation purposes, did not address the appropriate fluid thermal interaction phenomena.

This raises the question of the adequacy of the 180° downcomer studies. Perhaps three-dimensional calculations of the full 360° downcomer with multiple attached cold legs would demonstrate other asymmetries that did not appear in the 180° studies. In view of the complicated nature of these flows, that is entirely possible. For example, one asymmetry that is an integral part of the Calvert Cliffs geometry is that charging flow is injected into the intact loop cold leg in one 180° sector, but it is injected into the broken loop cold leg in the opposite 180° sector. However, there is reason to believe that an approximate 180° symmetry is preserved. In the transients that we have analyzed, there has been flow stagnation in the intact loop cold leg while loop flow has been maintained in the broken loop. This loop flow rate plus safety injection flow is generally an order of magnitude greater than the combined safety injection and charging flows in the intact loop. It is the loop flow that determines the type of flow circulation and therefore the fluid thermal mixing in the downcomer. The lack of charging flow in the intact cold leg would probably have little effect on these mixing processes.

REFERENCES

1. Bart. J. Daly and Martin D. Torrey, "SOLA-PTS: A Transient, Three-Dimensional Algorithm for Fluid-Thermal Mixing and Wall Heat Transfer in Complex Geometries," Los Alamos National Laboratory report in preparation.

2. Safety Code Development Group, "TRAC-PF1: An Advanced Best-Estimate Computer Program for Pressurized Water Reactor Analysis," Los Alamos National Laboratory report in preparation.

3. J. E. Koenig, G. D. Spriggs, and R. C. Smith, "TRAC Analyses of Potential Overcooling Transients at Calvert Cliffs-1 for PTS Risk Assessment," Los Alamos National Laboratory report in preparation.

4. Bart J. Daly and Martin D. Torrey, "Three Dimensional Thermalhydraulic Calculations using SOLA-PTS," Proceedings of the Eleventh Water Reactor Safety Research Information Meeting, Gaithersburg, MD, October 24-28, 1983, U. S. Nuclear Regulatory Commission report NUREG/CP-0048 2, 48 (1984).

5. J. D. Scarborough, Numerical Mathematical Analysis (The Johns Hopkins Press, 1958).

6. Combustion Engineering drawings 233-404 and J-8067-164-001.

7. Letter from Mr. Trevor Cook, Baltimore Gas and Electric Company, to Mr. Jason Chao, Nuclear Safety Analysis Center, January 27, 1983.

8. Gregory D. Spriggs, Los Alamos National Laboratory, personal communication.

9. Combustion Engineering drawing 233-580.

10. Combustion Engineering drawing 233-587.

11. Combustion Engineering drawing 233-586.

12. Combustion Engineering drawing 233-425.

13. P. H. Rothe and M. T. Ackerman, "Fluid and Thermal Mixing in a Model Cold Leg and Downcomer with Loop Flow," EPRI report NP-2312, April 1982.

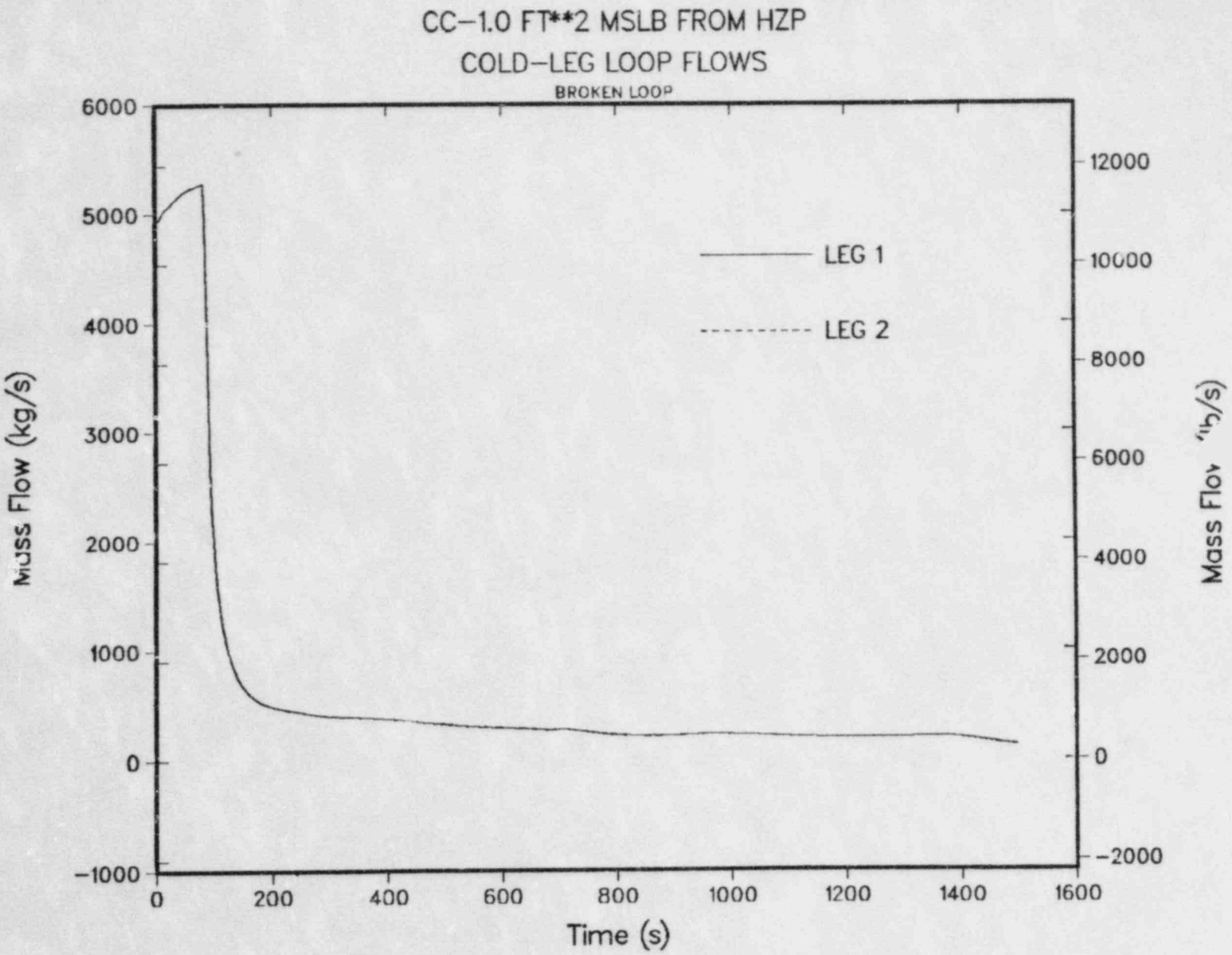

Fig. 1. Mass flow rate into the broken loop cold leg, from the TRAC calculation of Transient 1.

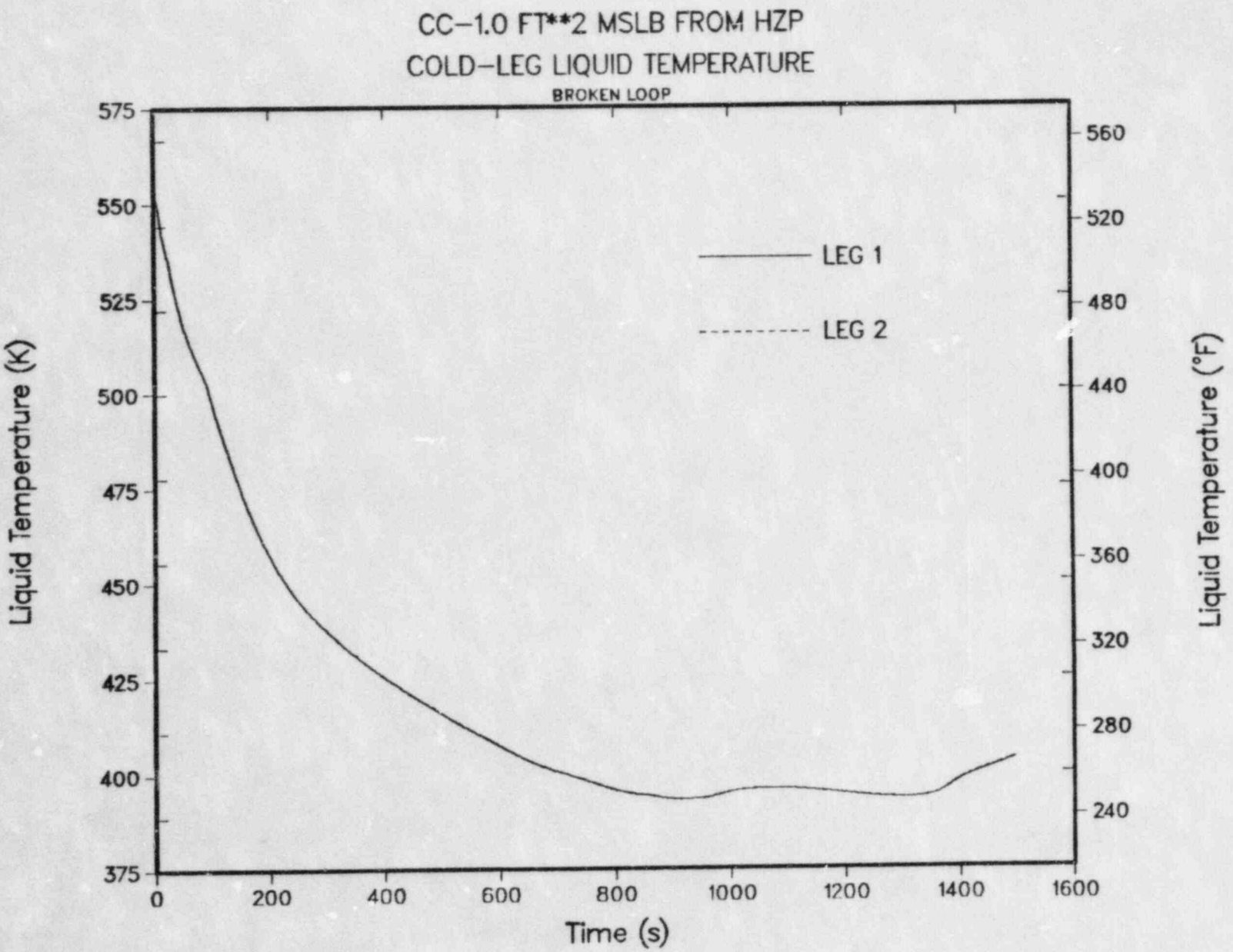

Fig. 2. Temperature of fluid flowing into the broken loop cold leg, from the TRAC calculation of Transient 1.

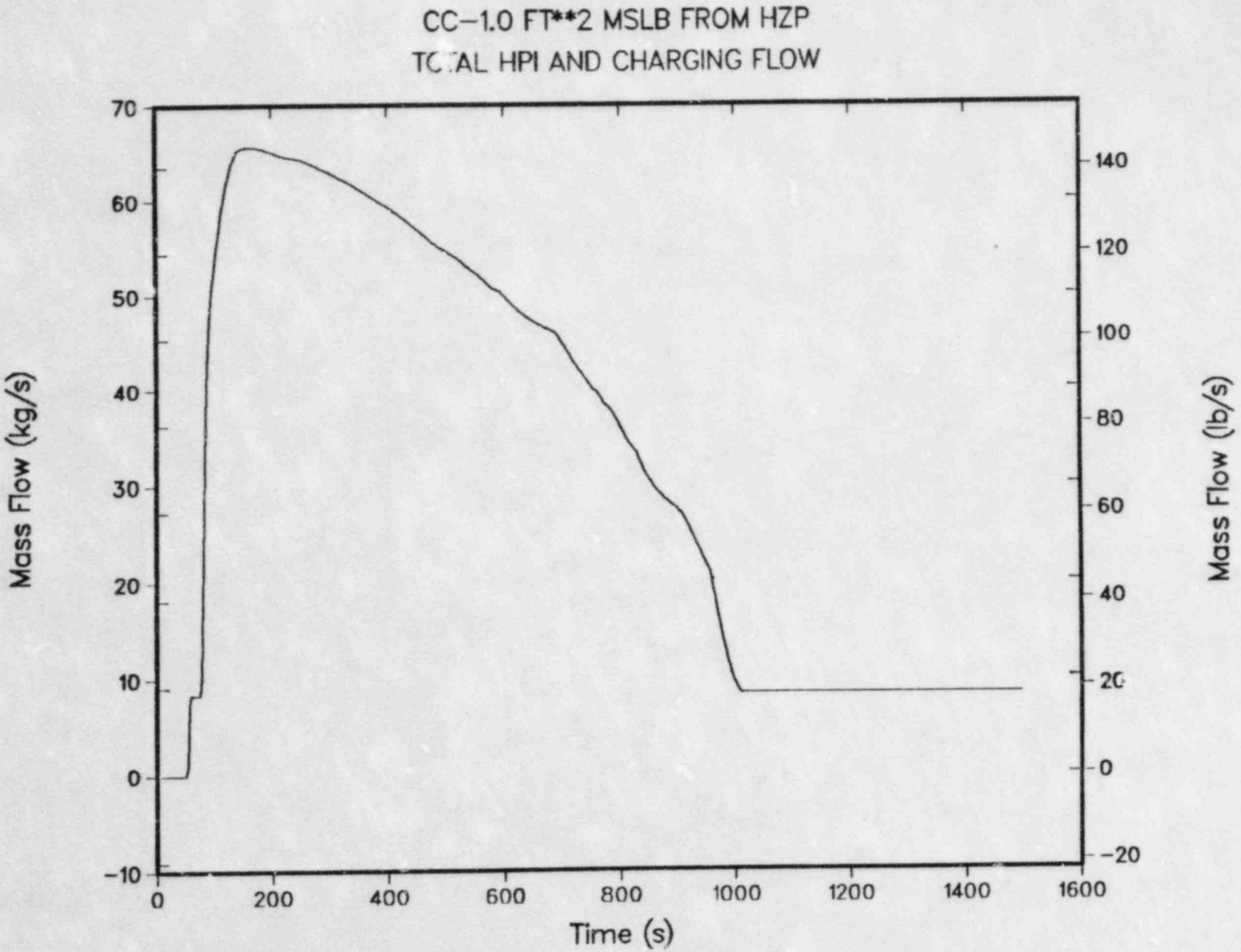

Fig. 3. Total safety injection and charging flow rates, from the TRAC calculation of Transient 1.

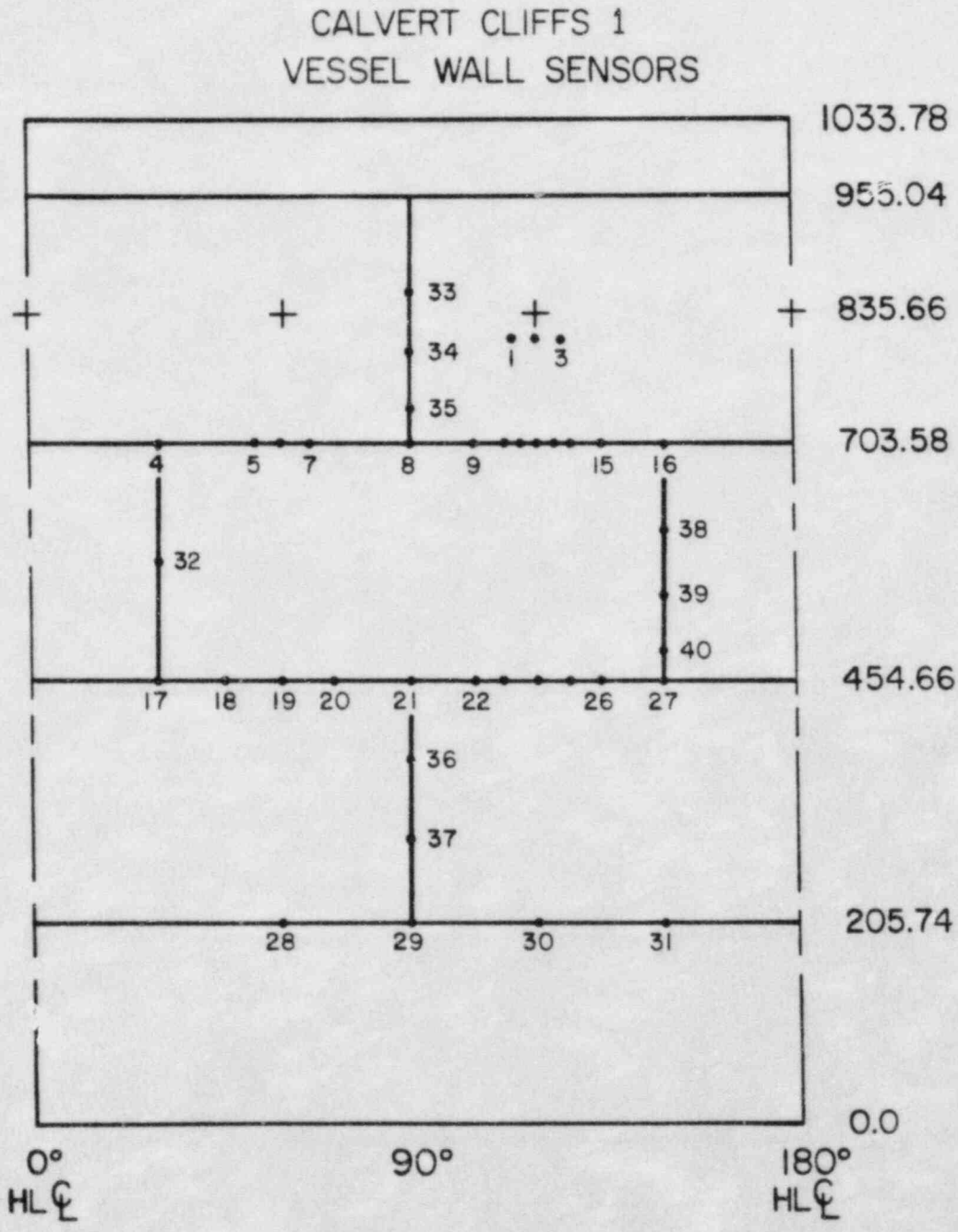

Fig. 4. Locations of vessel welds, hot and cold leg centerpoints, and temperature sensors for the SOLA-PTS calculations. Axial dimensions in cm.

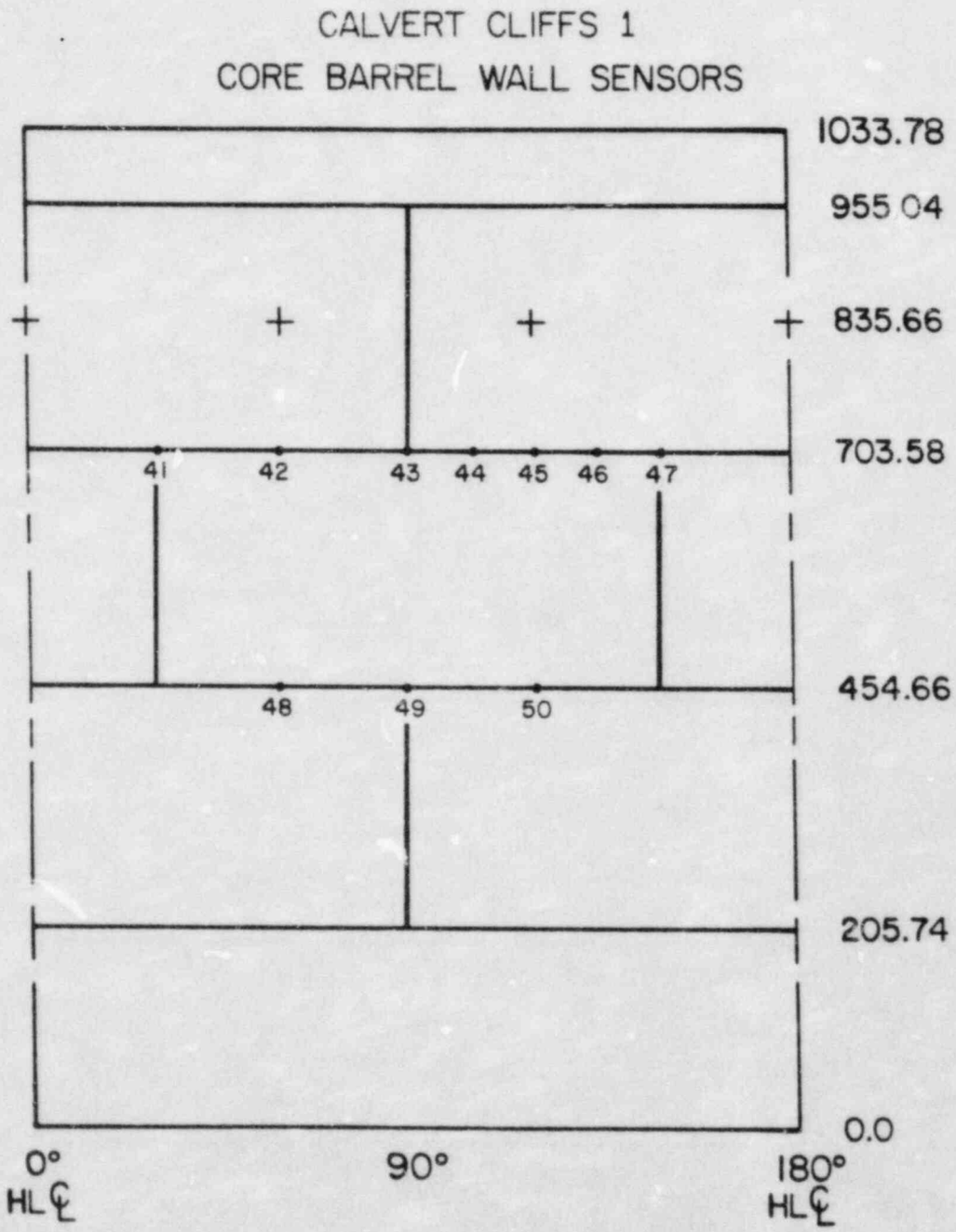

Fig. 5. Locations on the core barrel wall at which temperatures were recorded in the SOLA-PTS calculations. Axial dimensions in cm.

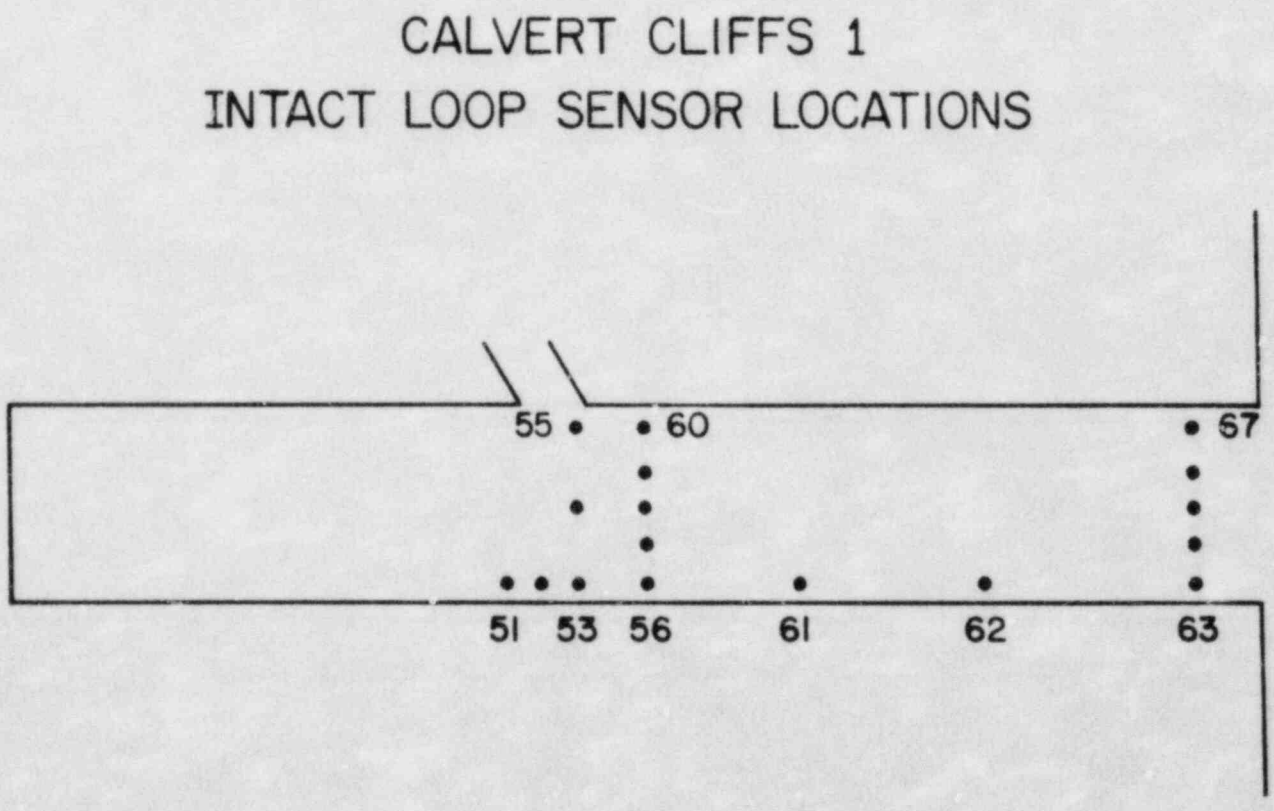

Fig. 6. Locations on the centerline of the intact loop cold leg at which temperatures were recorded for the SOLA-PTS calculations.

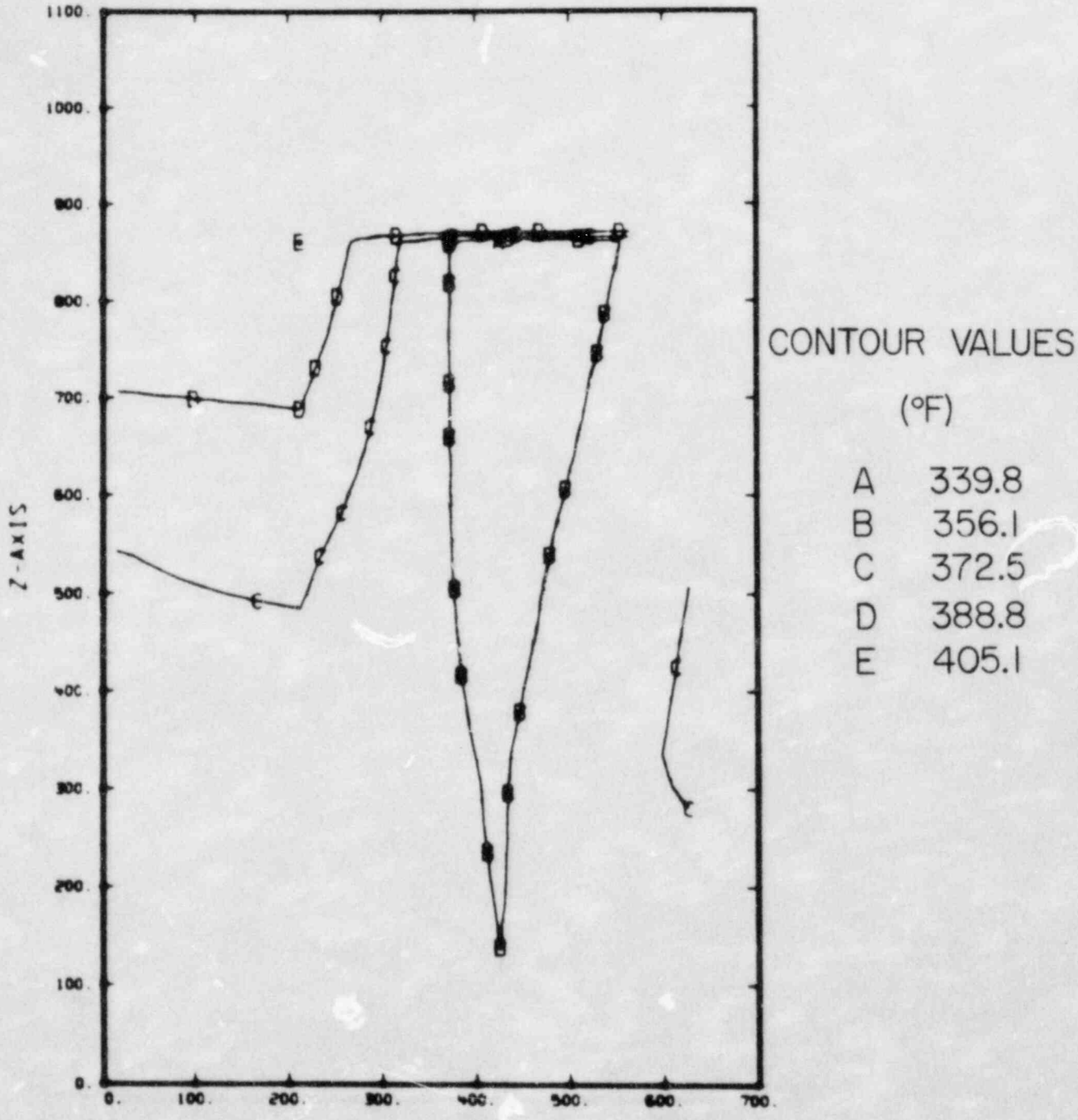

Fig. 7. Downcomer temperature distribution at t=300s, from the TRAC calculation of Transient 1.

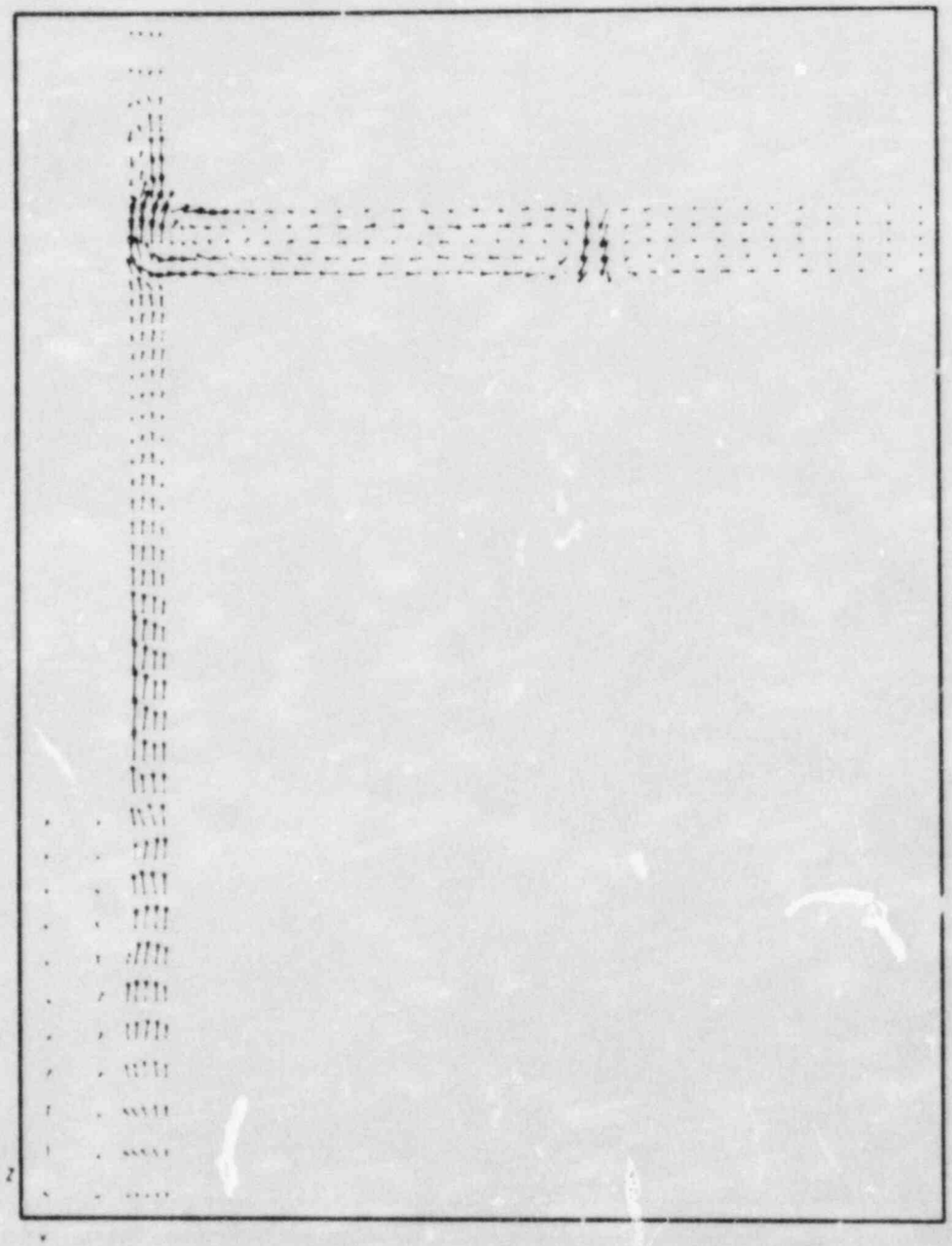

Fig. 8. Velocity vector plot in a vertical plane through the centerline of the intact loop cold leg for Transient 1 at t=650s, showing the core region on the left, the downcomer, and the cold leg. The arrowheads show the direction of flow.

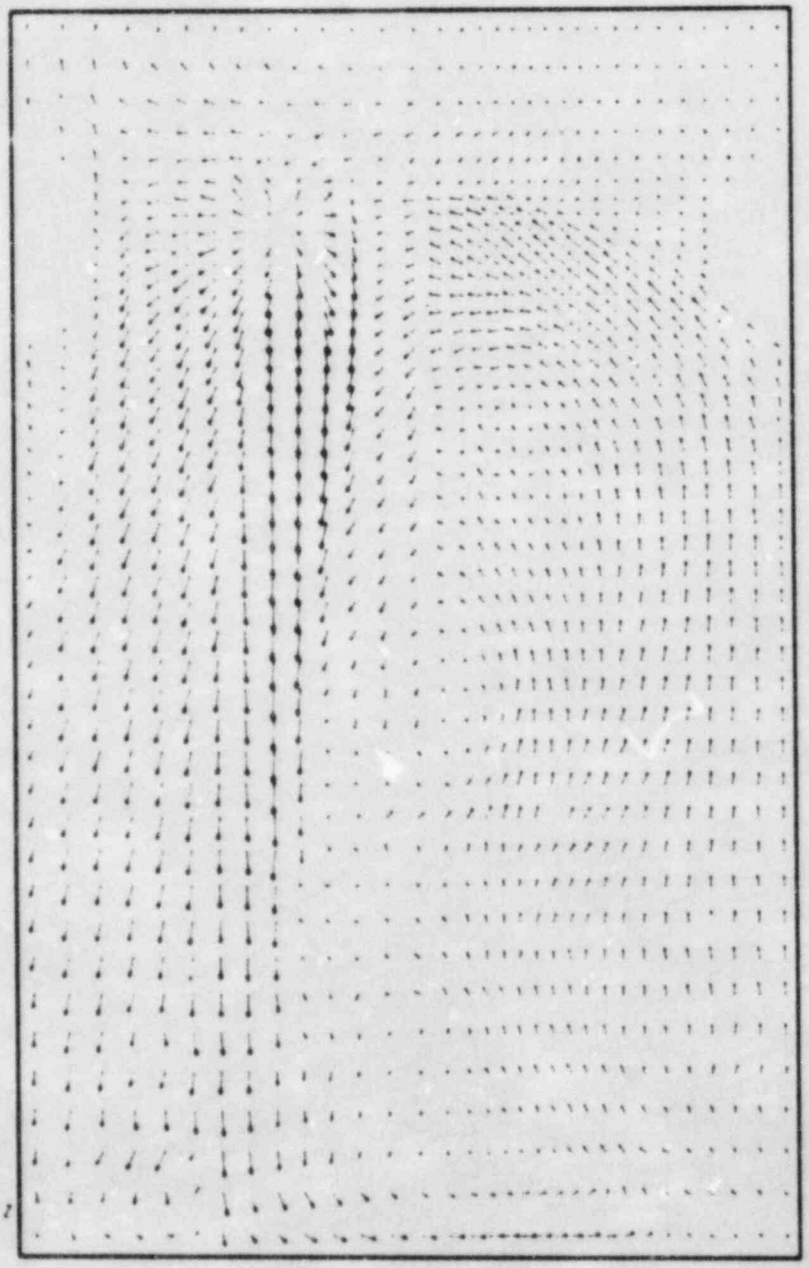

Fig. 9. Velocity vector plot in a vertical plane adjacent to the core barrel wall for Transient 1 at t=650s. Note the region of impact of the broken loop cold leg flow at the upper left. The blank regions are the hot leg obstacles.

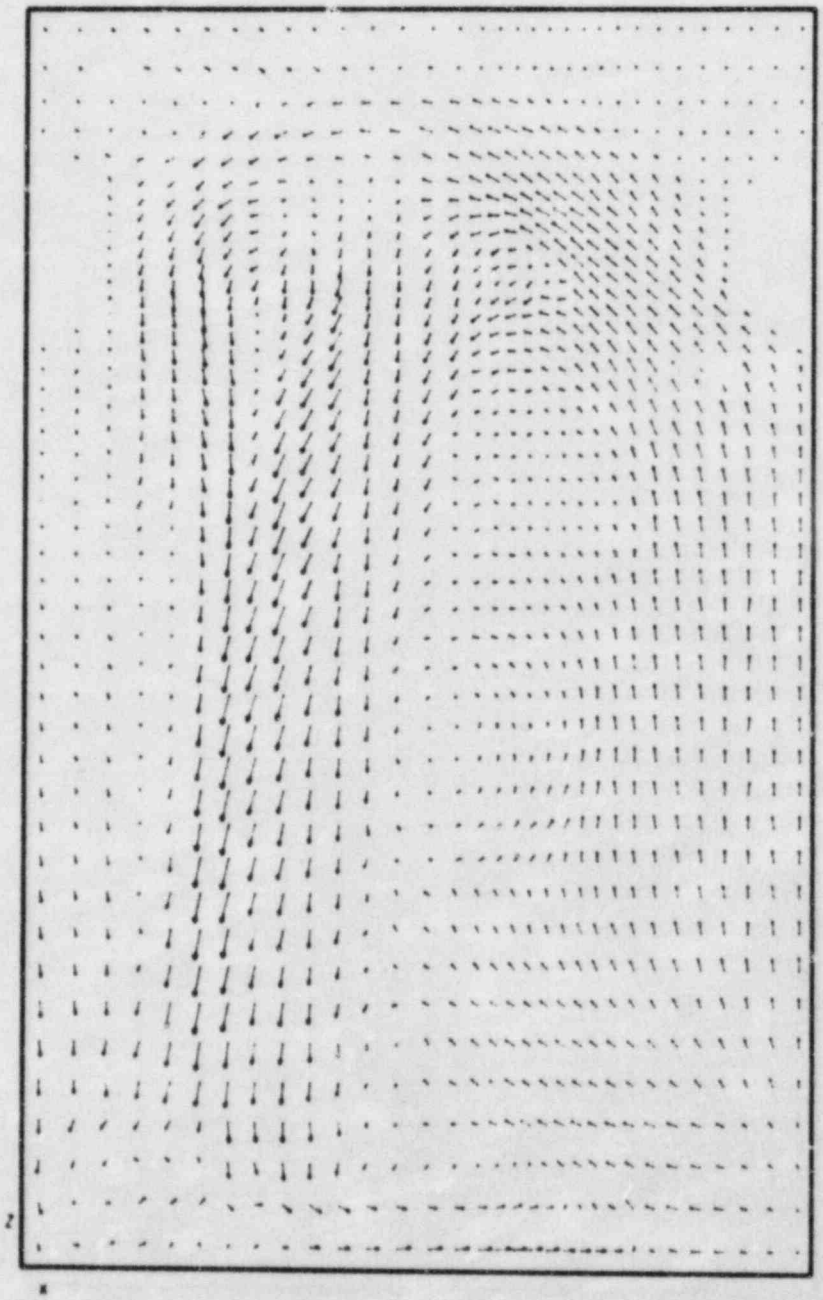

Fig. 10. Velocity vector plot in a vertical plane adjacent to the vessel wall for Transient 1 at t=650s. The flow patterns are diverted slightly by the incoming cold leg flows in the region between the hot leg obstacles.

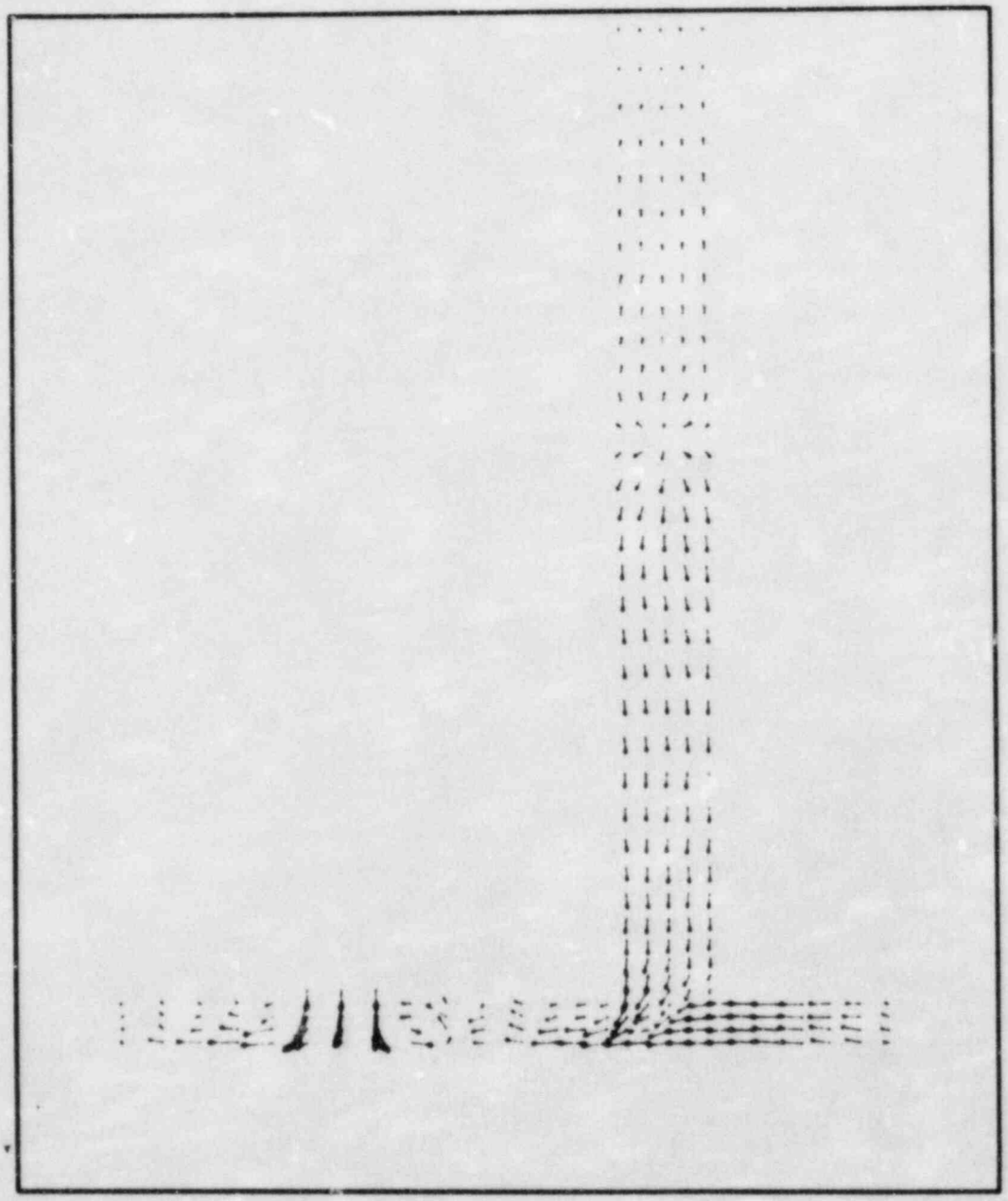

Fig. 11. Velocity vector plot in a horizontal plane through the bottom of the cold legs for Transient 1 at t=650s. The cold water from the bottom of the intact loop cold leg is entrained in the counterclockwise flow circulation in the downcomer and convected to the broken loop side. The blank regions at the left and right in the downcomer are occupied by the hot leg obstacles.

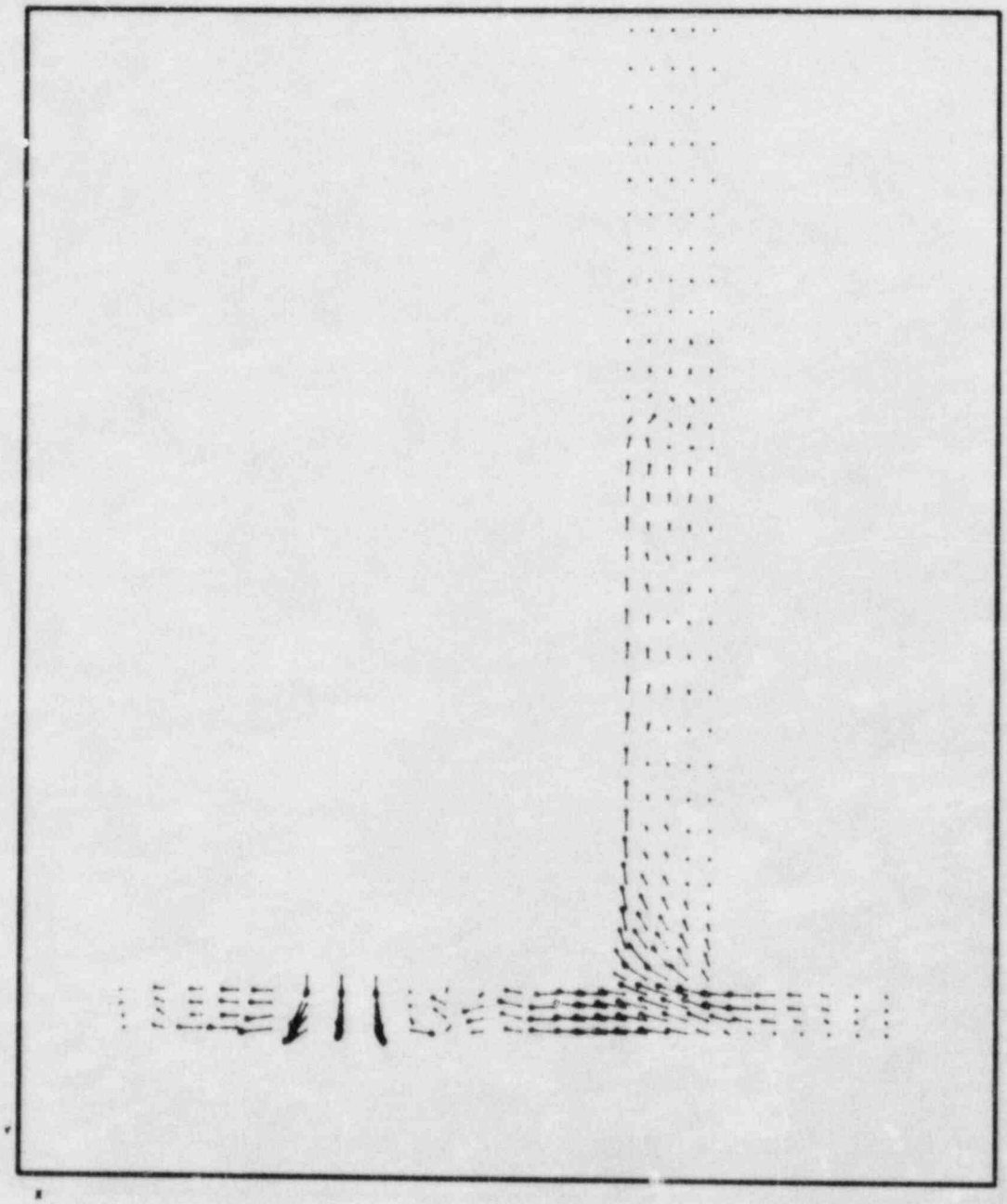

Fig. 12. Velocity vector plot in a horizontal plane through the top of the cold legs for Transient 1 at t=650s. Some of the circulating flow in the downcomer is entrained into the top of the intact loop cold leg.

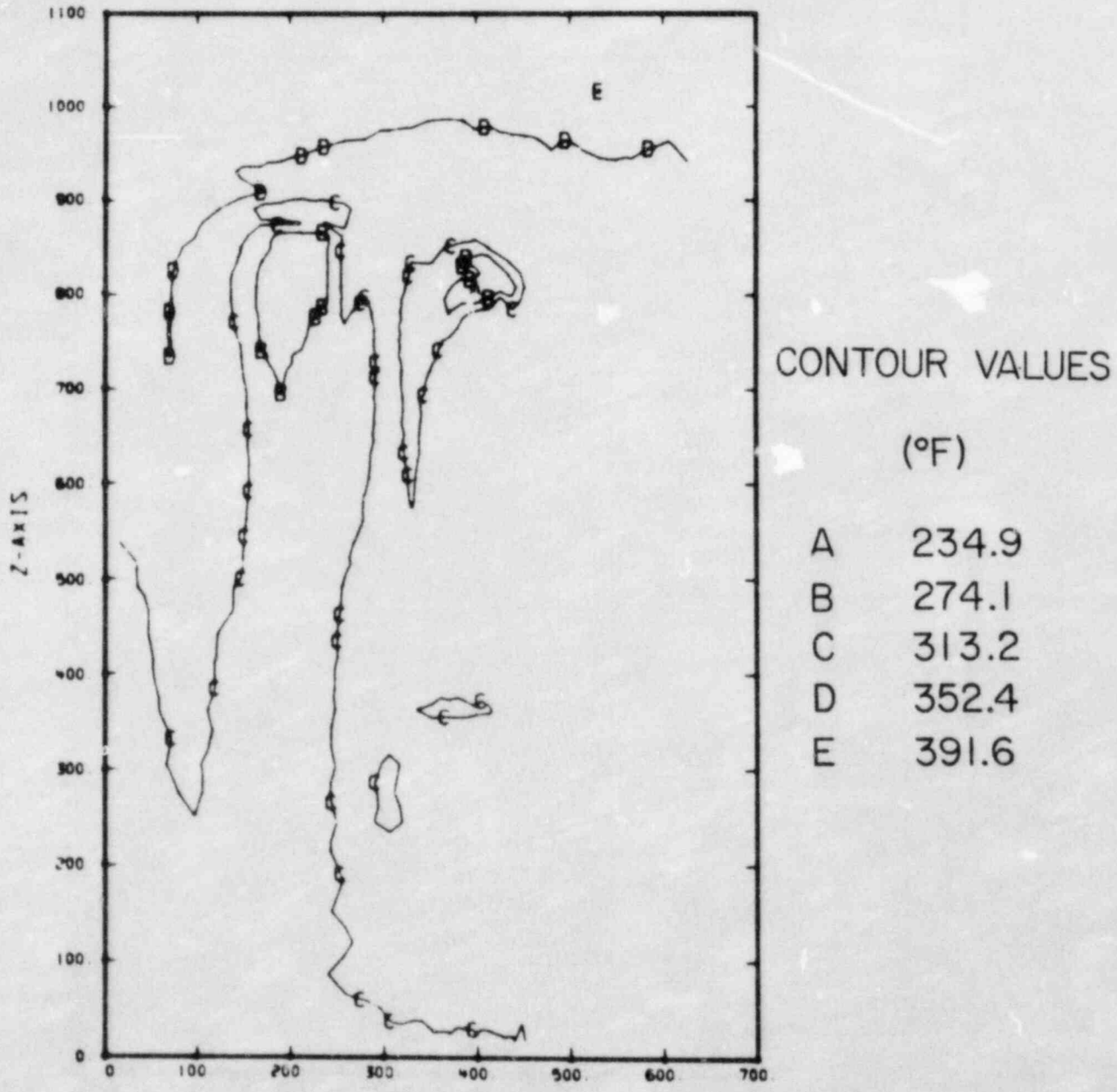

Fig. 13. Temperature contour plot in a vertical plane adjacent to the vessel wall for Transient 1 at t=650s. The contours show a cold fluid region below the broken loop cold leg and a warm region on the right side.

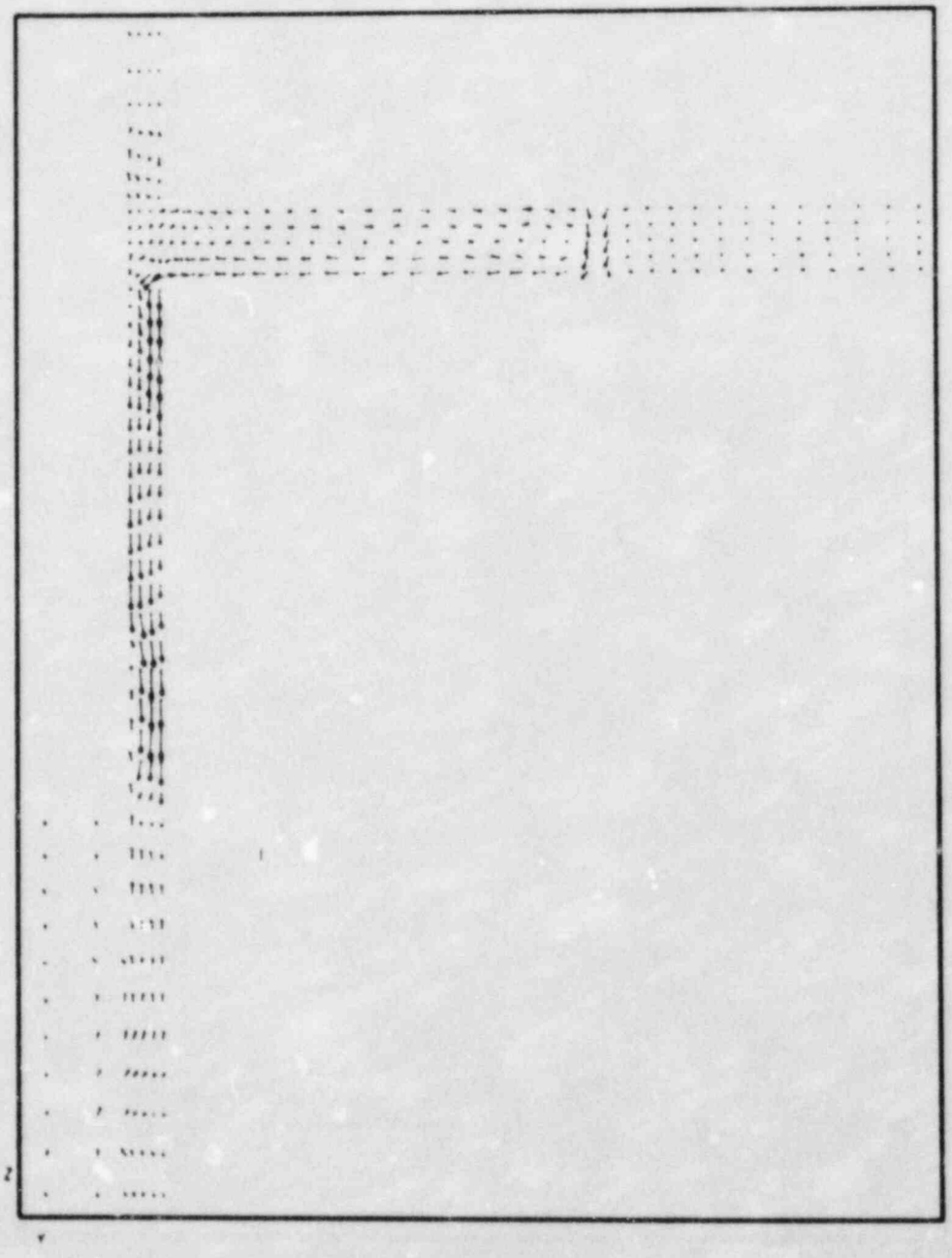

Fig. 14. Velocity vector plot in a vertical plane through the centerline of the intact loop cold leg for Transient 1 at t=850s. At this time, there is downward flow in the downcomer below the cold leg junction.

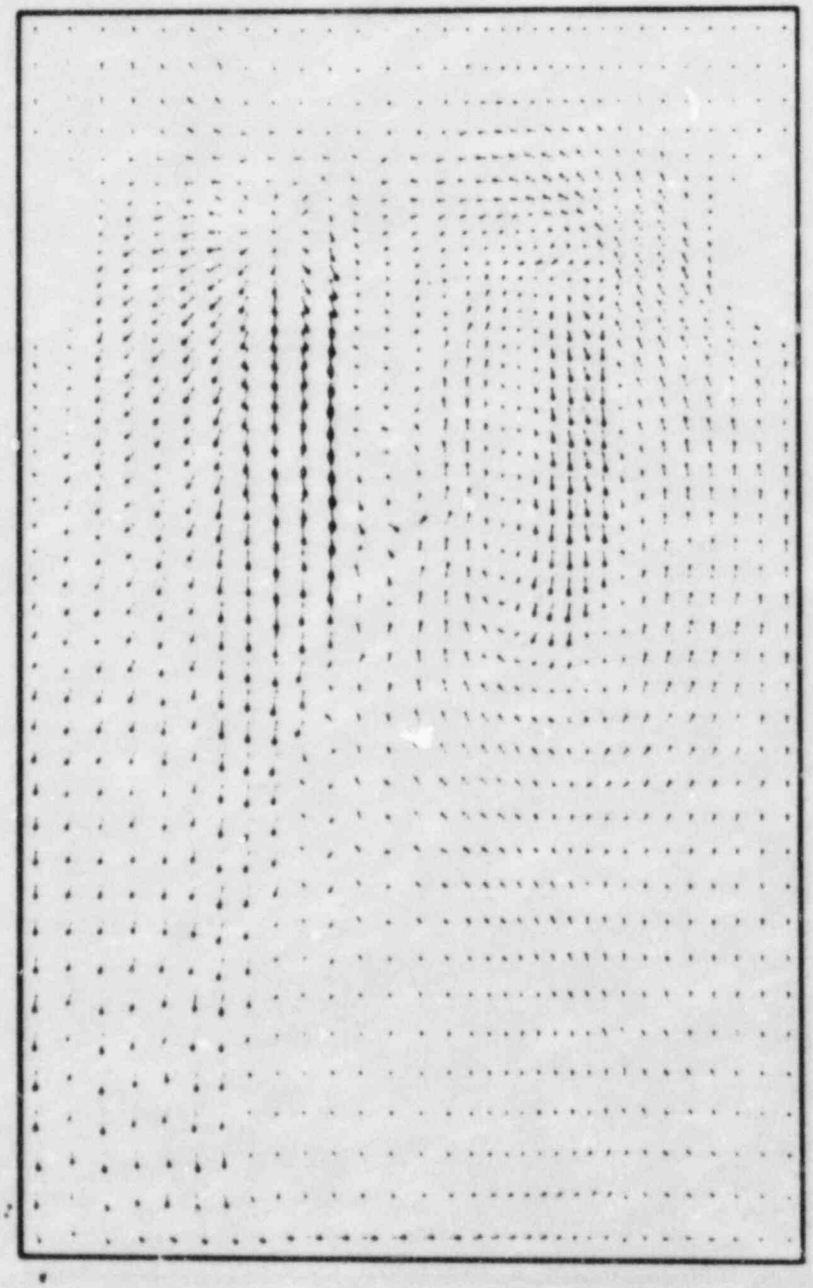

Fig. 15. Velocity vector plot in a vertical plane adjacent to the core barrel wall for Transient 1 at t=850s. There is downward flow beneath the intact loop cold leg at this time in the transient.

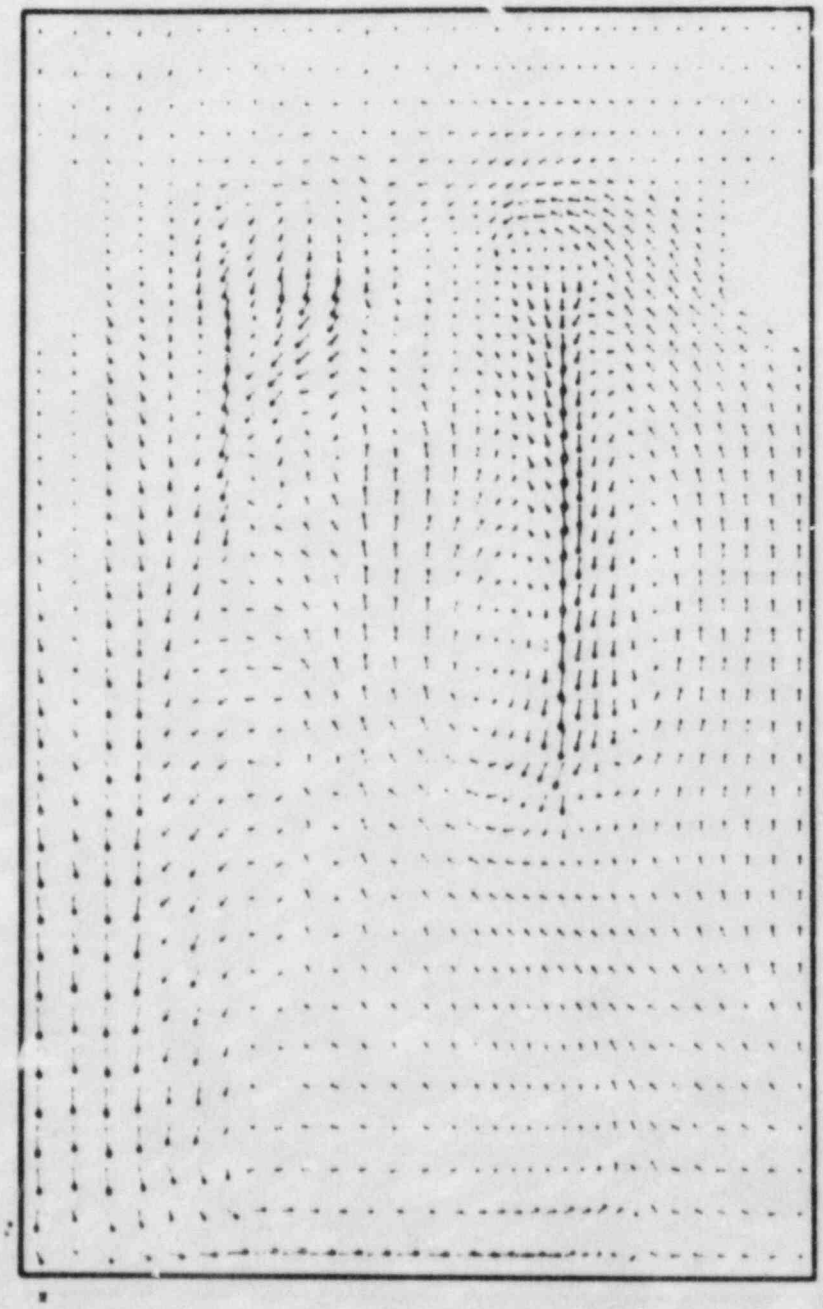

Fig. 16. Velocity vector plot in a vertical plane adjacent to the vessel wall for Transient 1 at t=850s. The cold stream at the bottom of the intact loop cold leg narrows as it falls in the downcomer.

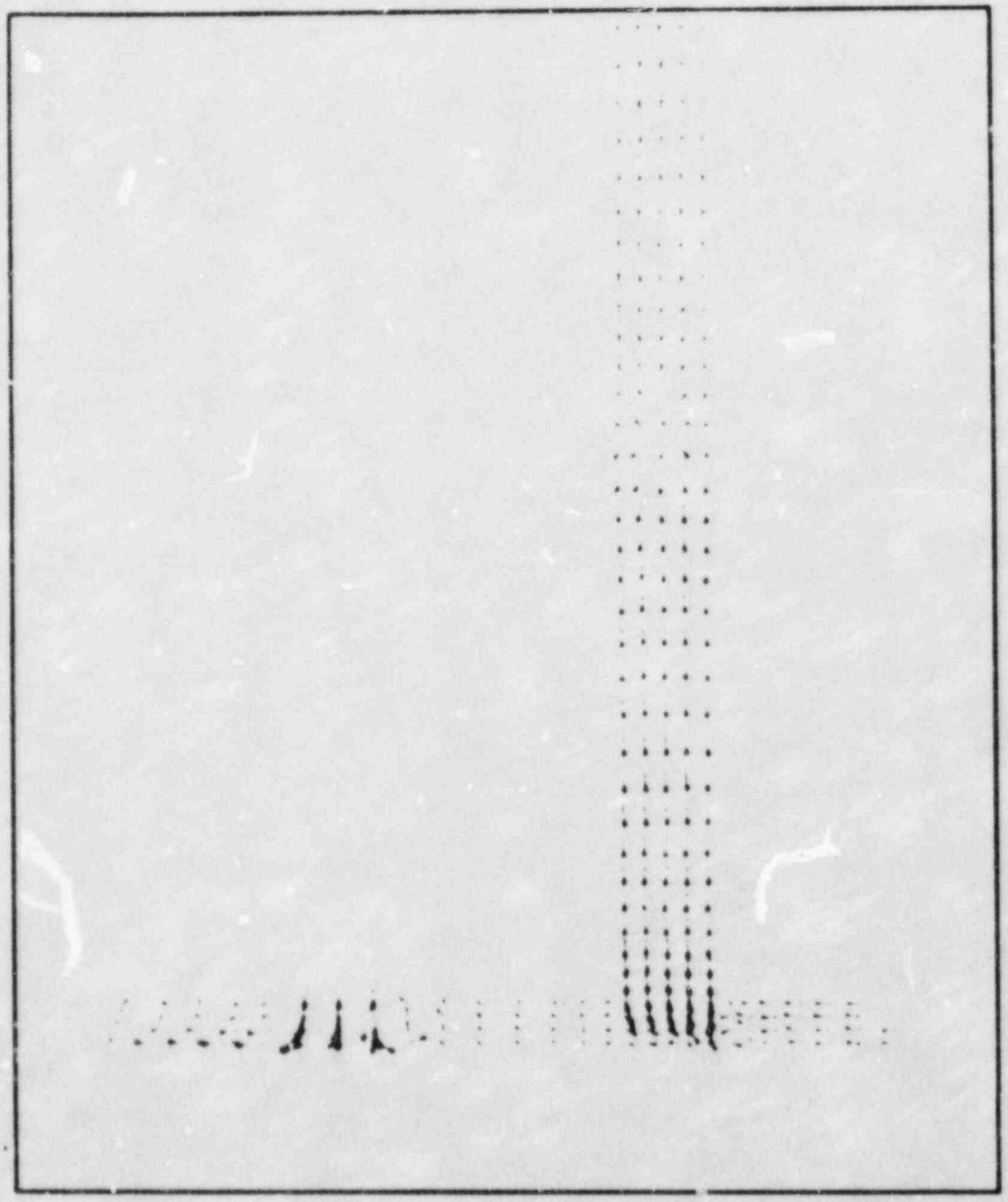

Fig. 17. Velocity vector plot in a horizontal plane through the bottom of the cold legs for Transient 1 at t=850s. The cold layer at the bottom of the intact loop cold leg falls vertically when it reaches the downcomer.

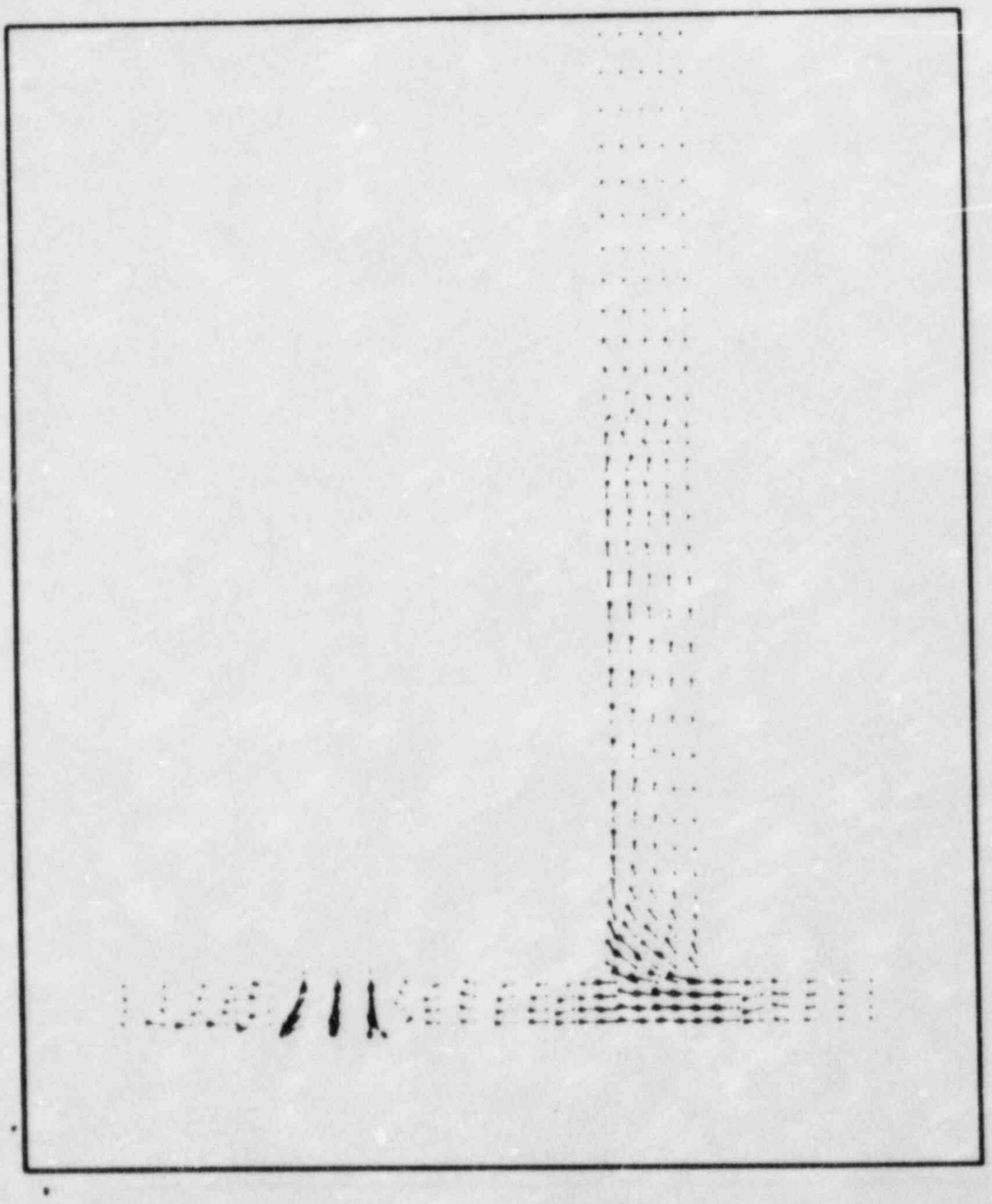

Fig. 18. Velocity vector plot in a horizontal plane through the top of the cold legs for Transient 1 at t=850s. The flow field looks very similar to that of Fig. 12.

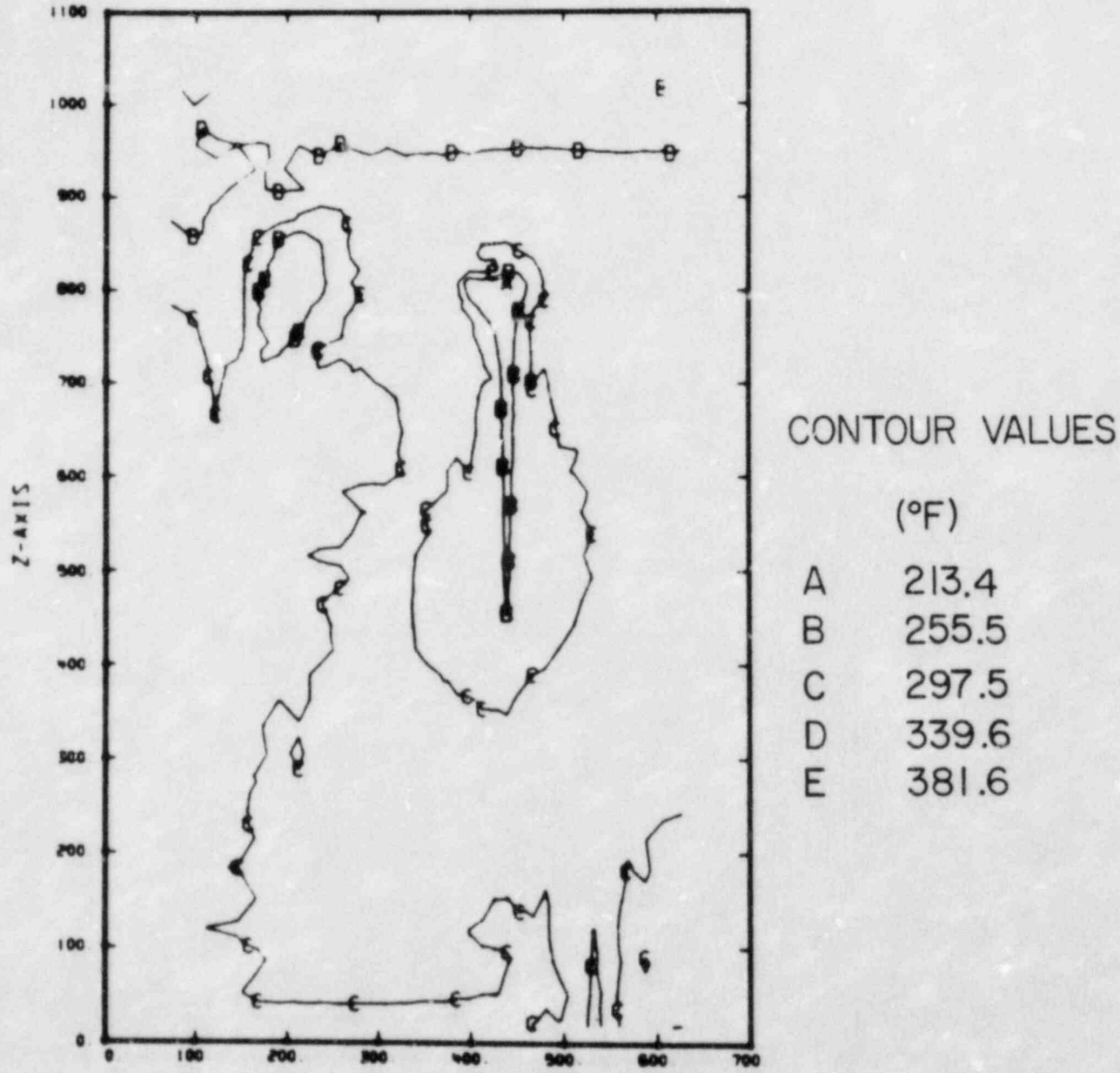

Fig. 19. Temperature contour plot in a vertical plane adjacent to the vessel wall for Transient 1 at t=850s. The cold stream from the stratified layer at the bottom of the intact loop cold leg narrows as it falls in the downcomer.

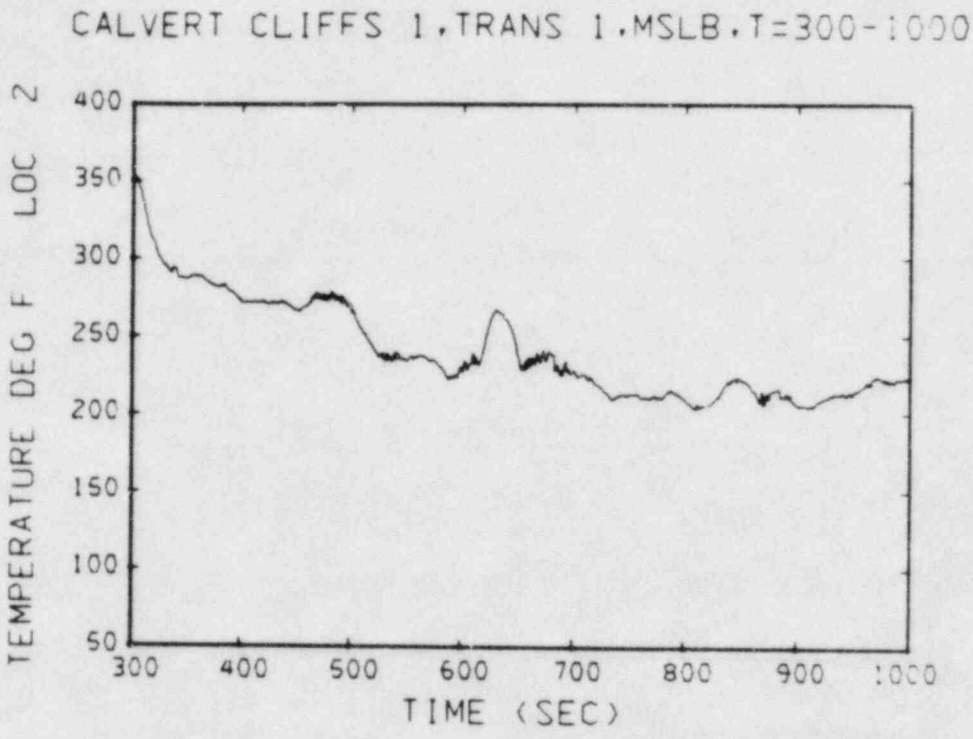

Fig. 20. Transient temperature plot at location 2, Fig. 4.

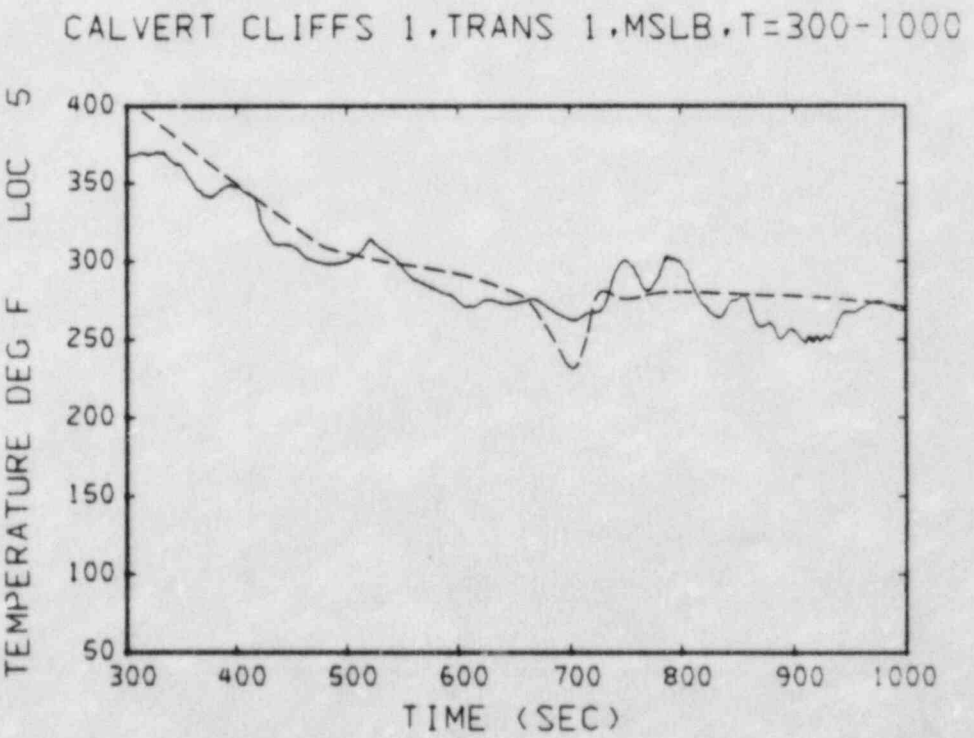

Fig. 21. Transient temperature plot at location 5, Fig. 4. The dashed line shows the TRAC downcomer temperatures (Ref. 3) at approximately the same location.

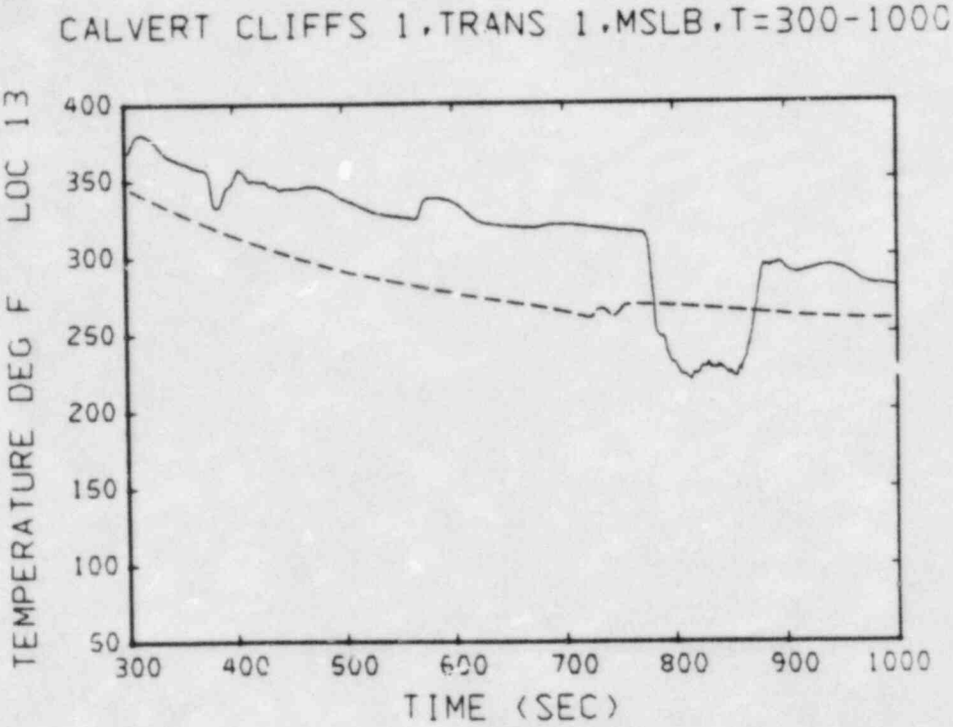

Fig. 22. Transient temperature plot at location 13, Fig. 4. The dashed line shows the TRAC downcomer temperatures (Ref. 3) at approximately the same location.

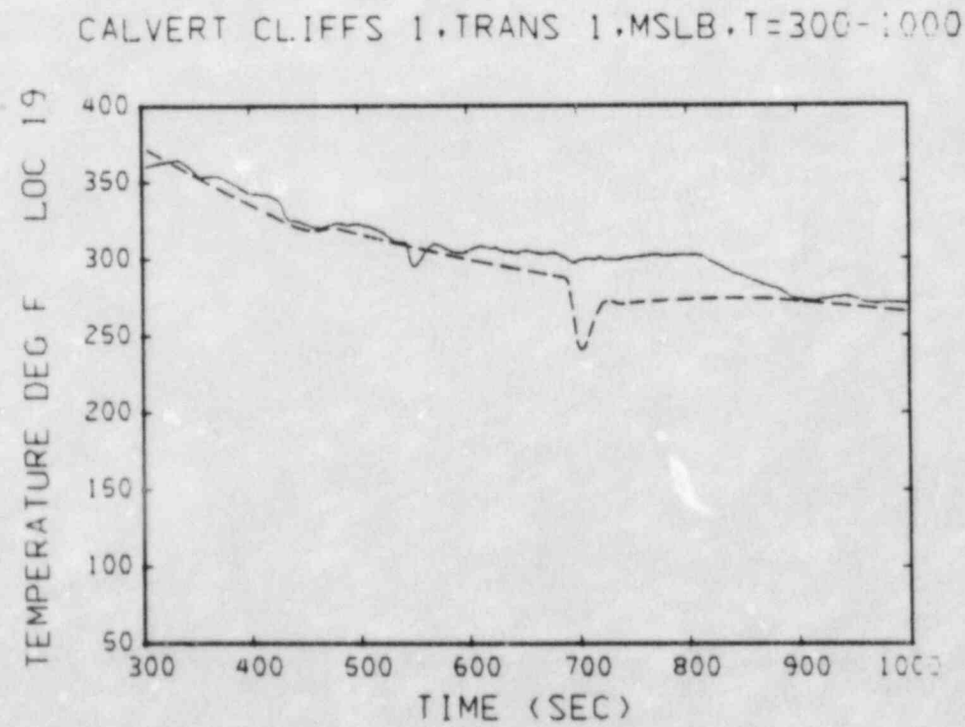

Fig. 23. Transient temperature plot at location 19, Fig. 4. The dashed line shows the TRAC downcomer temperatures (Ref. 3) at approximately the same location.

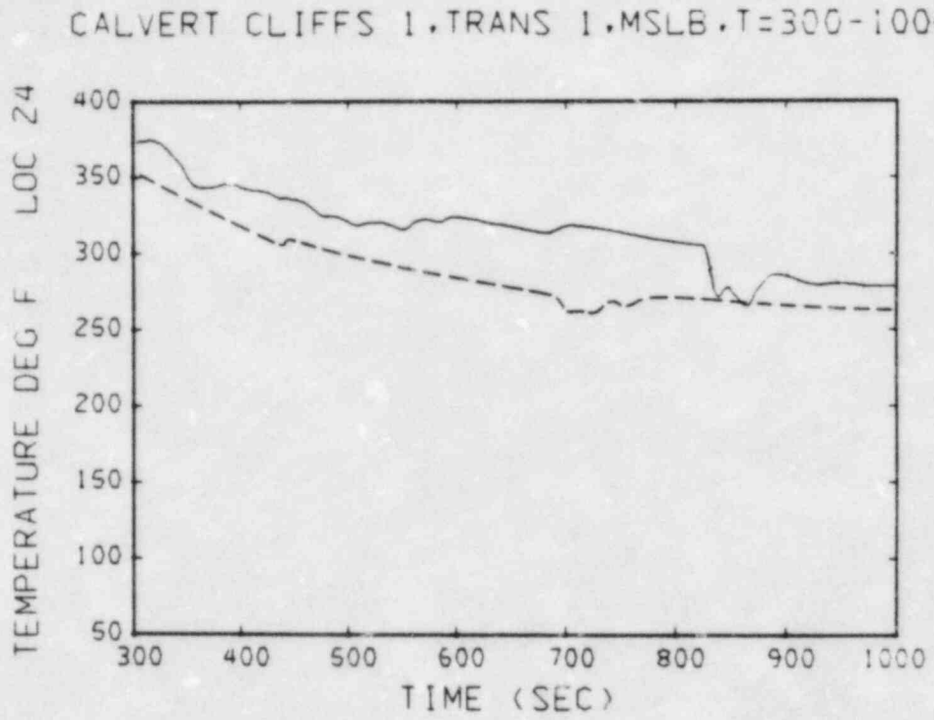

Fig. 24. Transient temperature plot at location 24, Fig. 4. The dashed line shows the TRAC downcomer temperatures (Ref. 3) at approximately the same location.

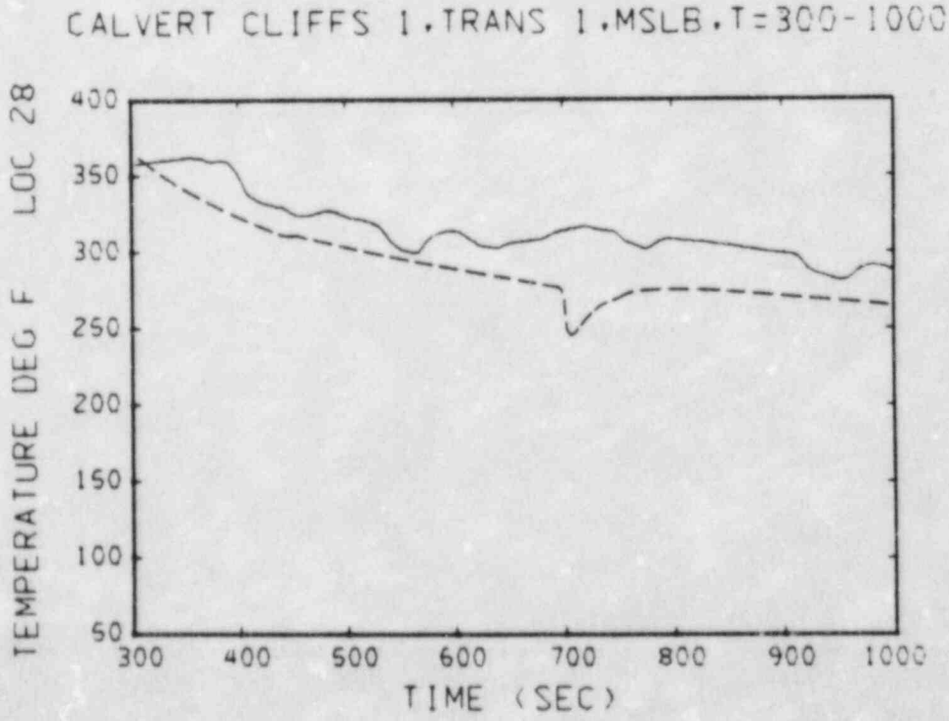

Fig. 25. Transient temperature plot at location 28, Fig. 4. The dashed line shows the TRAC downcomer temperatures (Ref. 3) at approximately the same location.

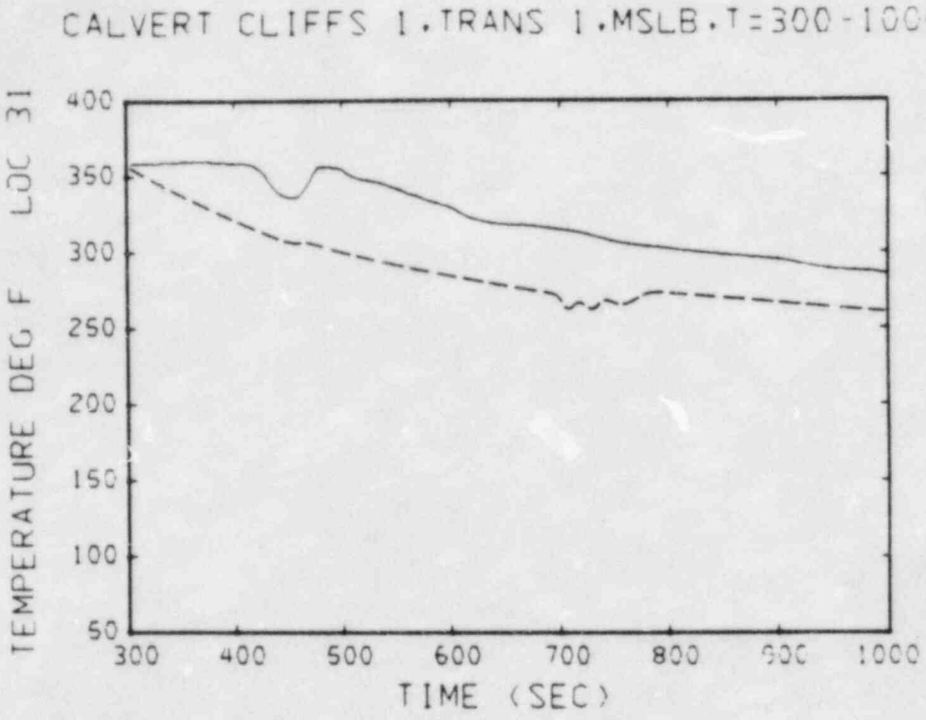

Fig. 26. Transient temperature plot at location 31, Fig. 4. The dashed line shows the TRAC downcomer temperatures (Ref. 3) at approximately the same location.

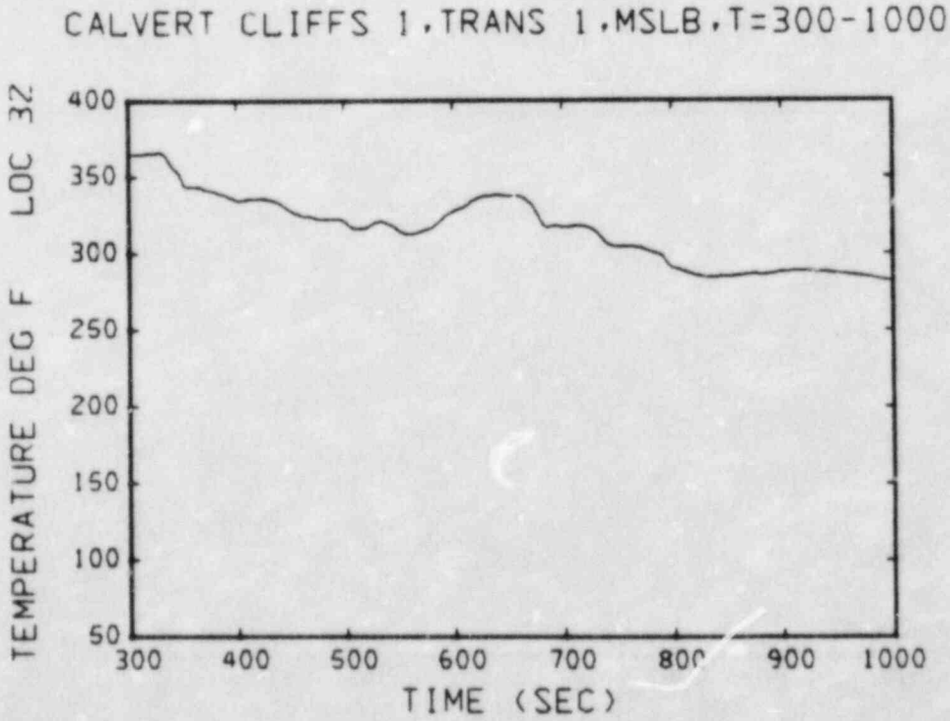

Fig. 27. Transient temperature plot at location 32, Fig. 4.

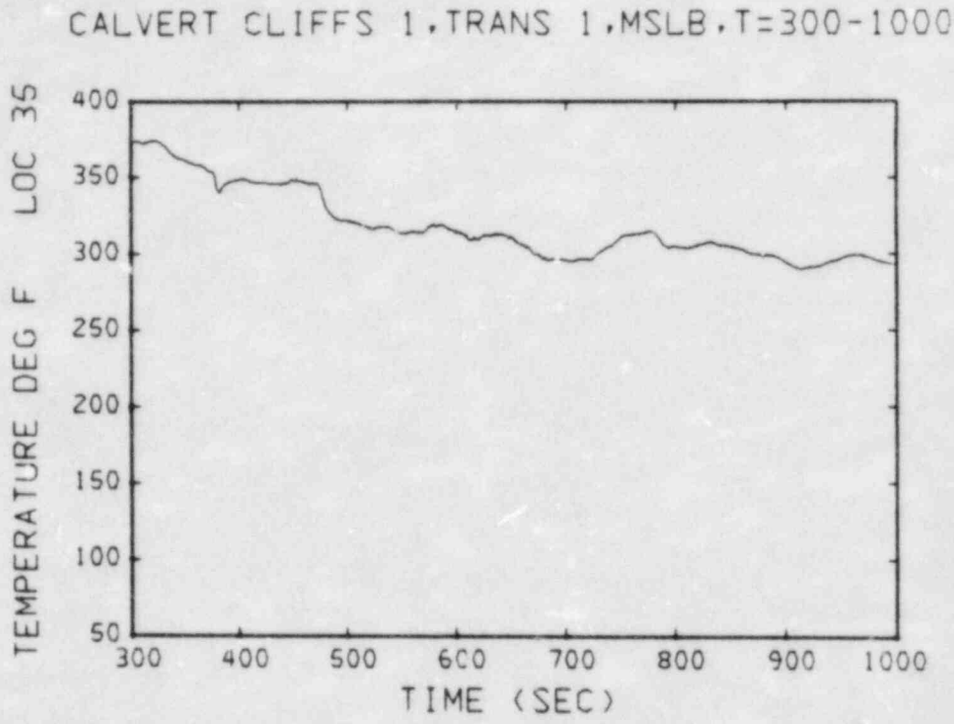

Fig. 28. Transient temperature plot at location 35, Fig. 4.

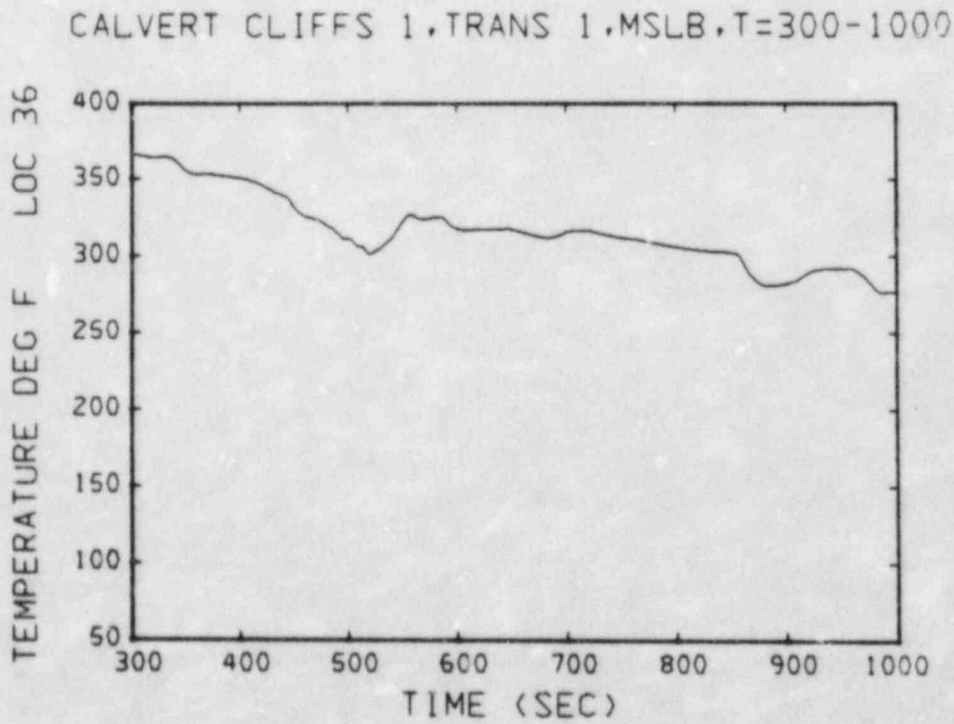

Fig. 29. Transient temperature plot at location 36, Fig. 4.

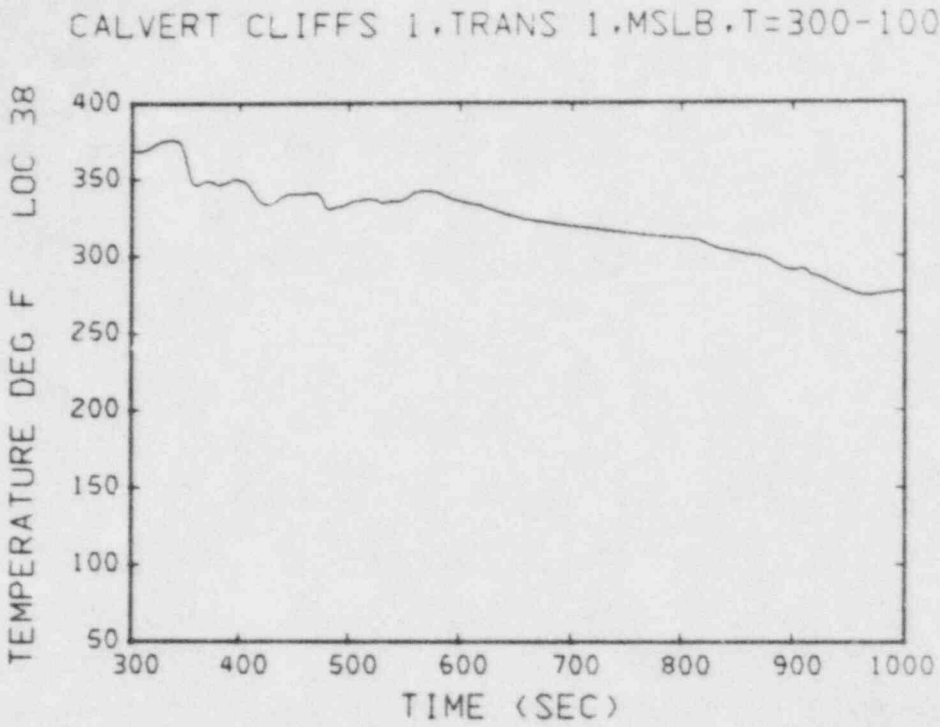

Fig. 30. Transient temperature plot at location 38, Fig. 4.

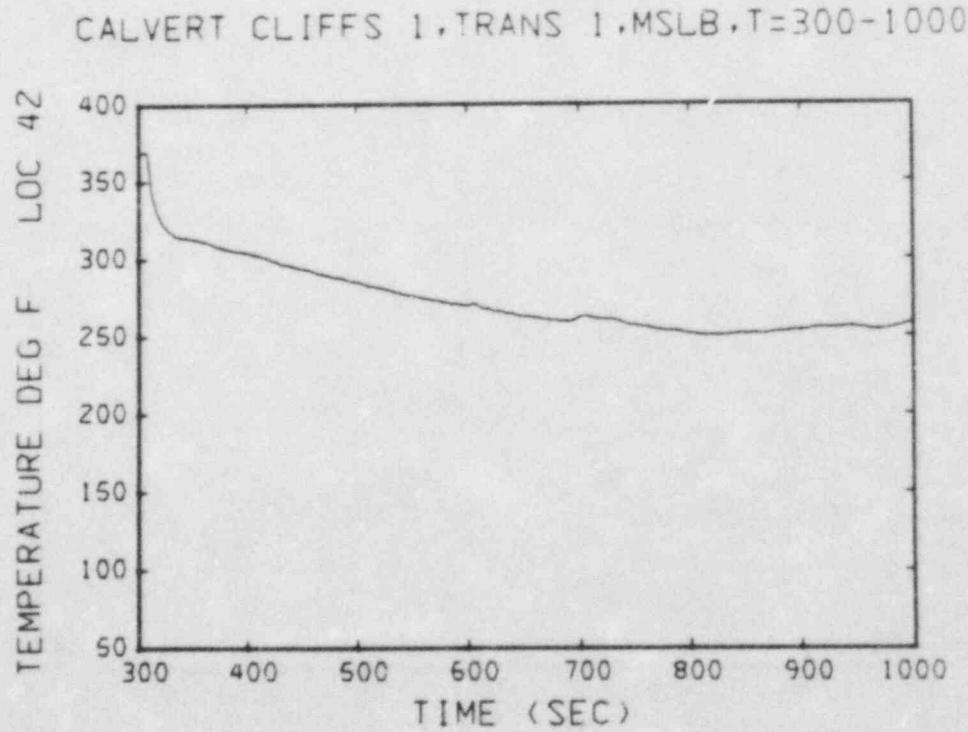

Fig. 31. Transient temperature plot at location 42, Fig. 5.

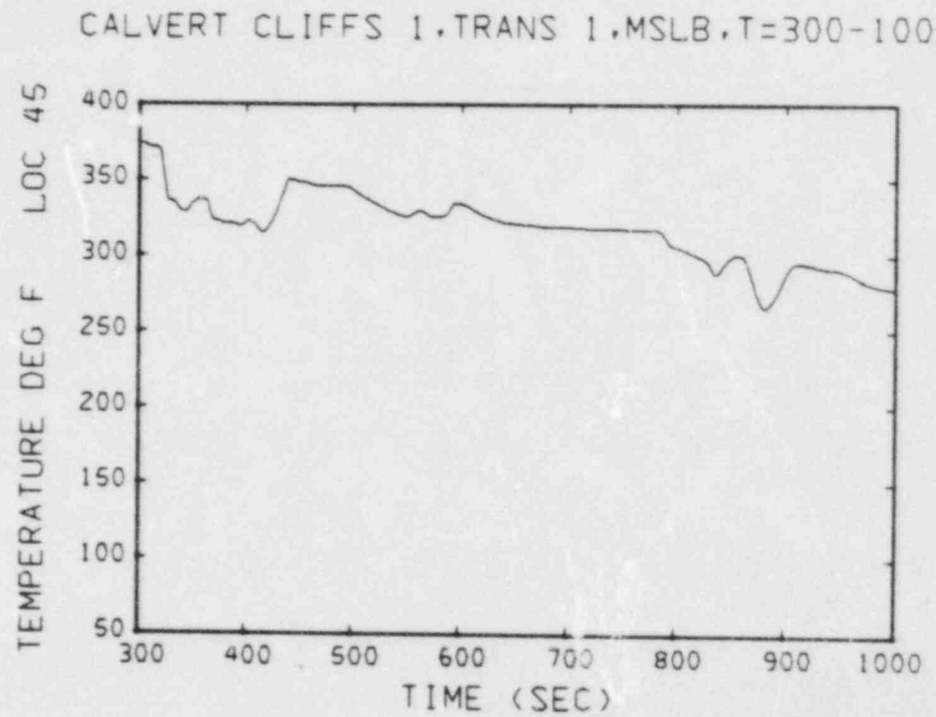

Fig. 32. Transient temperature plot at location 45, Fig. 5.

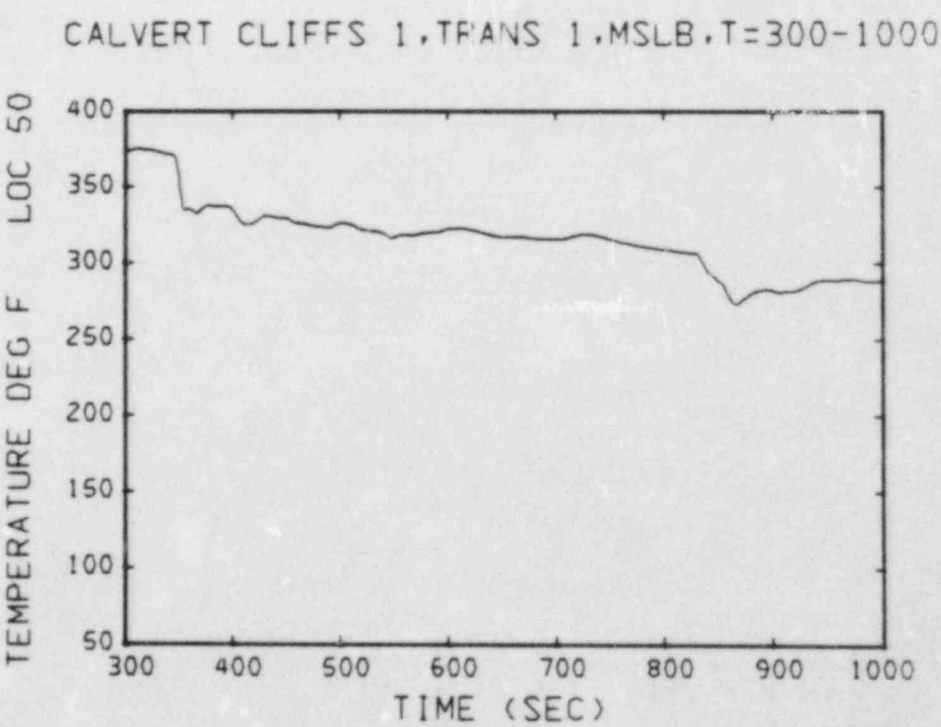

Fig. 33. Transient temperature plot at location 50, Fig. 5.

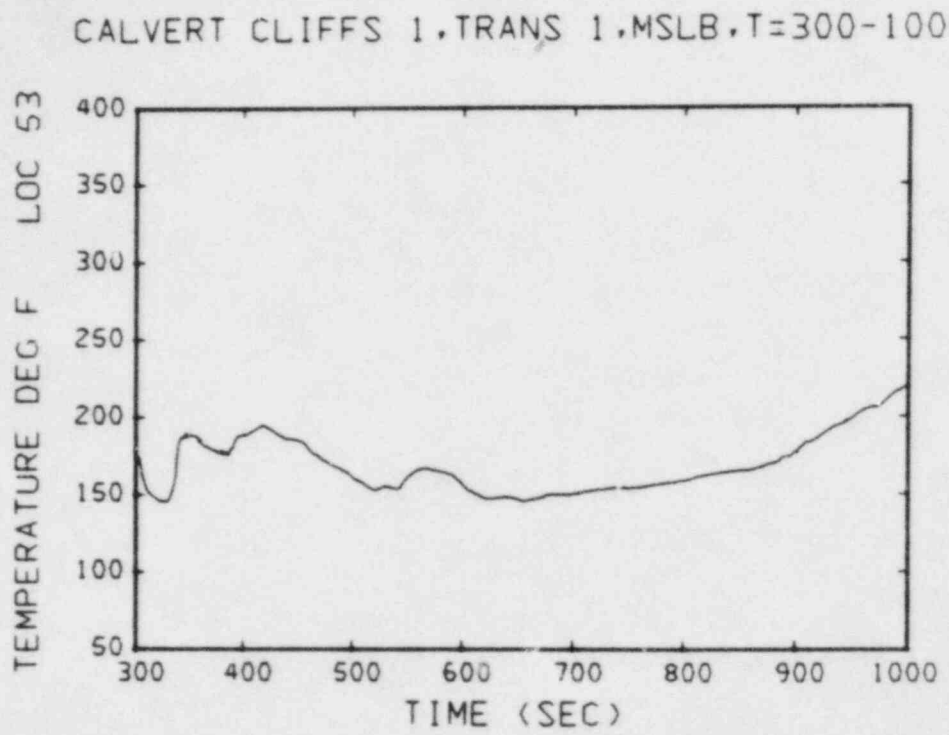

Fig. 34. Transient temperature plot at location 53, Fig. 6.

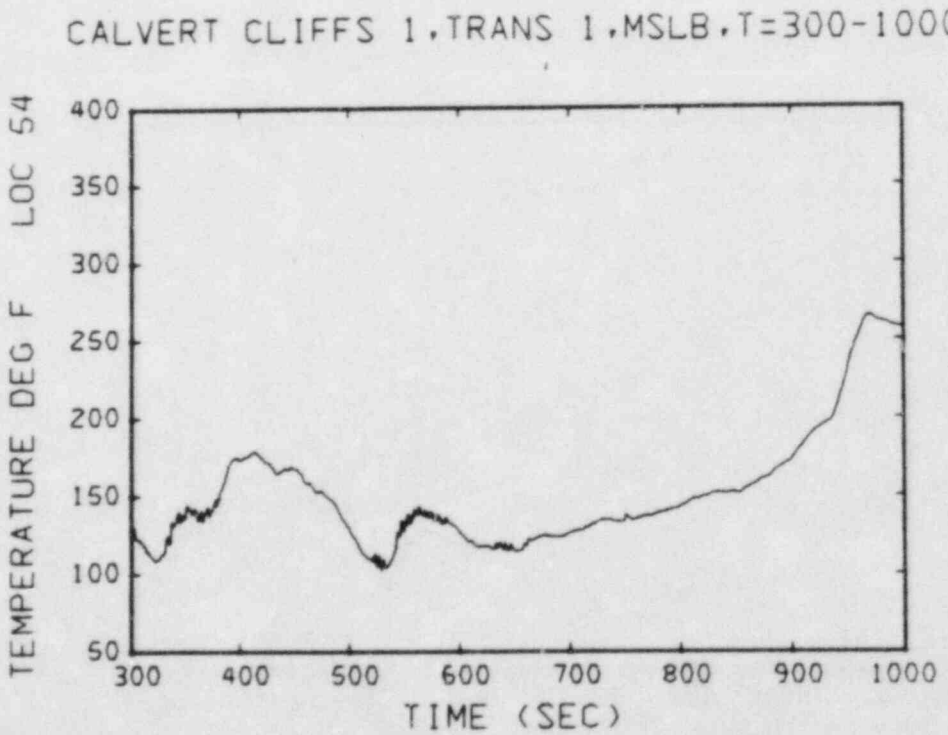

Fig. 35. Transient temperature plot at location 54, Fig. 6.

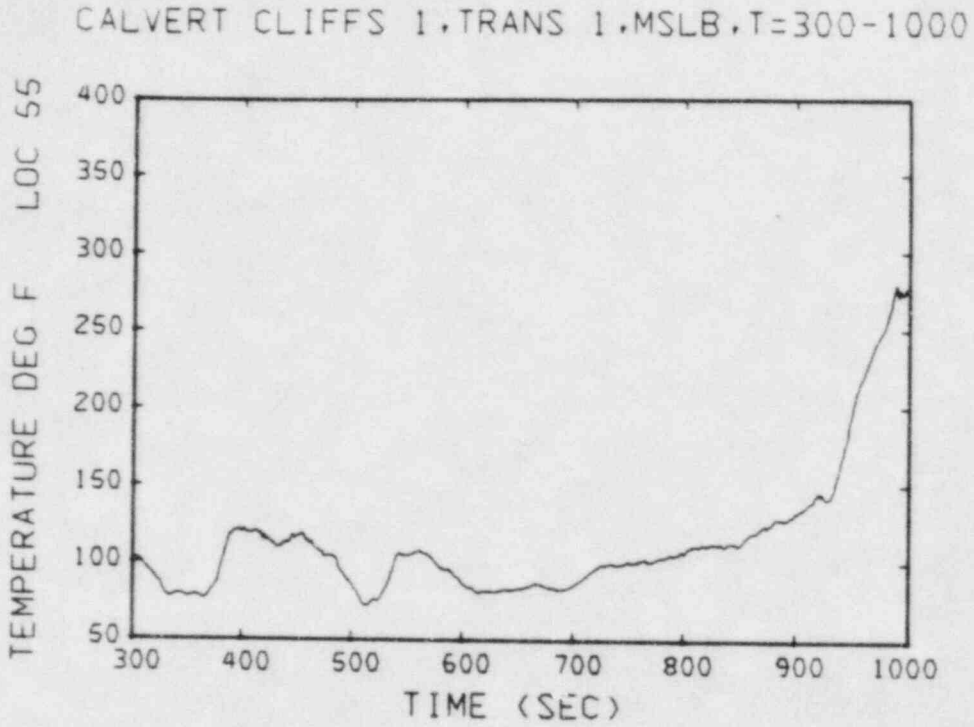

Fig. 36. Transient temperature plot at location 55, Fig. 6.

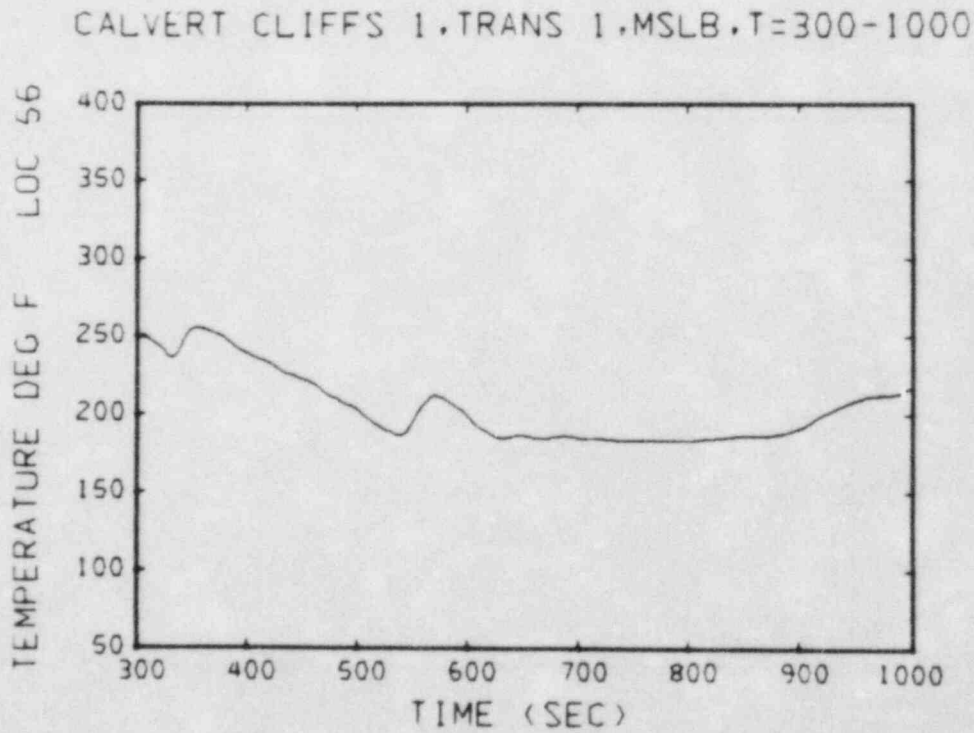

Fig. 37. Transient temperature plot at location 56, Fig. 6.

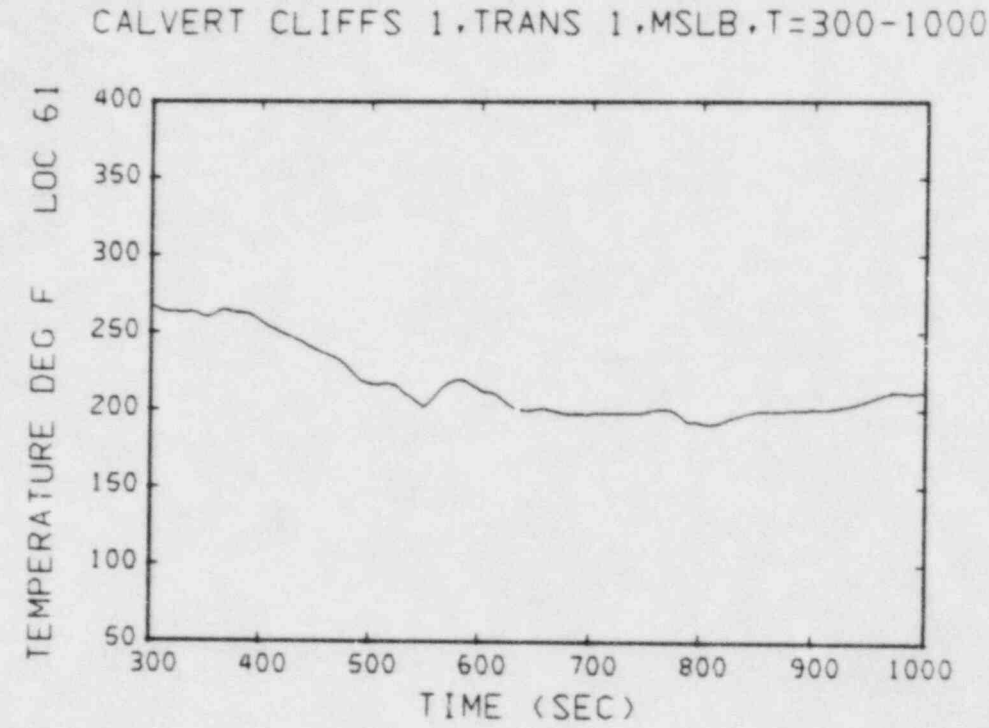

Fig. 38. Transient temperature plot at location 61, Fig. 6.

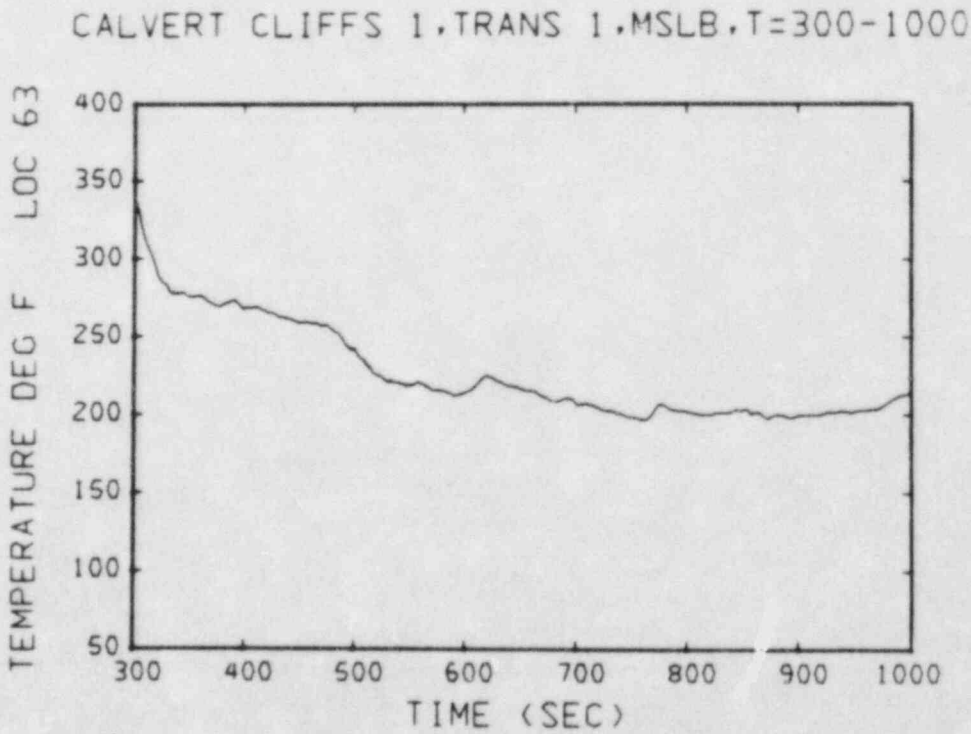

Fig. 39. Transient temperature plot at location 63, Fig. 6.

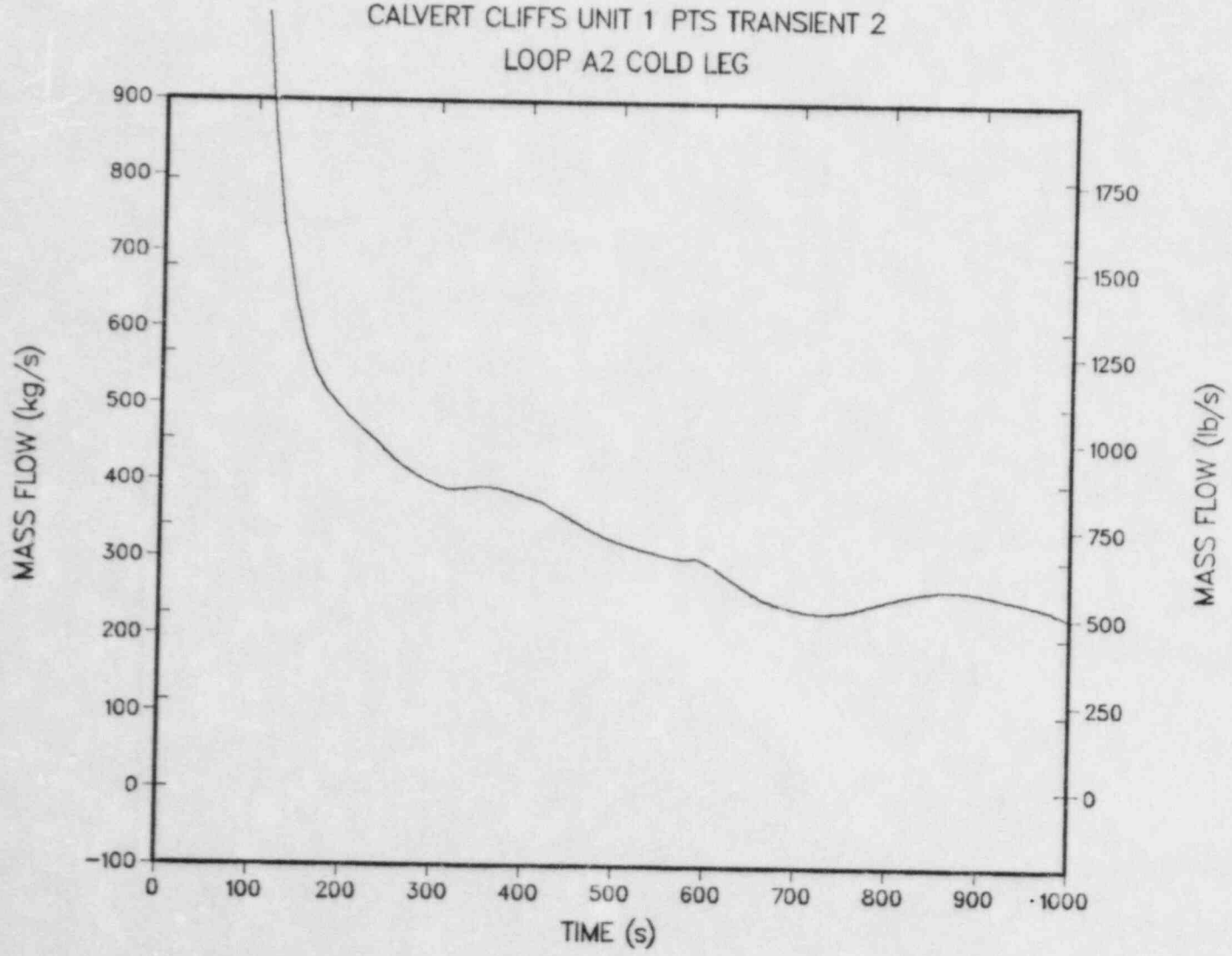

Fig. 40. Mass flow rate into the broken loop cold leg, from the TRAC calculation of Transient 2.

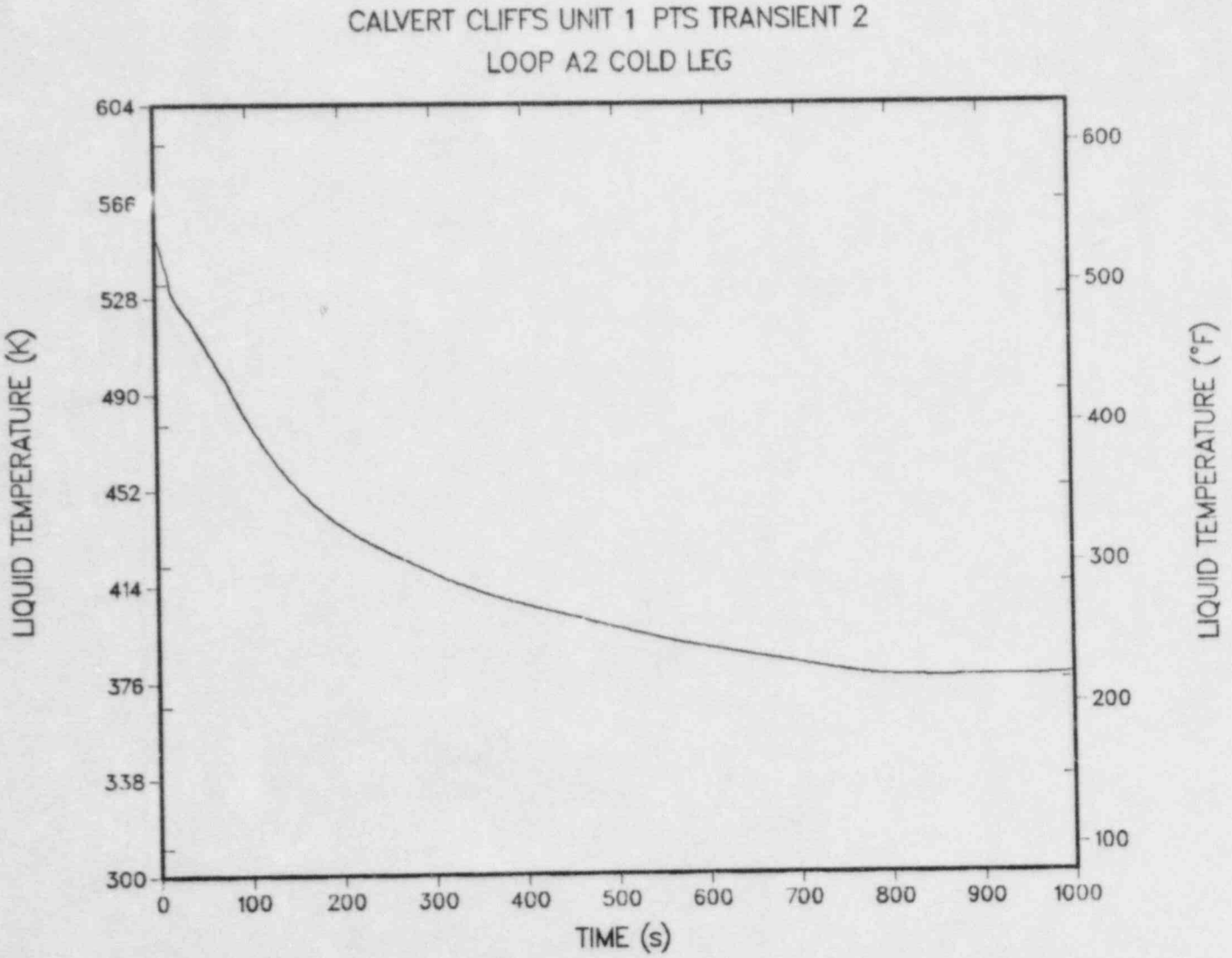

Fig. 41. Temperature of fluid flowing into the broken loop cold leg, from the TRAC calculation of Transient 2.

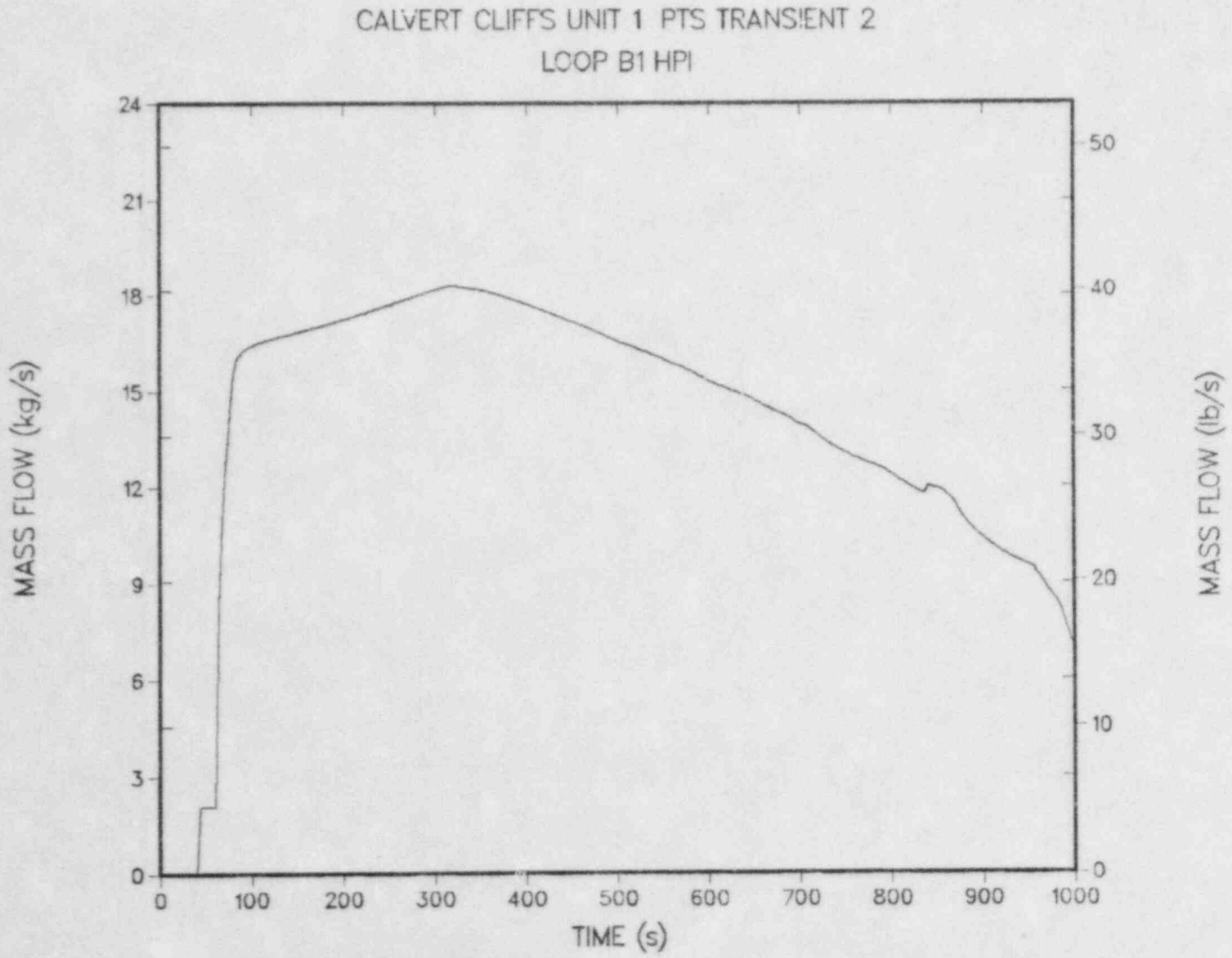

Fig. 42. One-fourth of the total safety injection and charging flow rates, from the TRAC calculation of Transient 2.

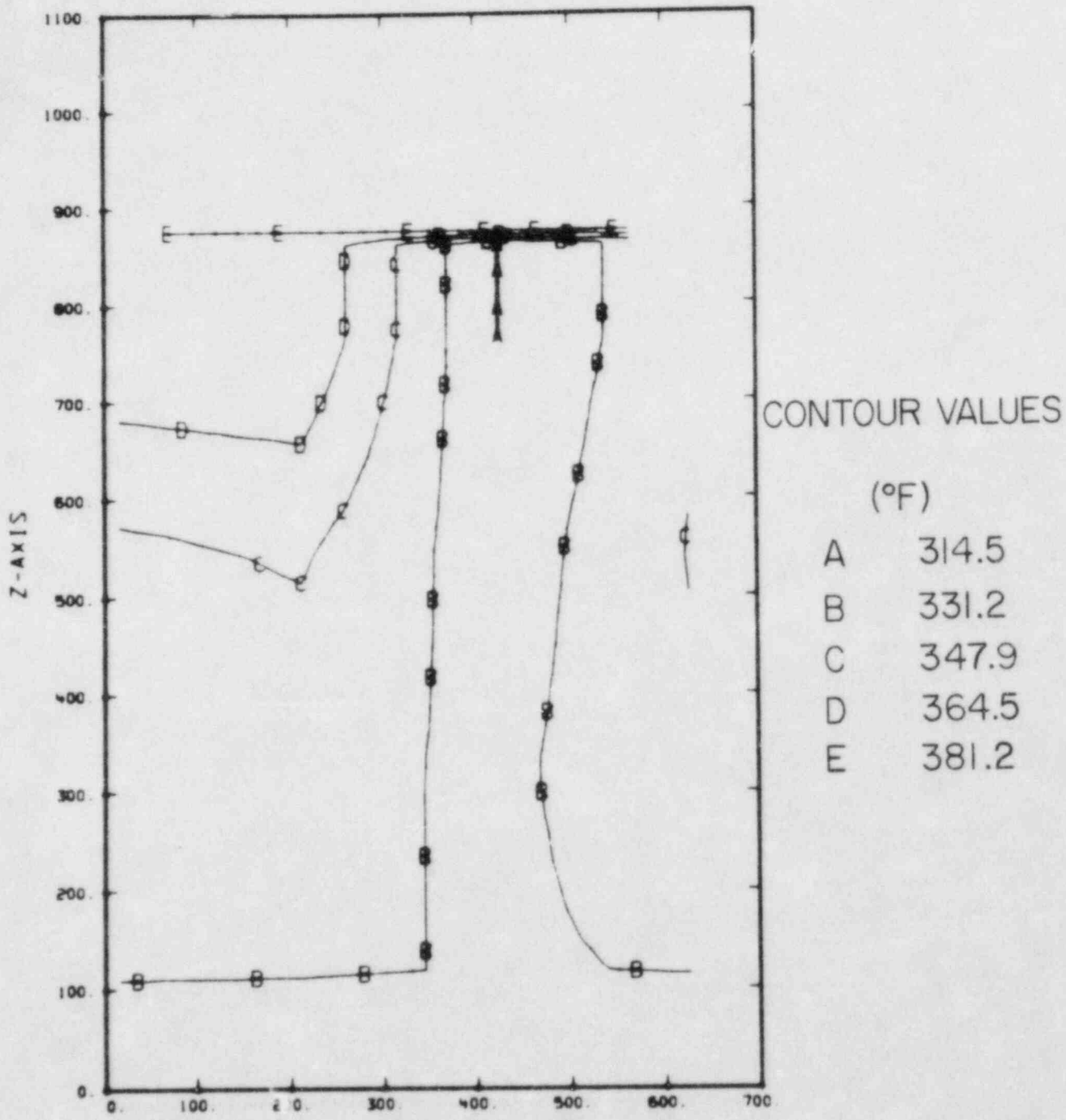

Fig. 43. Downcomer temperature distribution at t=300s from the TRAC calculation of Transient 2.

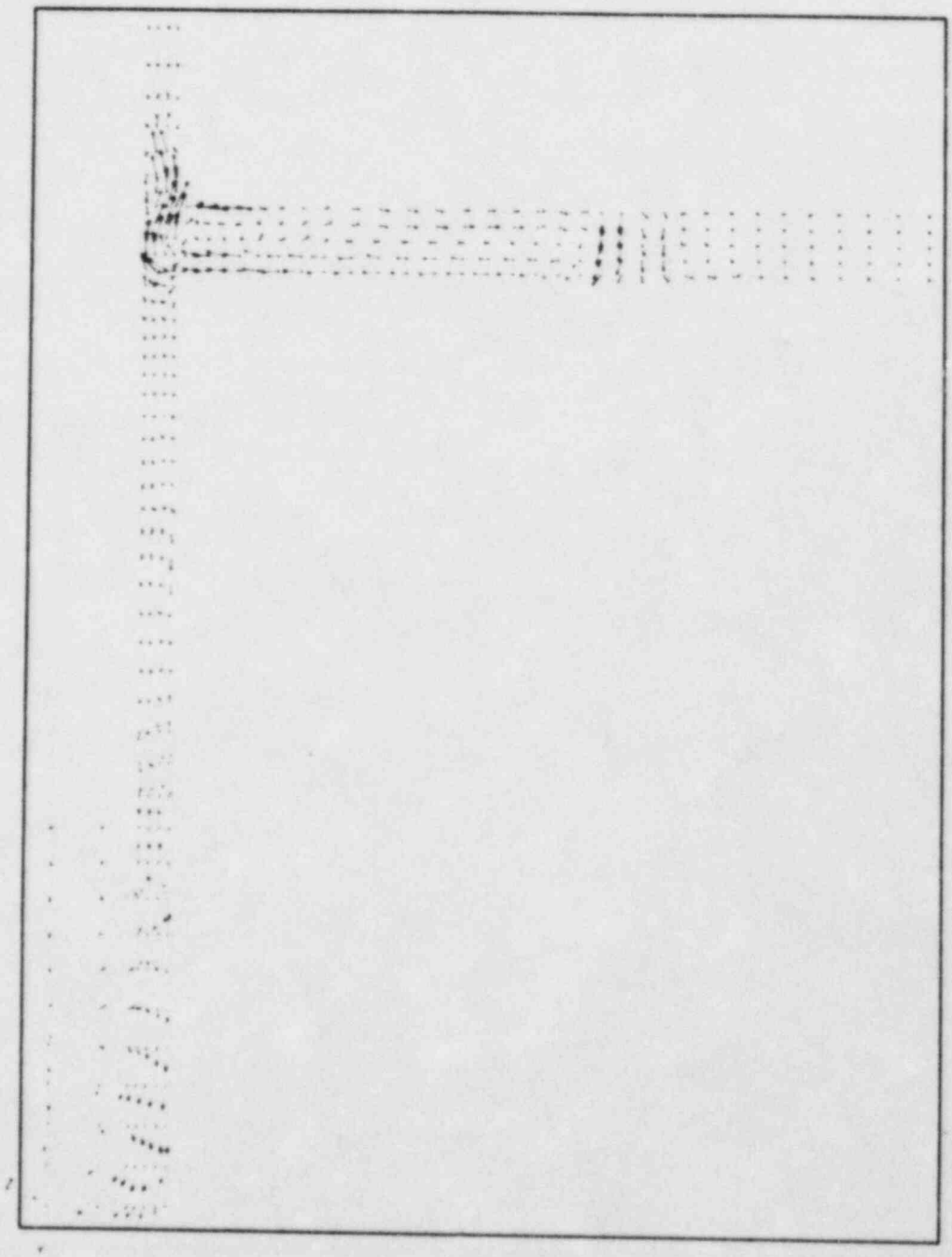

Fig. 44. Velocity vector plot in a vertical plane through the centerline of the intact loop cold leg for Transient 2 at t=800s. The cold water exiting from this cold leg is carried upward and azimuthally toward the broken loop side by the strong circulating flow in the downcomer.

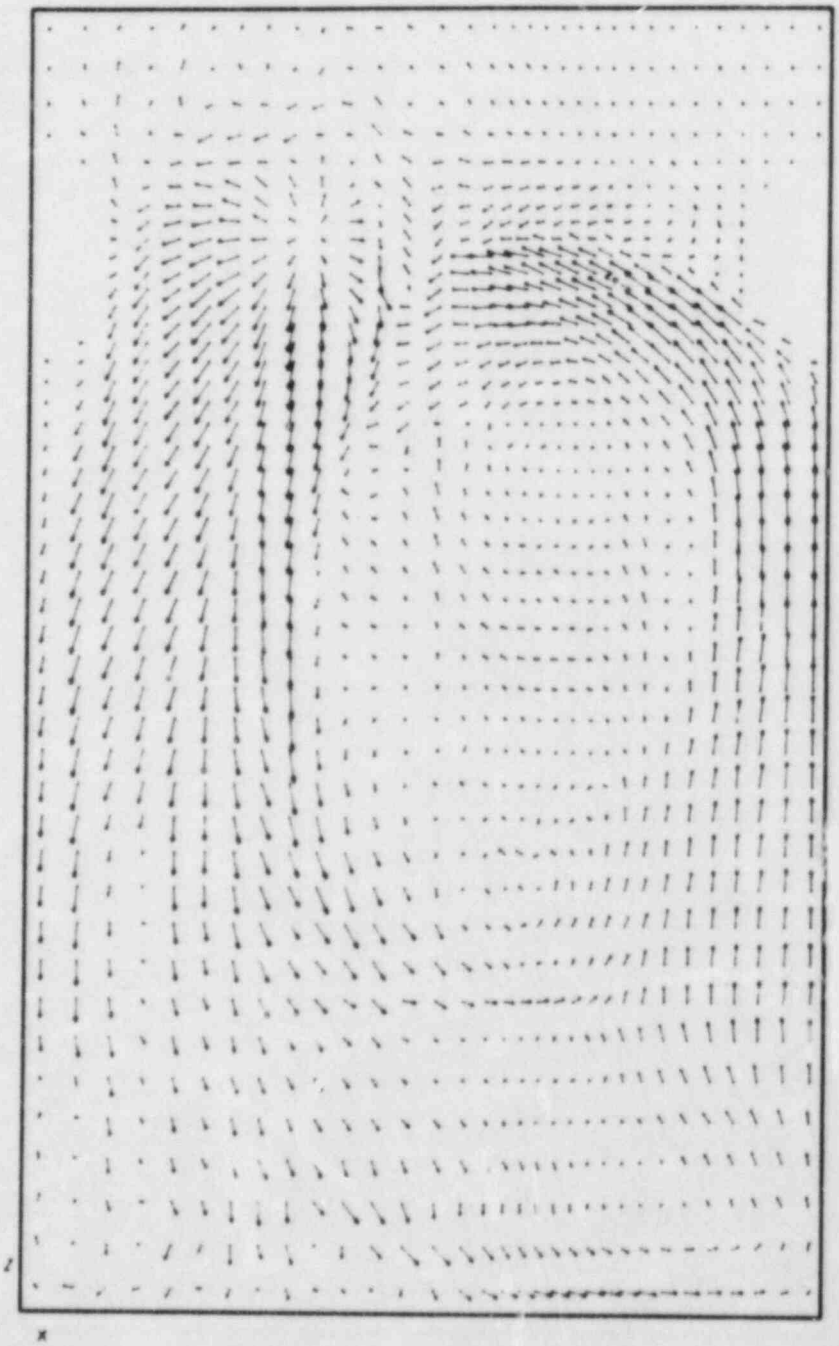

Fig. 45. Velocity vector plot in a vertical plane adjacent to the core barrel wall for Transient 2 at t=800s. Note the region of impact of the broken loop cold leg flow at the upper left. The strong circulating flow in the downcomer diverts the flow from the intact loop cold leg before it impacts on the core barrel.

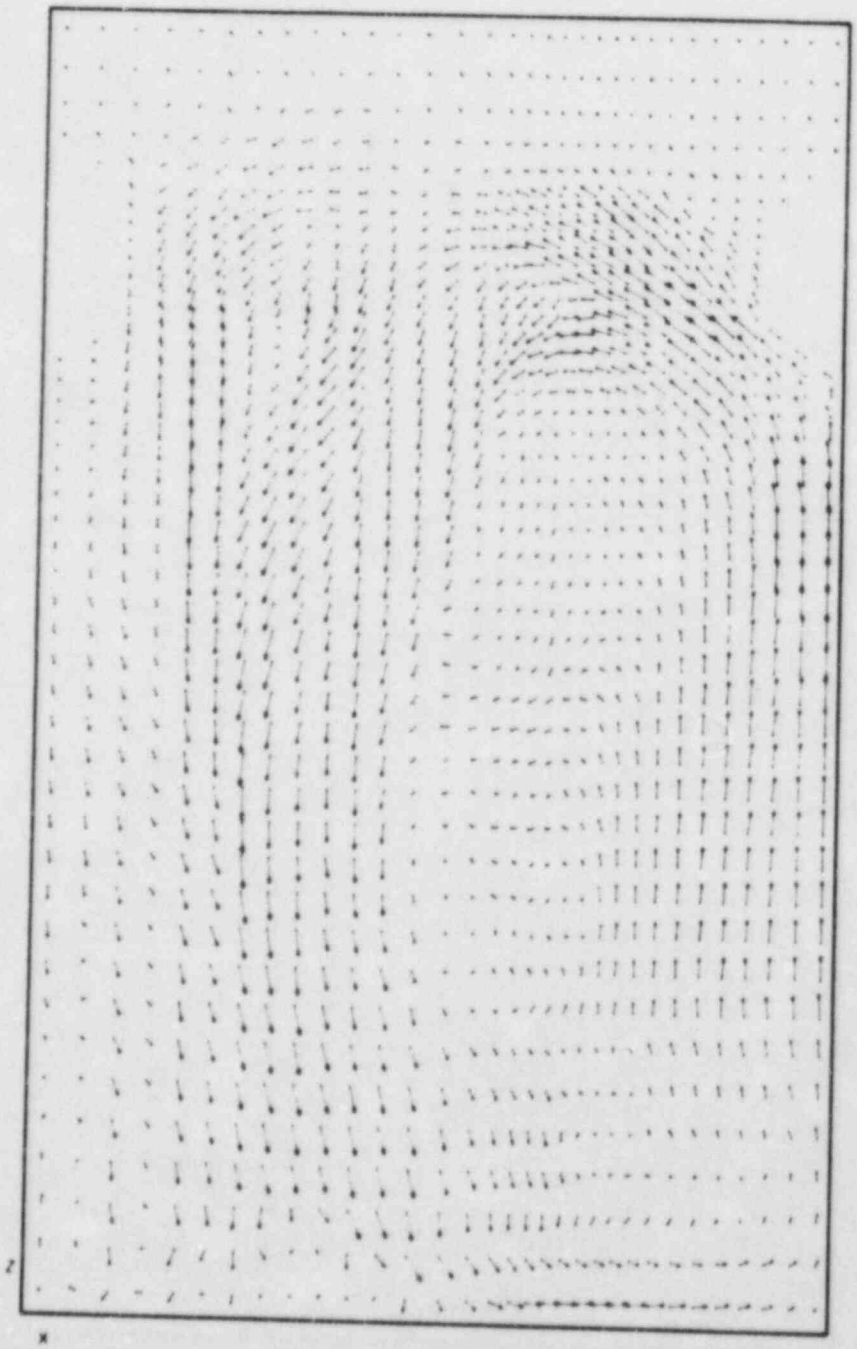

Fig. 46. Velocity vector plot in a vertical plane adjacent to the vessel wall for Transient 2 at t=800s. The circulating flow in the downcomer carries cold water from the intact loop cold leg to the broken loop side.

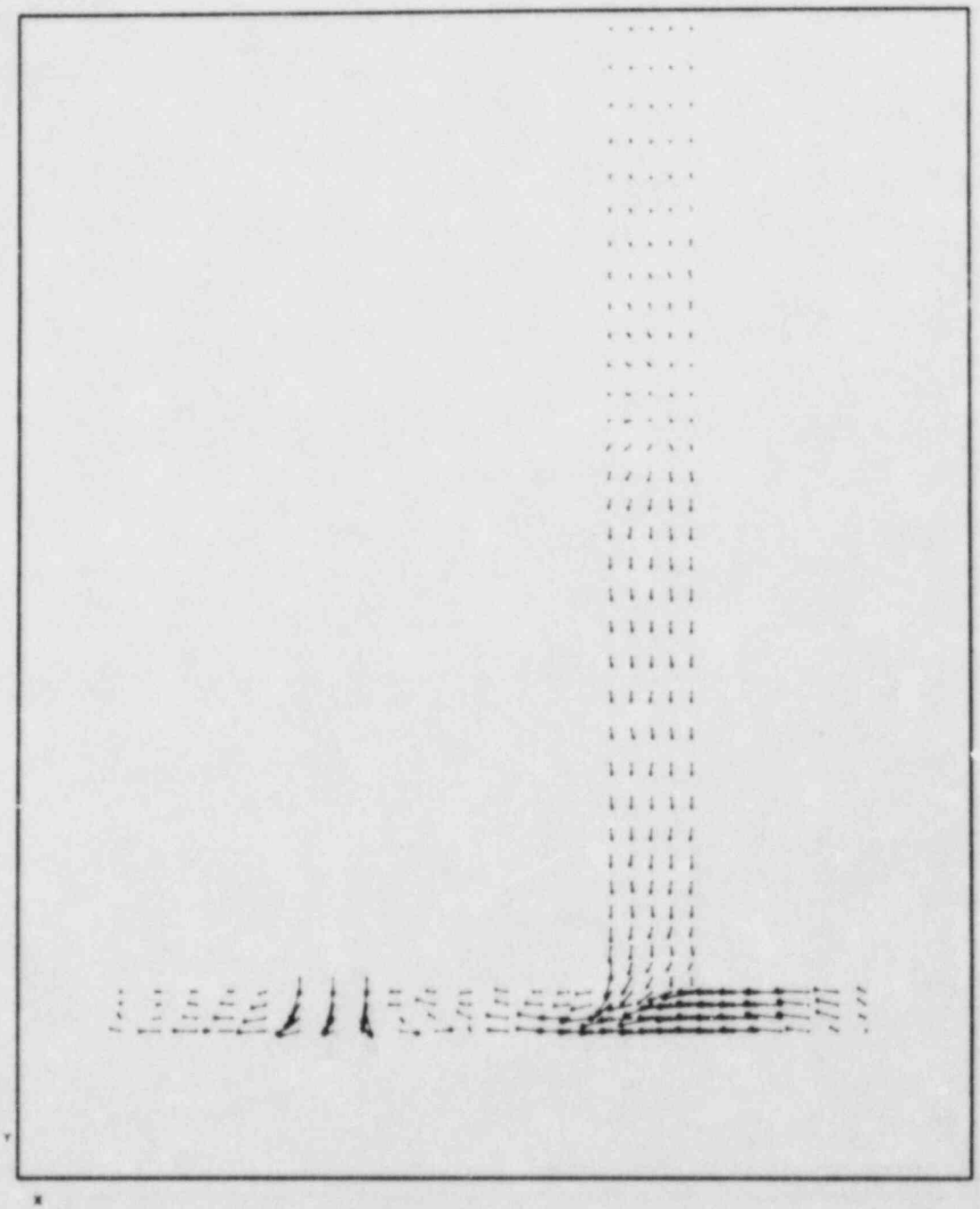

Fig. 47. Velocity vector plot in a horizontal plane through the bottom of the cold legs for Transient 2 at t=800s. The strong downcomer circulation diverts the flow from both cold legs to the left.

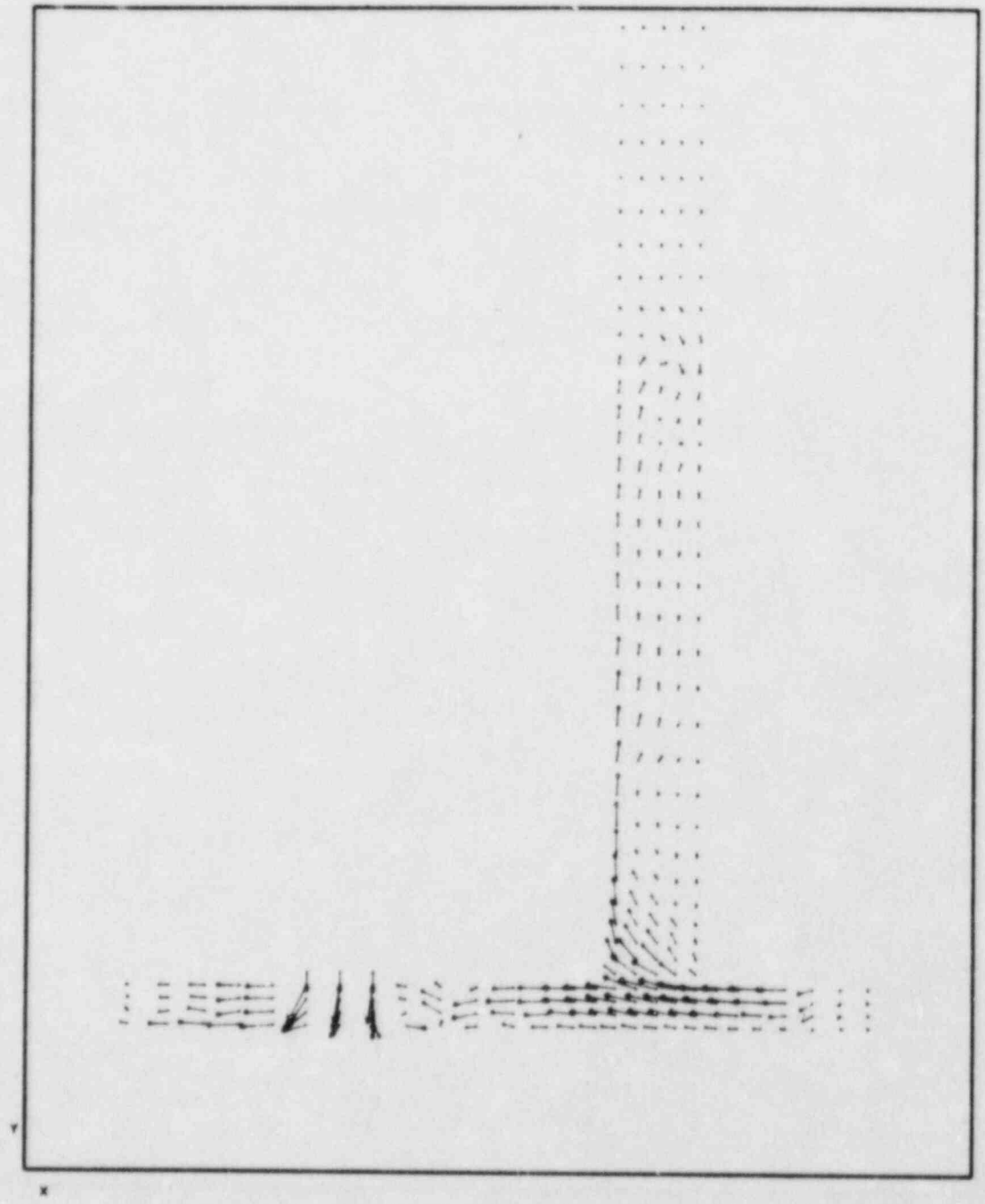

Fig. 48. Velocity vector plot in a horizontal plane through the top of the cold legs for Transient 2 at t=800s. Some of the circulating fluid is entrained into the intact loop cold leg.

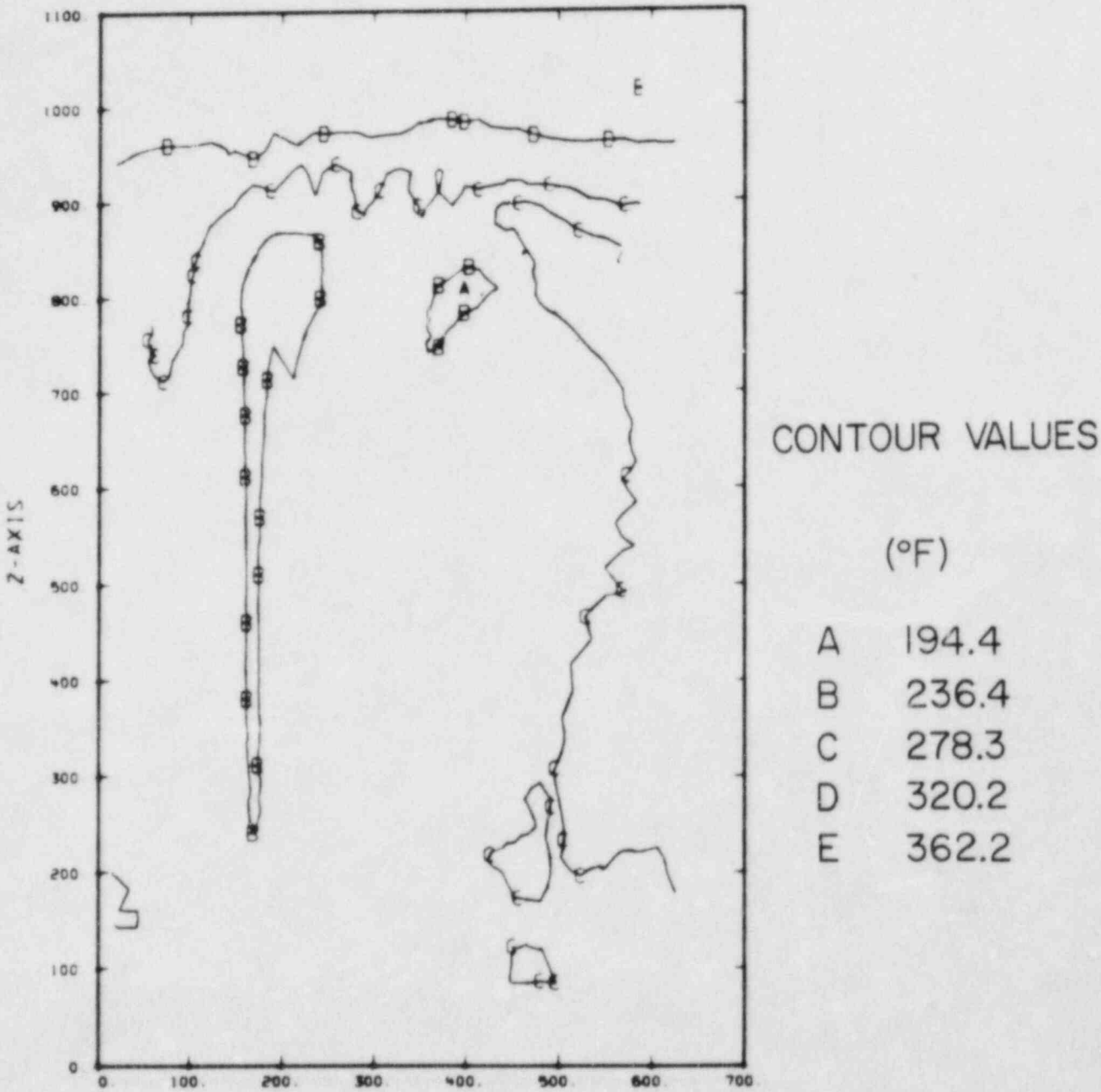

Fig. 49. Temperature contour plot in a vertical plane adjacent to the vessel wall for Transient 2 at t=800s. The coldest region below the broken loop cold leg is confined to a narrow spike.

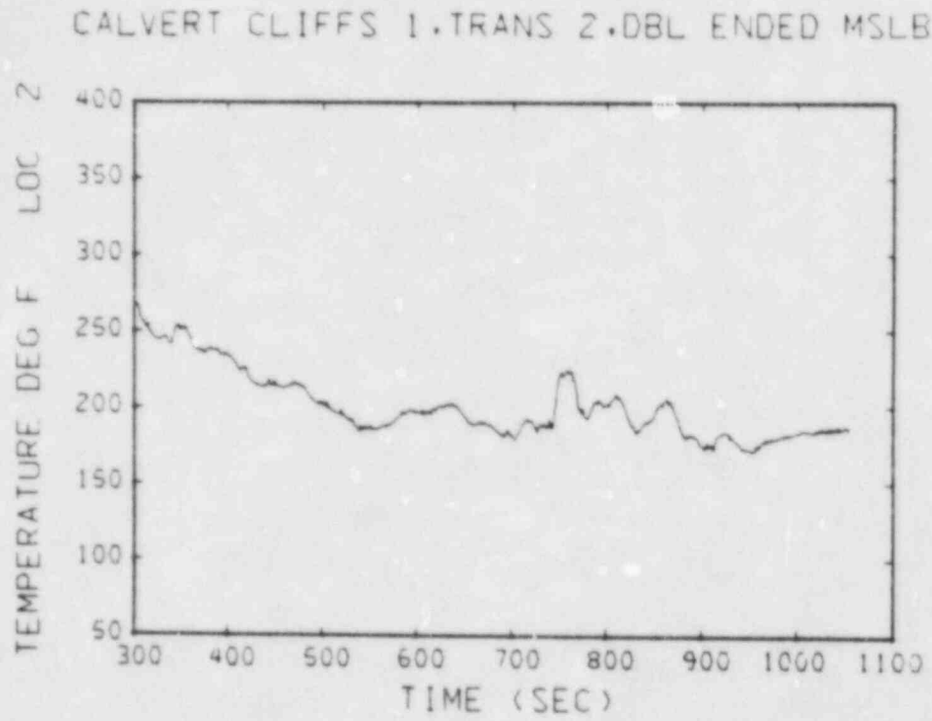

Fig. 50. Transient temperature plot at location 2, Fig. 4.

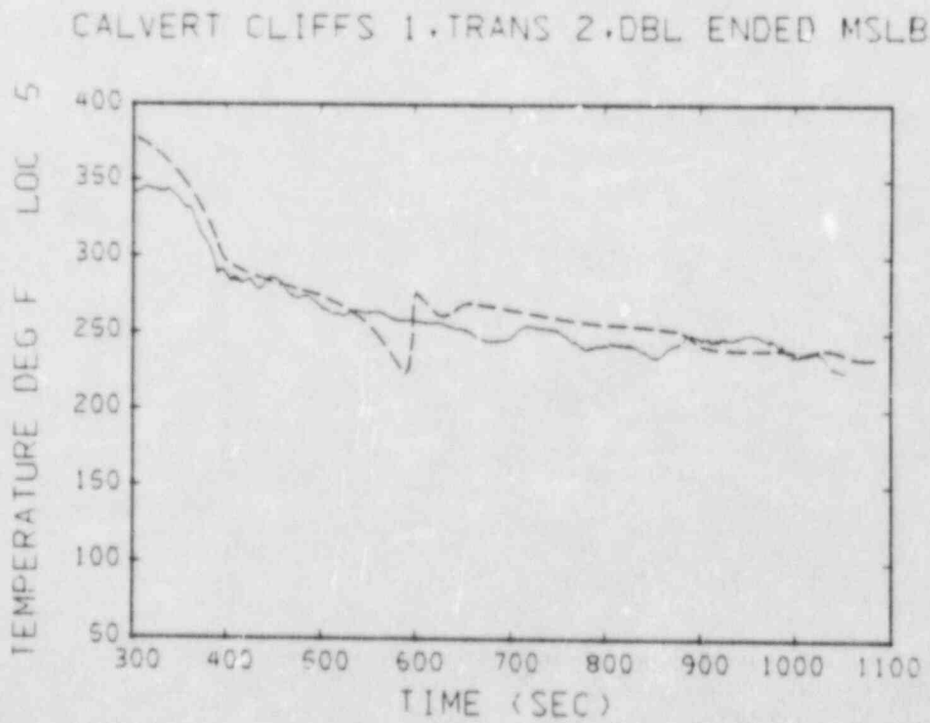

Fig. 51. Transient temperature plot at location 5, Fig. 4. The dashed line shows the TRAC downcomer temperatures (Ref. 3) at approximately the same location.

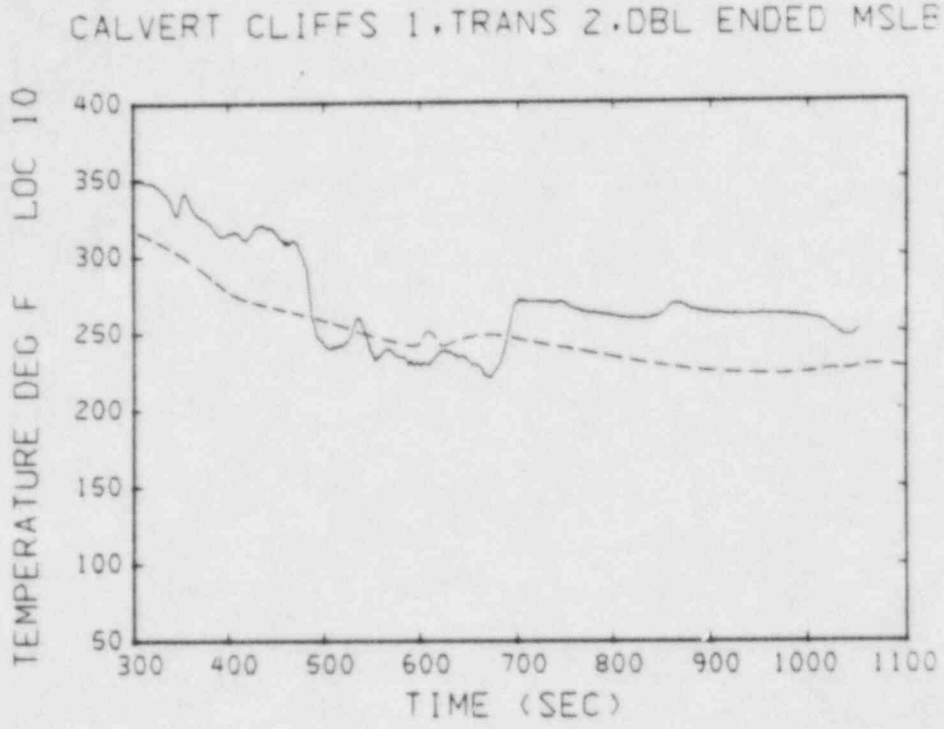

Fig. 52. Transient temperature plot at location 10, Fig. 4. The dashed line shows the TRAC downcomer temperatures (Ref. 3) at approximately the same location.

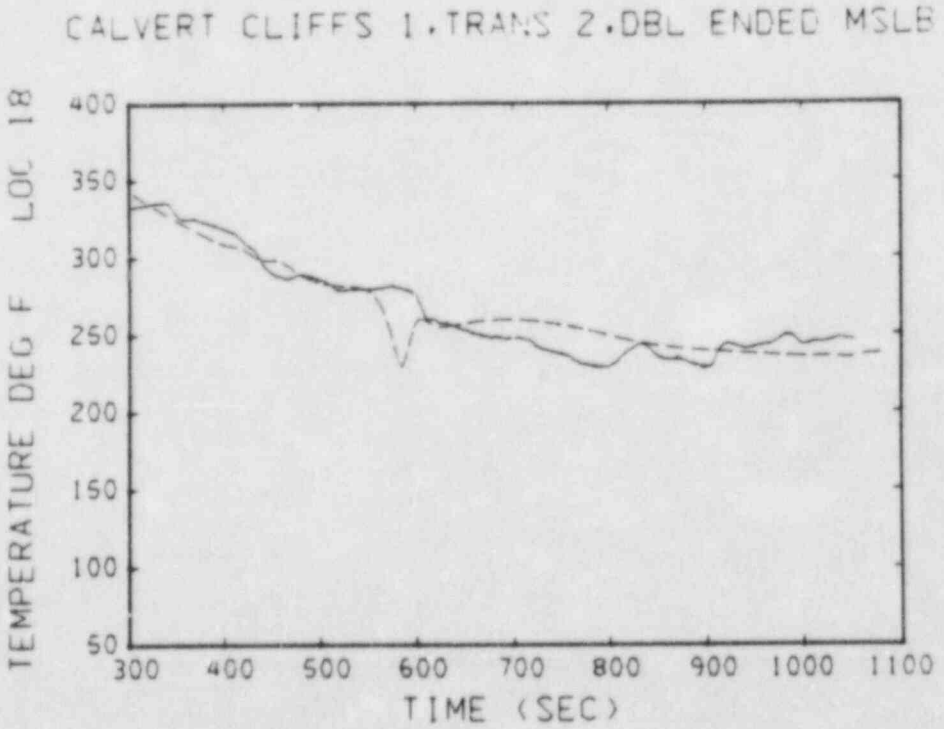

Fig. 53. Transient temperature plot at location 18, Fig. 4. The dashed line shows the TRAC downcomer temperatures (Ref. 3) at approximately the same location.

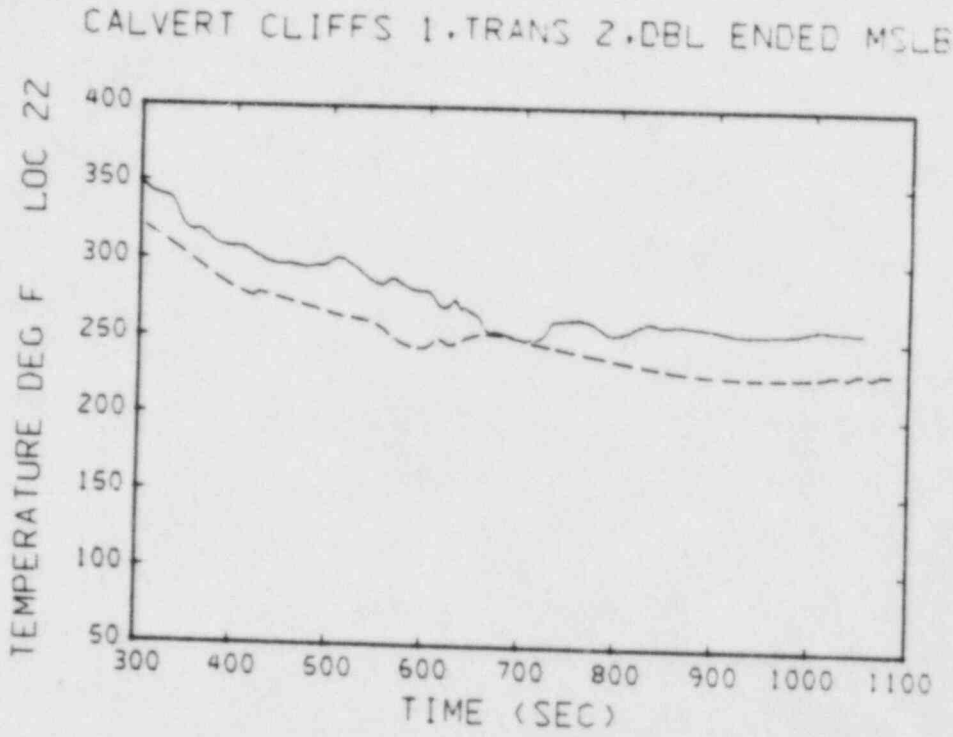

Fig. 54. Transient temperature plot at location 22, Fig. 4. The dashed line shows the TRAC downcomer temperatures (Ref. 3) at approximately the same location.

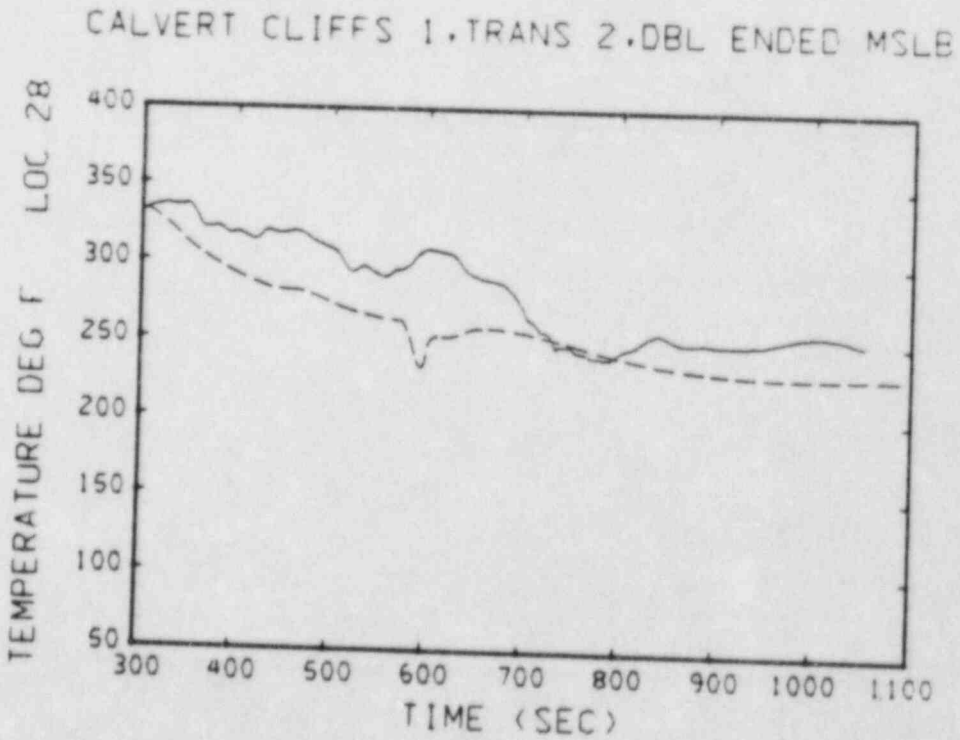

Fig. 55. Transient temperature plot at location 28, Fig. 4. The dashed line shows the TRAC downcomer temperatures (Ref. 3) at approximately the same location.

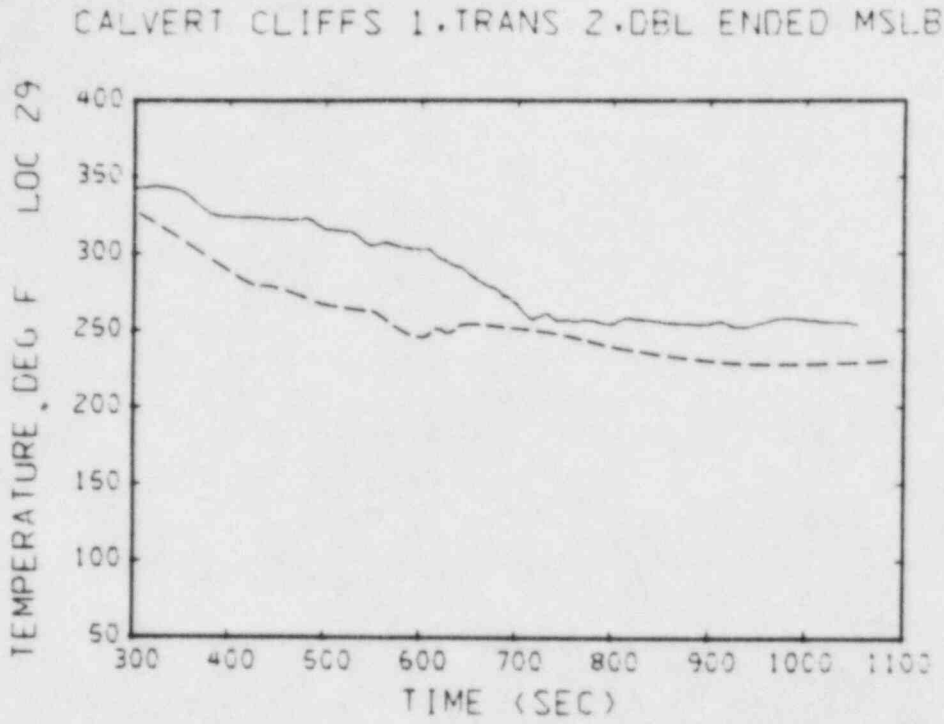

Fig. 56. Transient temperature plot at location 29, Fig. 4. The dashed line shows the TRAC downcomer temperatures (Ref. 3) at approximately the same location.

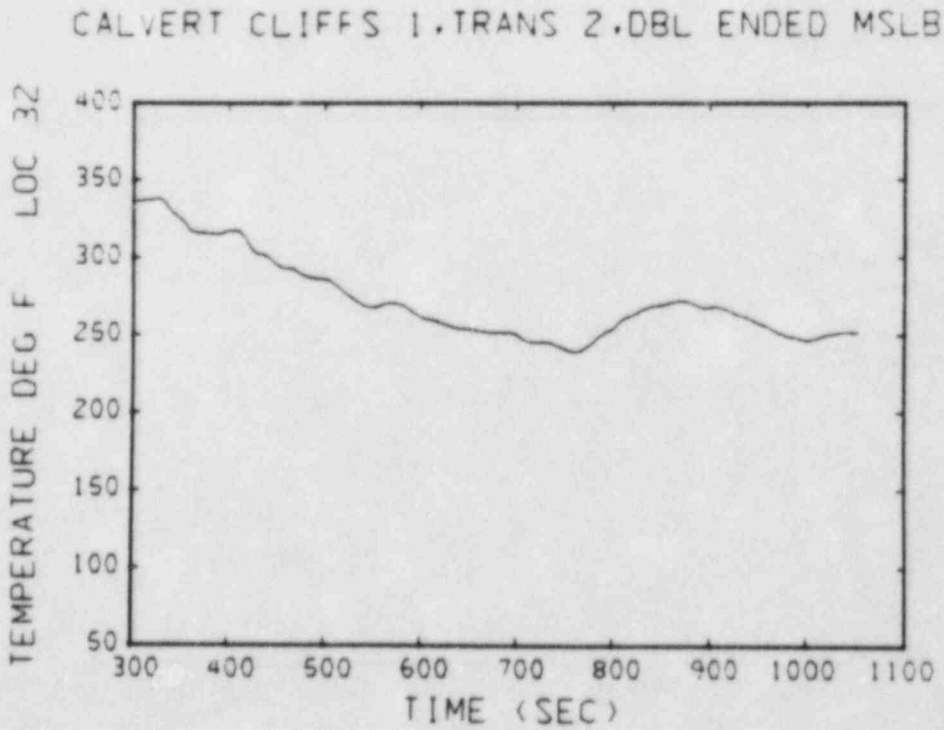

Fig. 57. Transient temperature plot at location 32, Fig. 4.

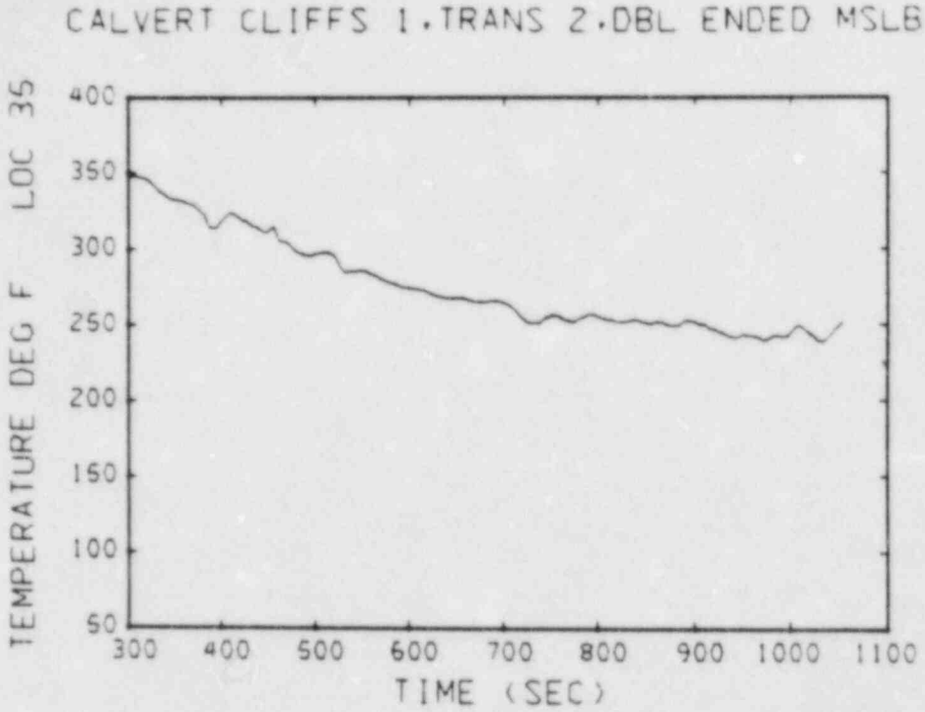

Fig. 58. Transient temperature plot at location 35, Fig. 4.

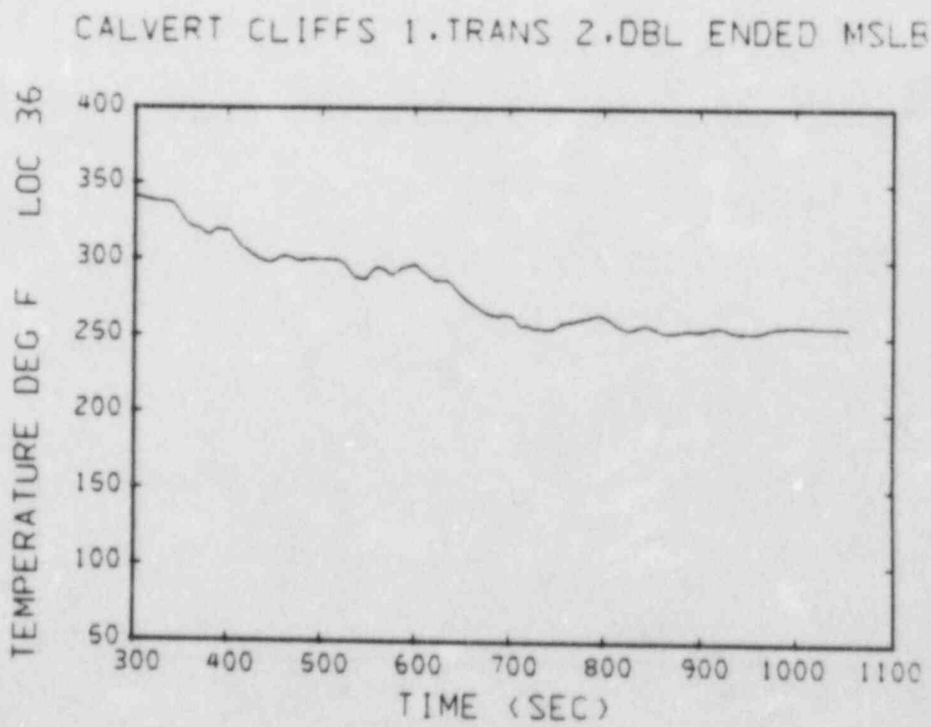

Fig. 59. Transient temperature plot at location 36, Fig. 4.

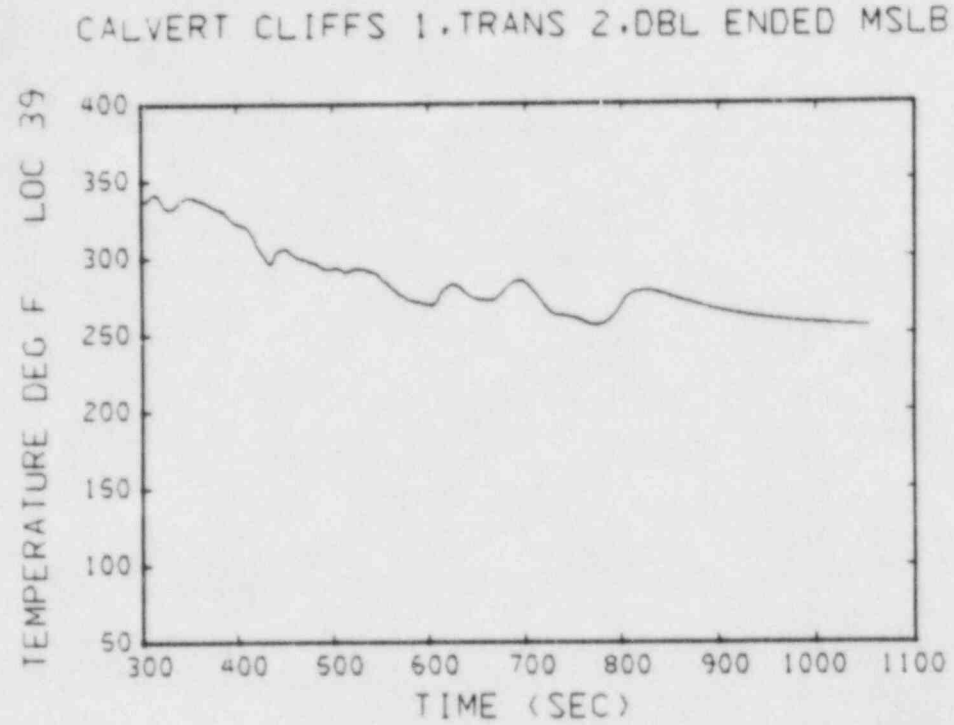

Fig. 60. Transient temperature plot at location 39, Fig. 4.

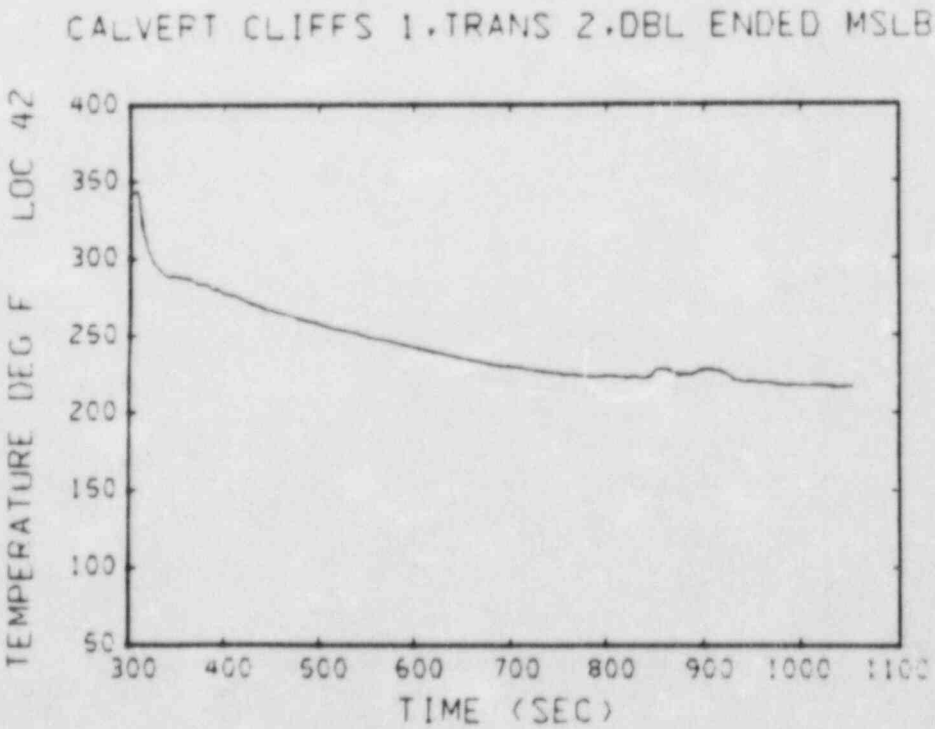

Fig. 61. Transient temperature plot at location 42, Fig. 5.

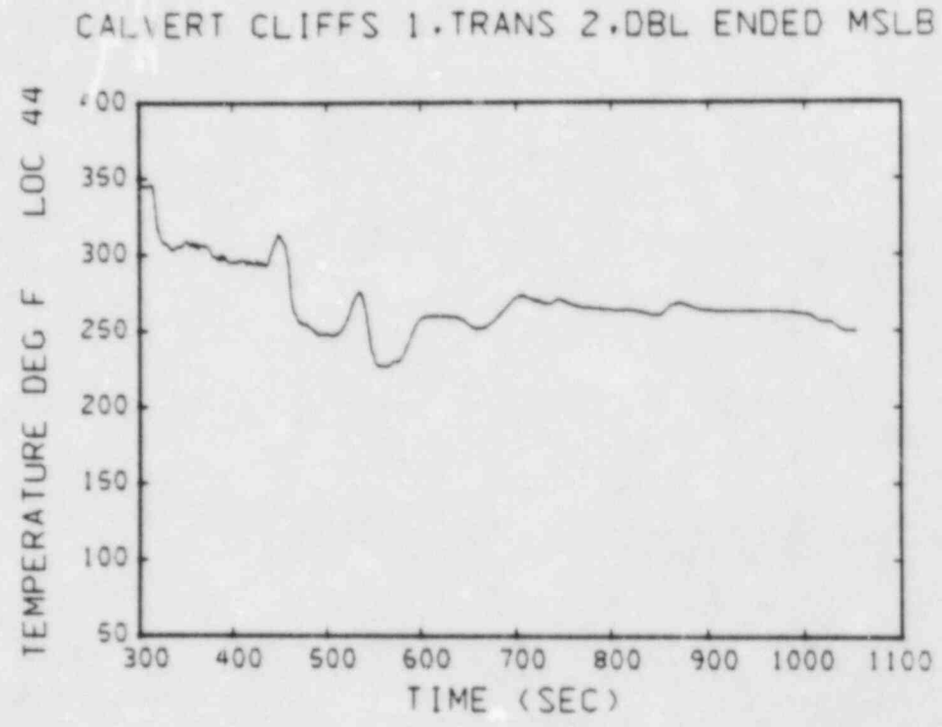

Fig. 62. Transient temperature plot at location 44, Fig. 5.

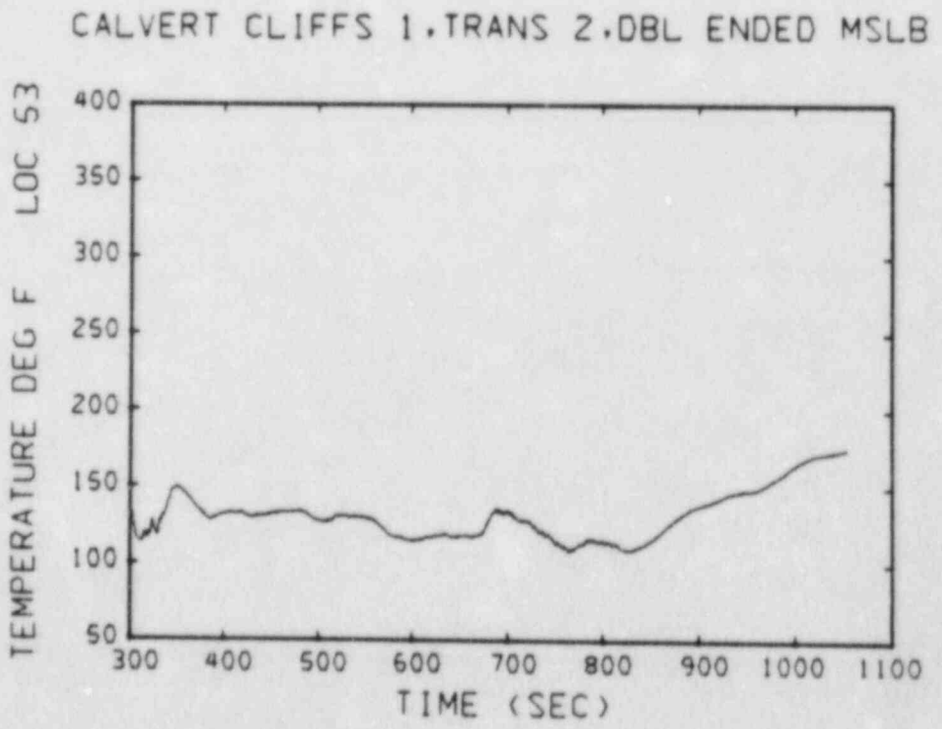

Fig. 63. Transient temperature plot at location 53, Fig. 6.

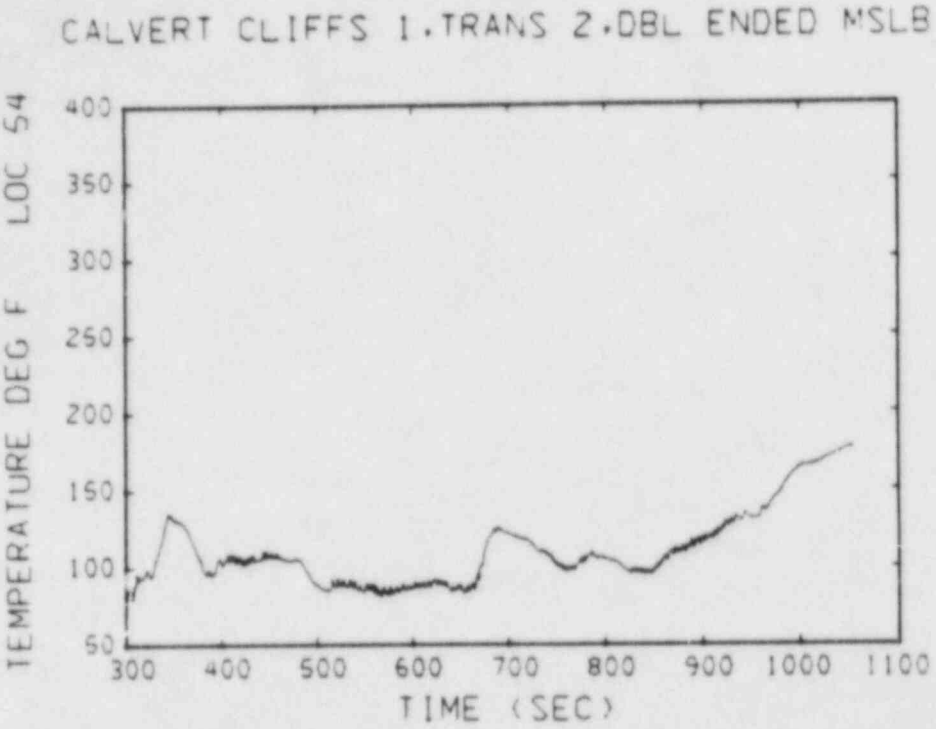

Fig. 64. Transient temperature plot at location 54, Fig. 6.

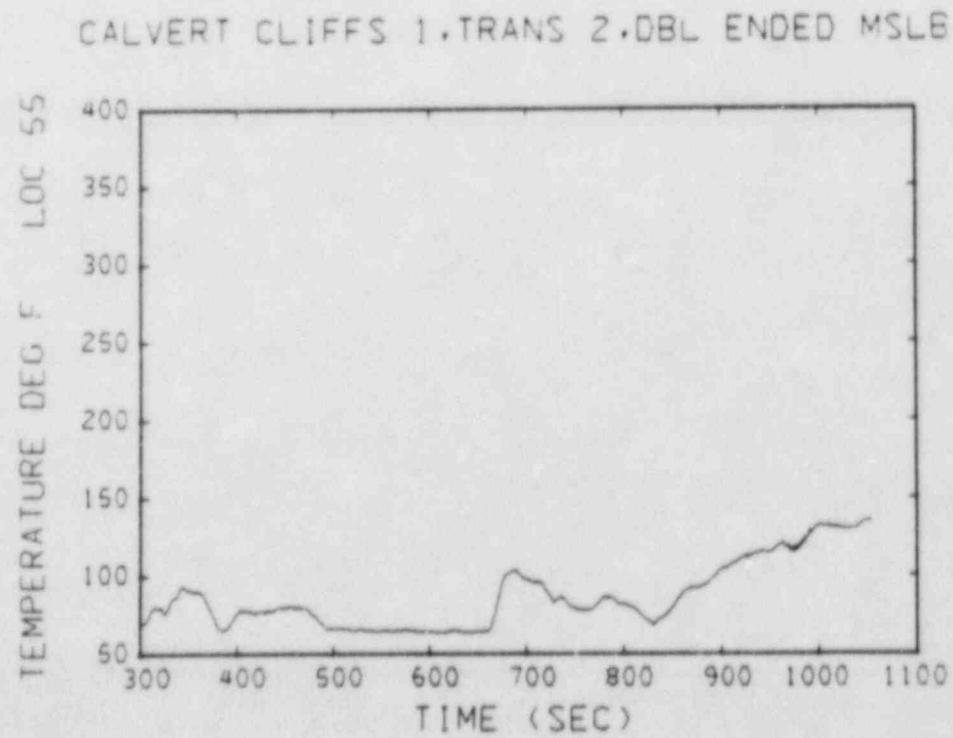

Fig. 65. Transient temperature plot at location 55, Fig. 6.

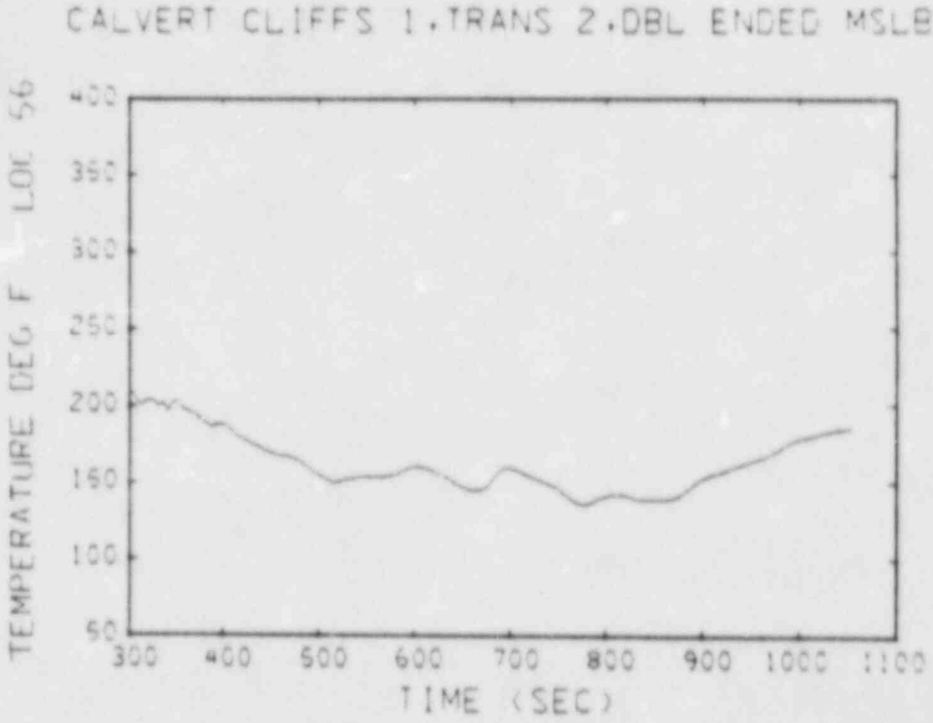

Fig. 66. Transient temperature plot at location 56, Fig. 6.

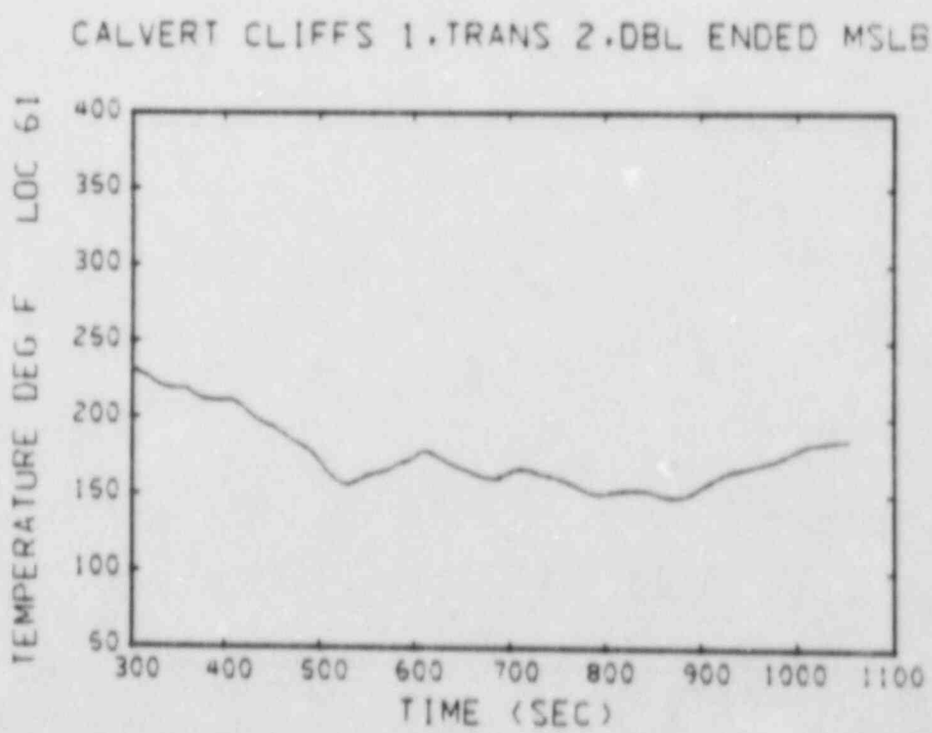

Fig. 67. Transient temperature plot at location 61, Fig. 6.

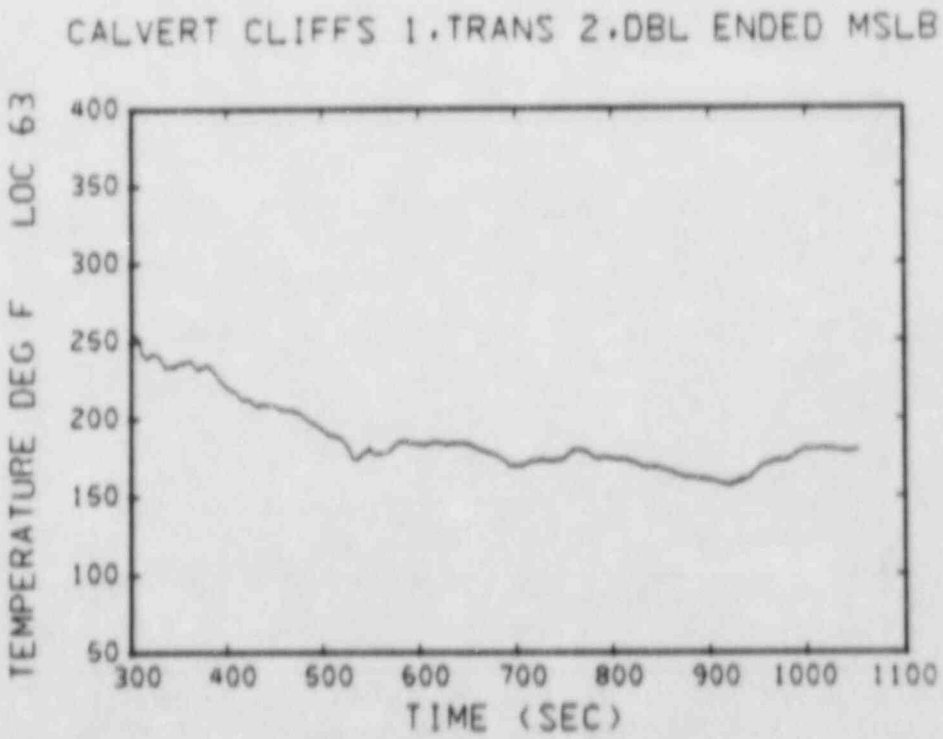

Fig. 68. Transient temperature plot at location 63, Fig. 6.

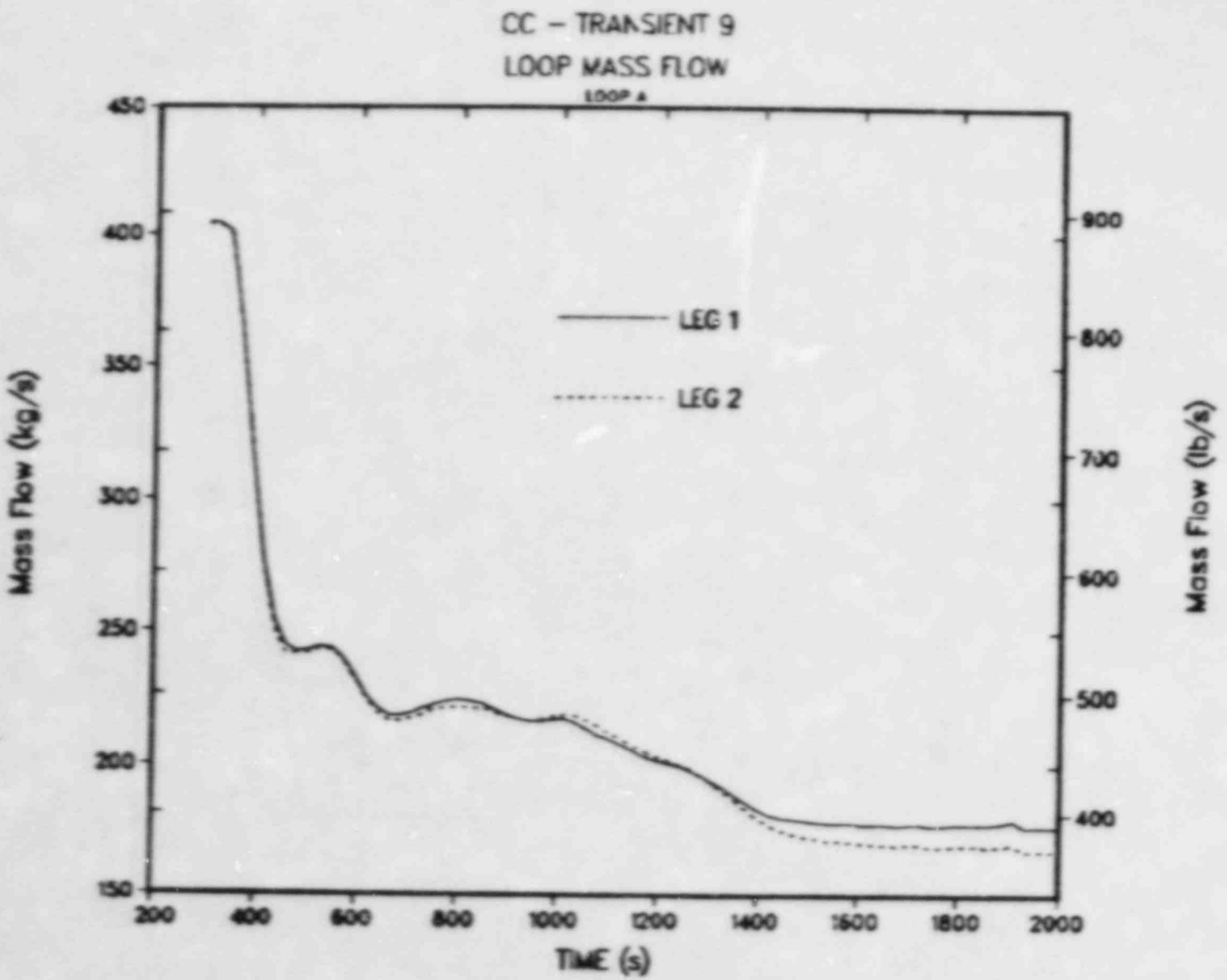

Fig. 69. Mass flow rate into the broken loop cold leg, from the TRAC calculation of Transient 9.

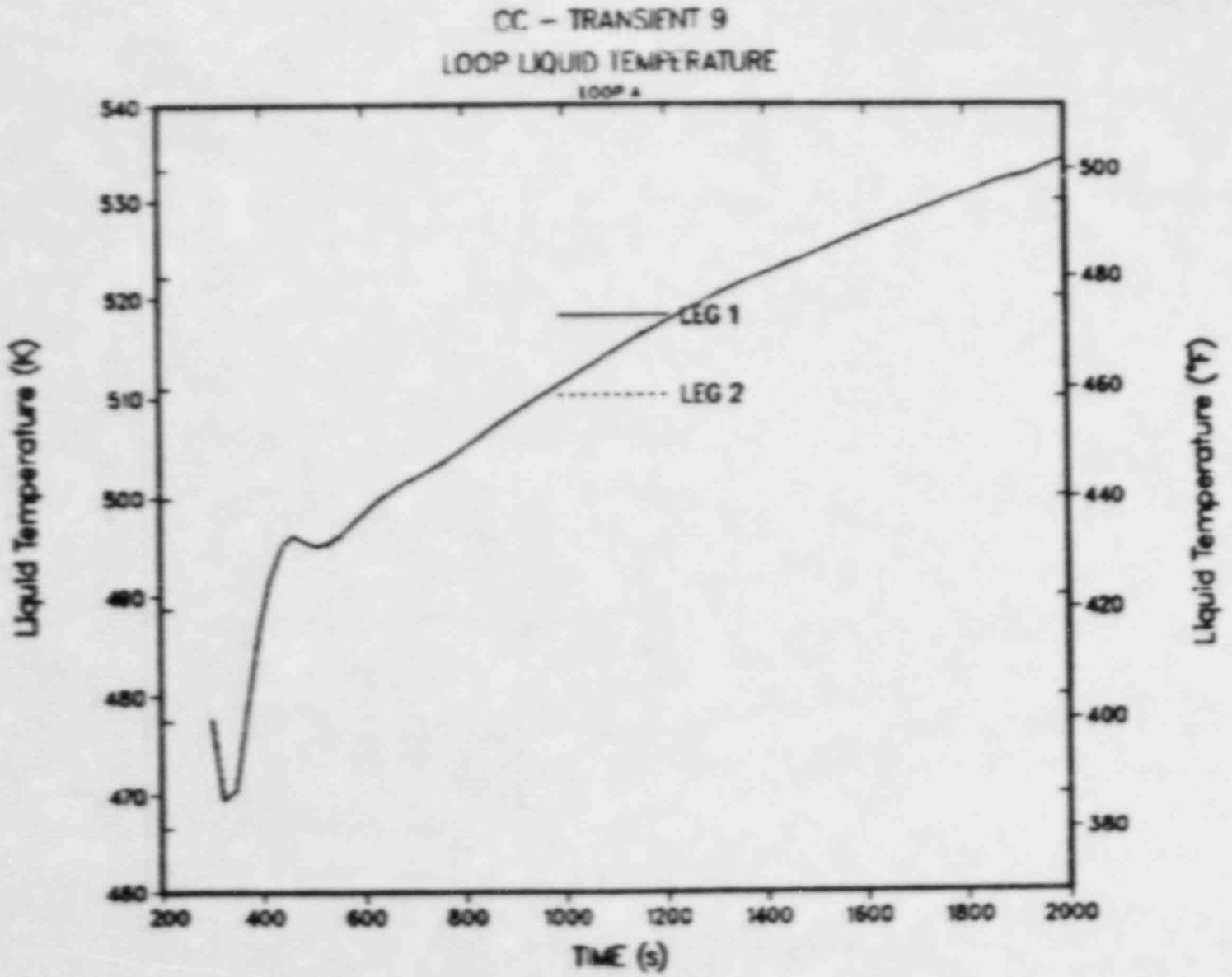

Fig. 70. Temperature of fluid flowing into the broken loop cold leg, from the TRAC calculation of Transient 9.

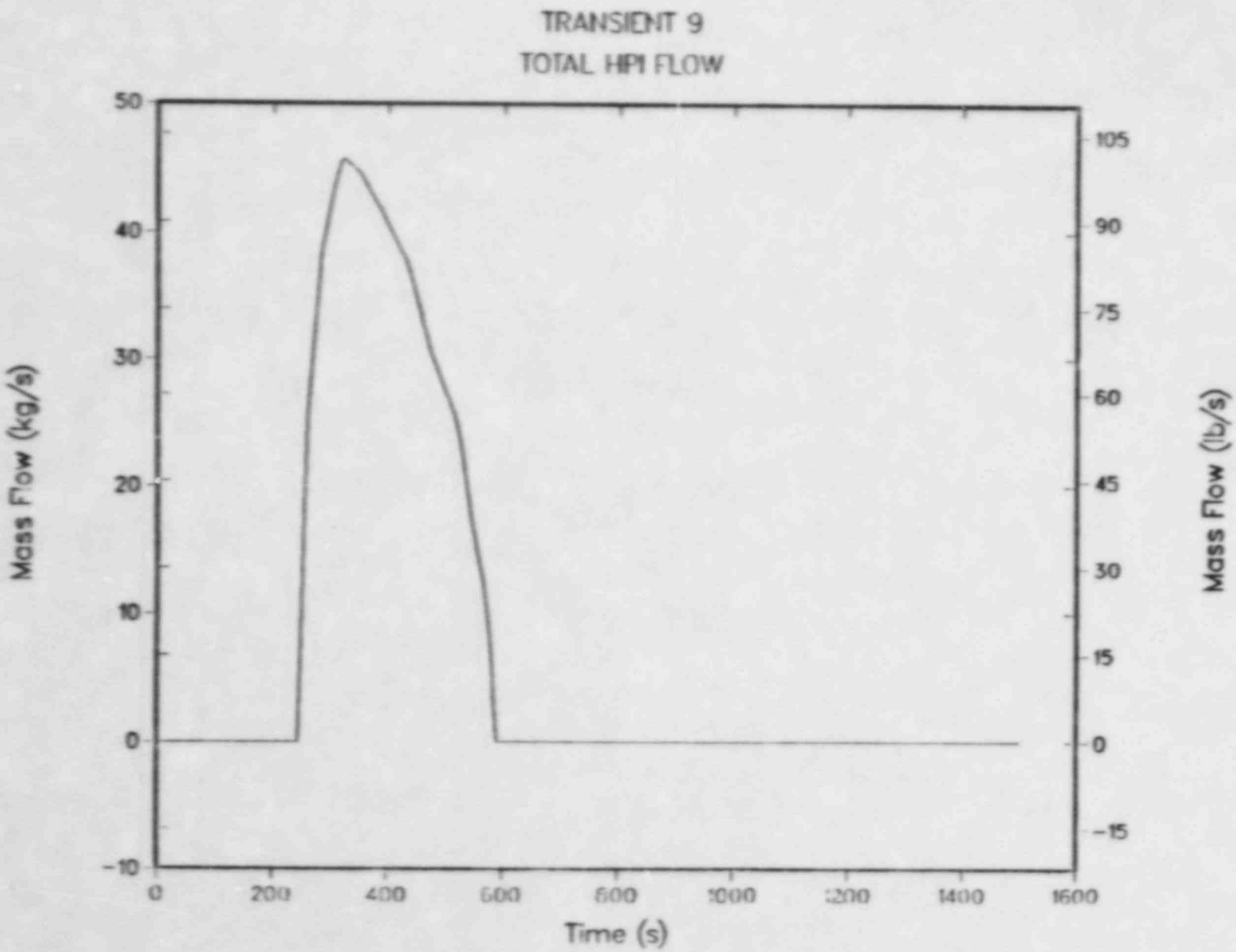

Fig. 71. Total safety injection flow rate, from the TRAC calculation of Transient 9.

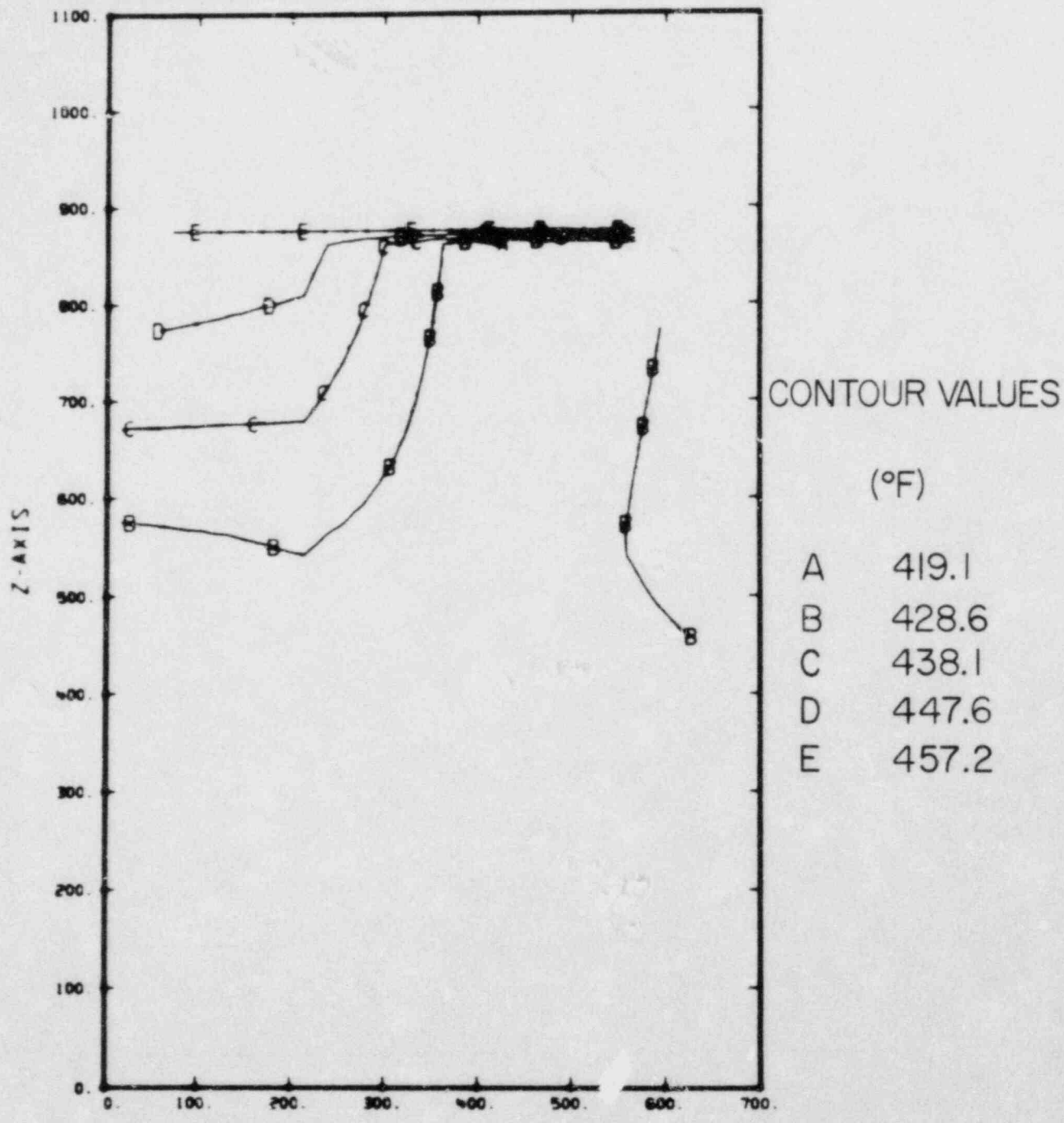

Fig. 72. Downcomer temperature distribution at t=400s, from the TRAC calculation of Transient 9.

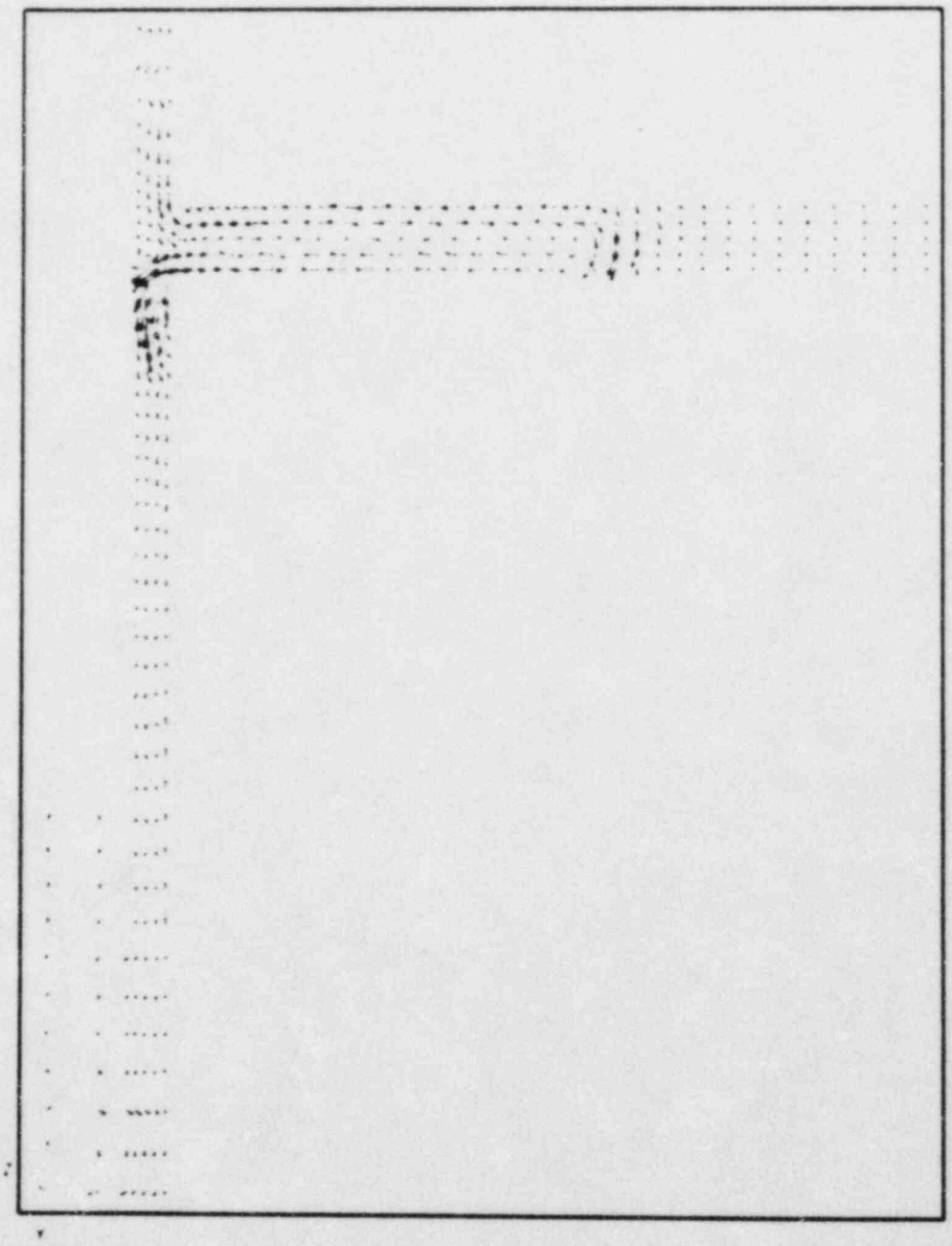

Fig. 73. Velocity vector plot in a vertical plane through the centerline of the intact loop cold leg for Transient 9 at t=600s. Warm water is entrained into the cold leg from above and mixes with the injected fluid so that the temperature of the exiting flow is higher than in the previous transients.

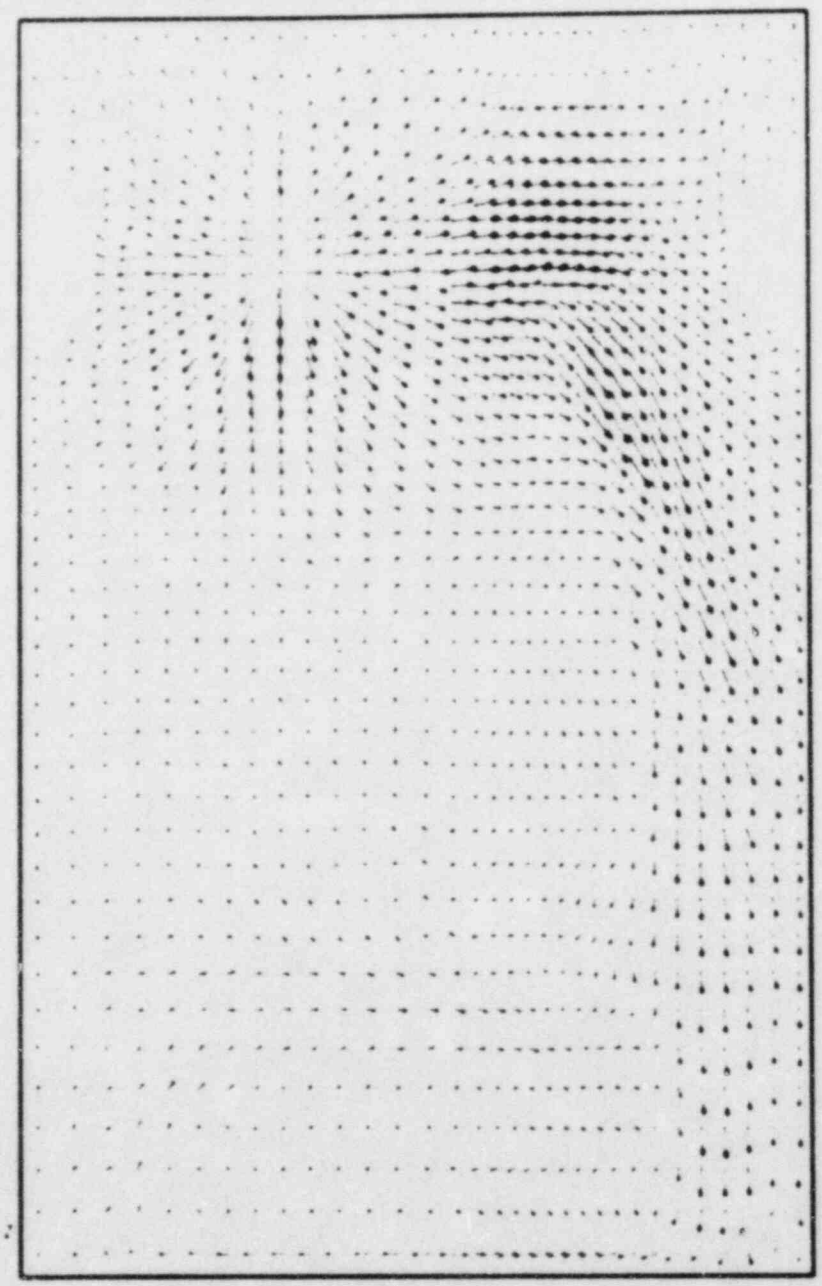

Fig. 74. Velocity vector plot in a vertical plane adjacent to the core barrel wall for Transient 9 at t=600s. Unlike the previous transients the downflow is on the right.

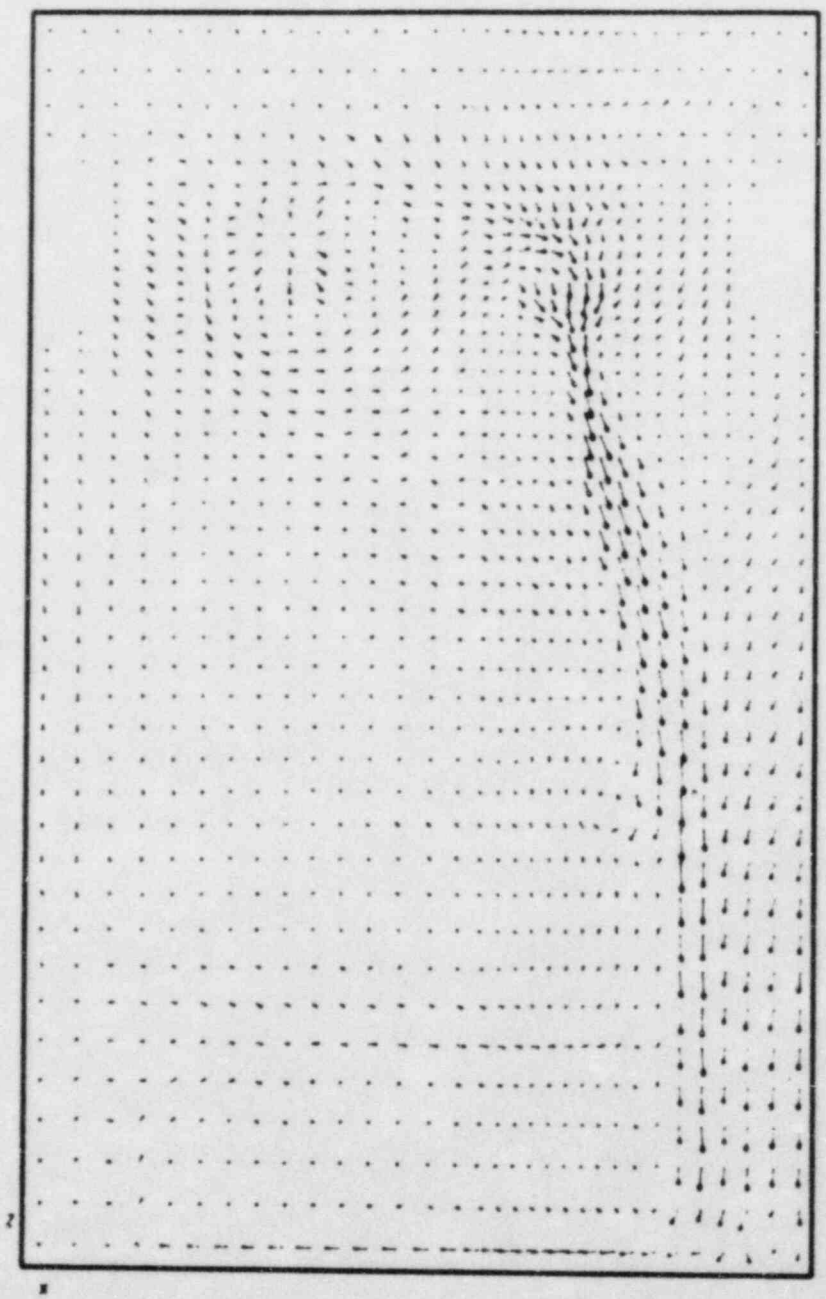

Fig. 75. Velocity vector plot in a vertical plot adjacent to the vessel wall for Transient 9 at t=600s. The flow from the intact loop cold leg penetrates to the bottom of the downcomer.

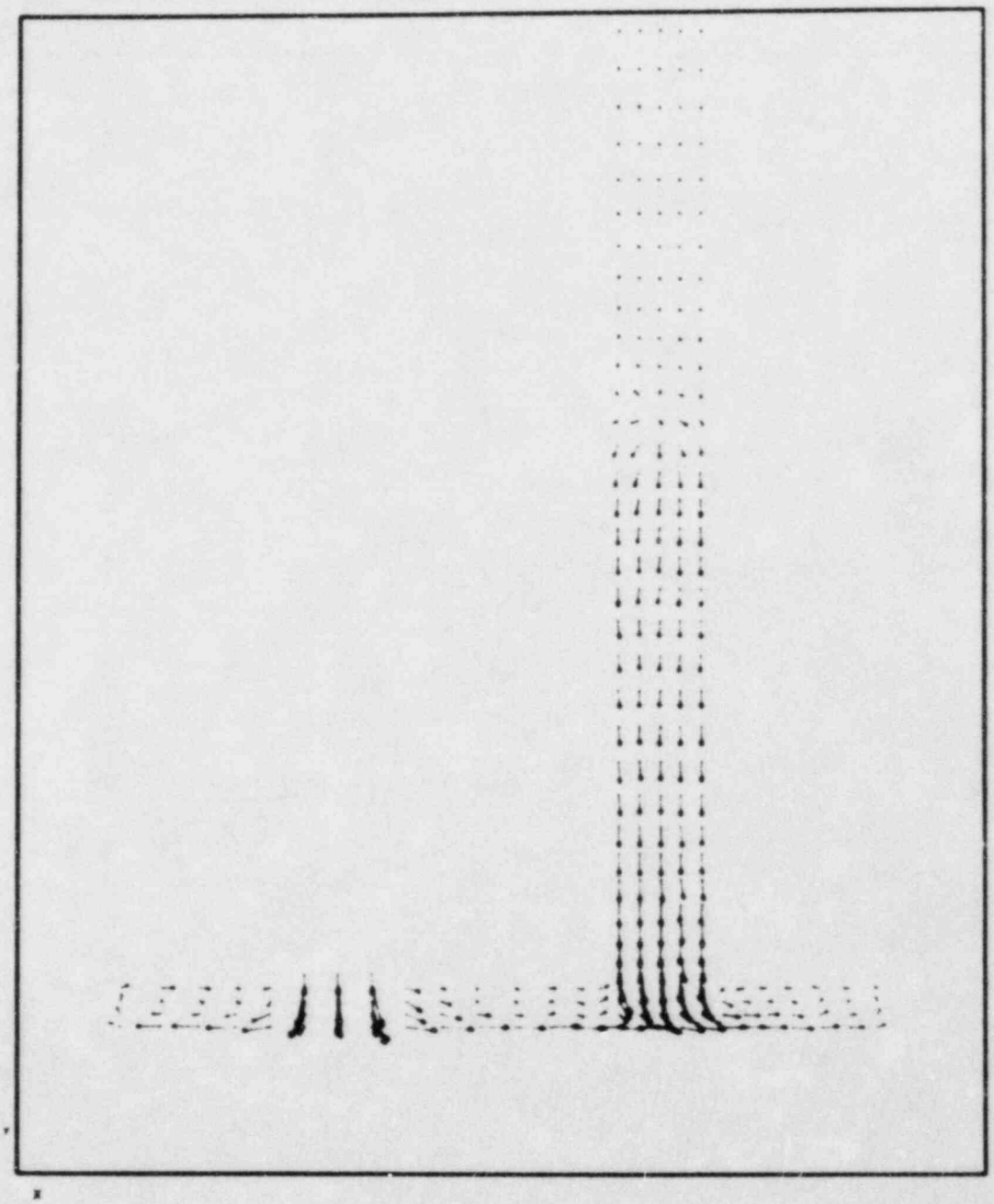

Fig. 76. Velocity vector plot in a horizontal plane through the bottom of the cold legs for Transient 9 at t=600s. The flow from the broken loop spreads along the core barrel wall and confines the flow from the intact loop to the vessel side where a recirculating flow has formed.

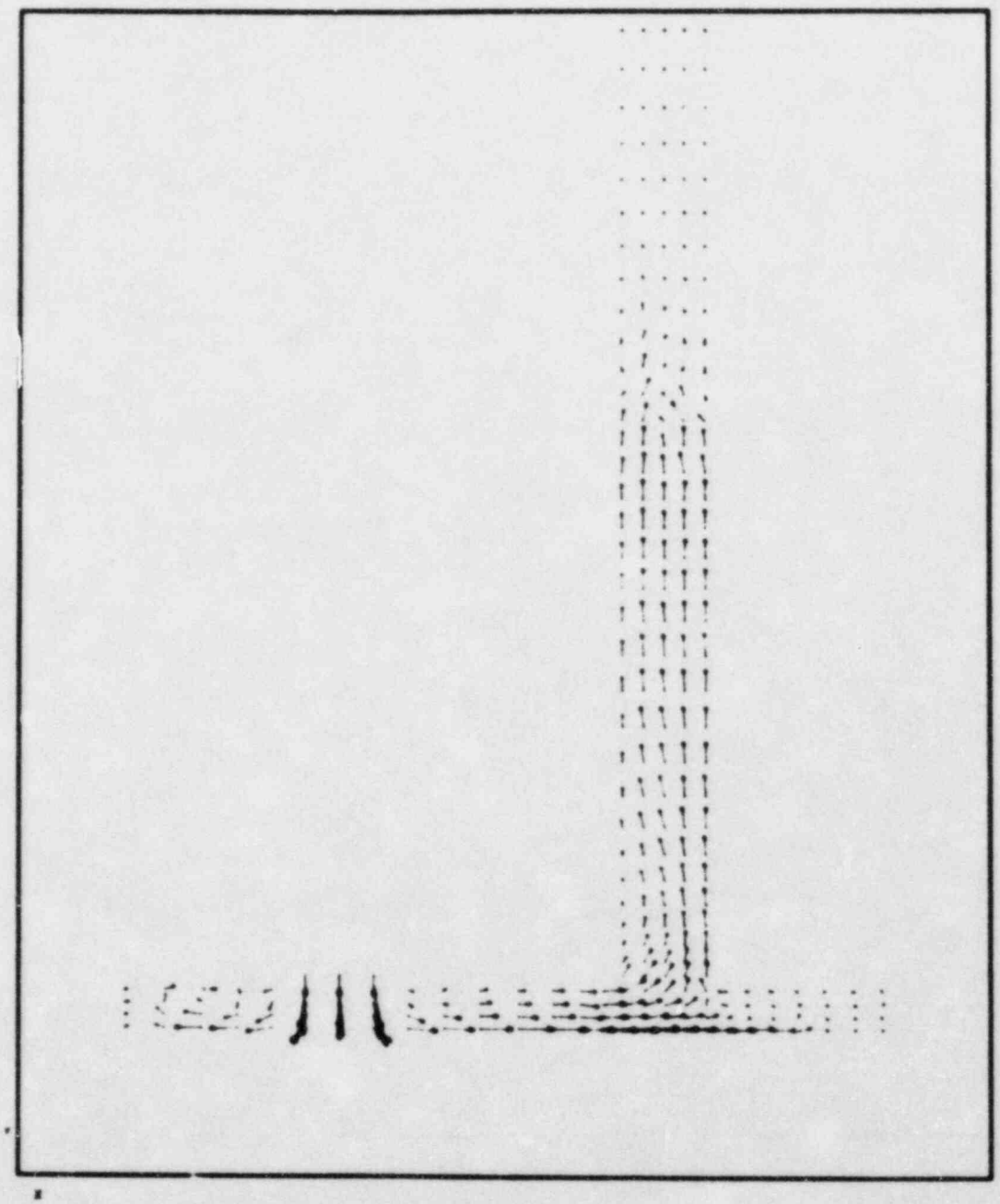

Fig. 77. Velocity vector plot in a horizontal plane through the tops of the cold legs for Transient 9 at t=600s. A large volume of fluid from the broken loop is entrained into the intact loop cold leg.

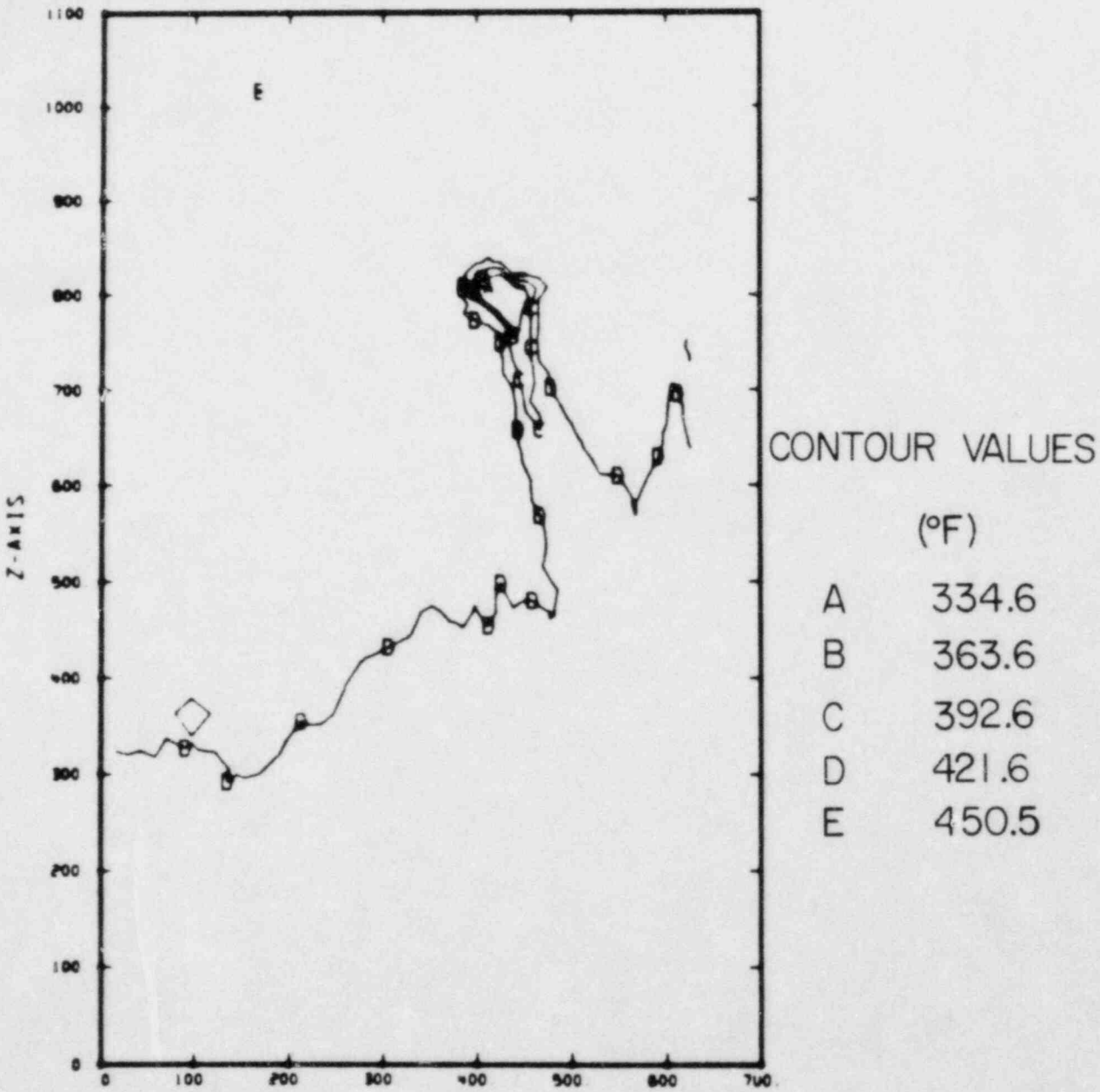

Fig. 78. Temperature plot in a vertical plane adjacent to the vessel wall for Transient 9 at t=600s. The temperature variation is slight except in a small channel downstream from the intact loop cold leg exit.

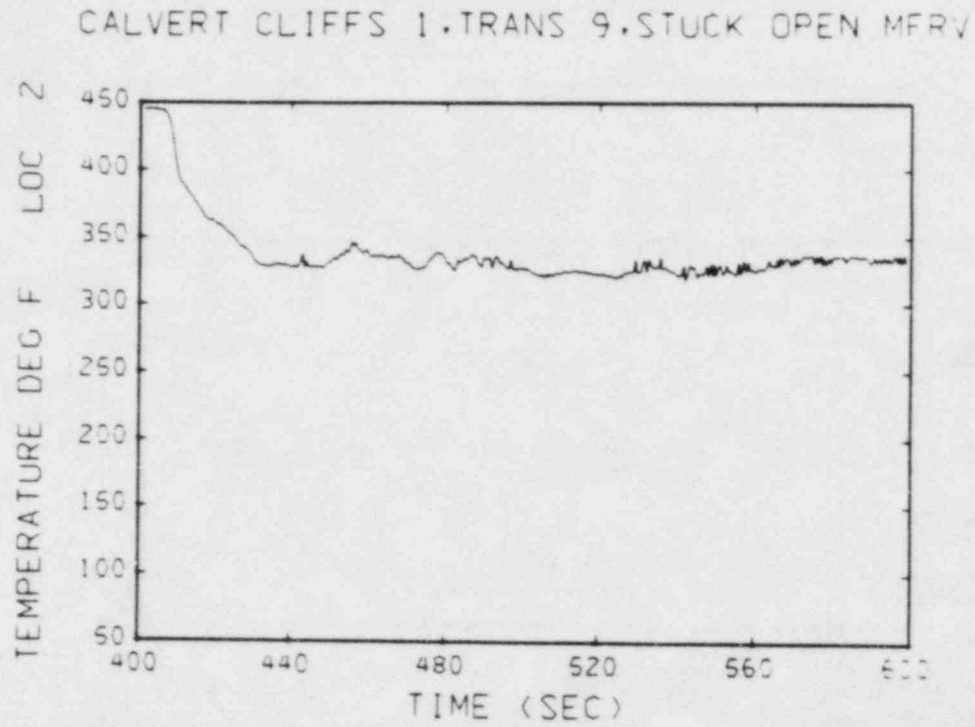

Fig. 79. Transient temperature plot at location 2, Fig. 4.

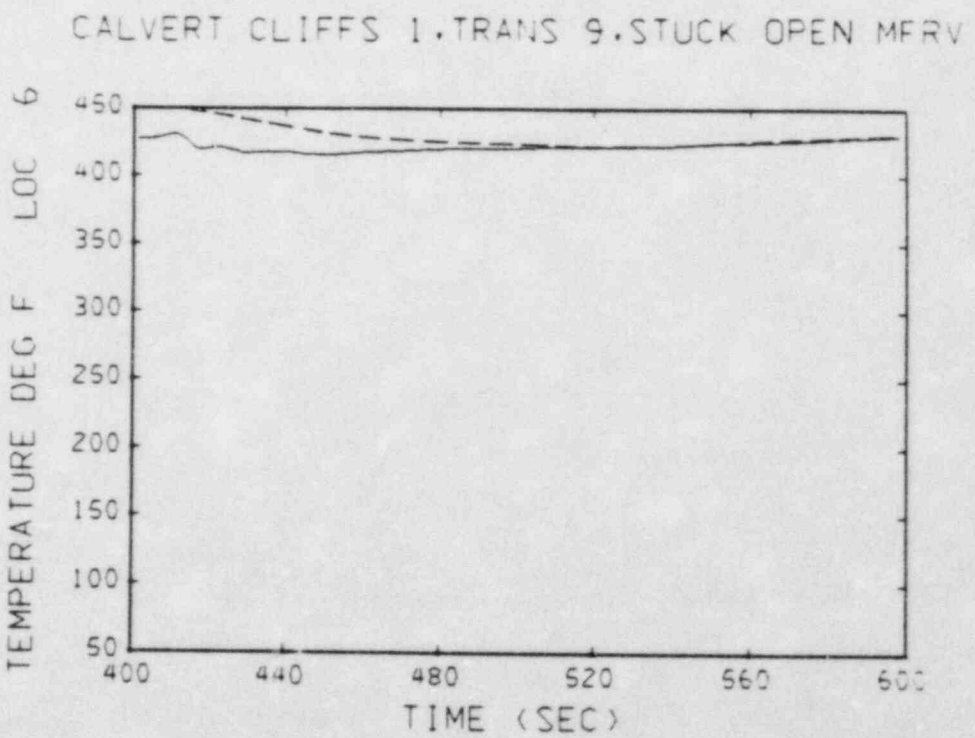

Fig. 80. Transient temperature plot at location 6, Fig. 4. The dashed line shows the TRAC downcomer temperatures (Ref. 3) at approximately the same location.

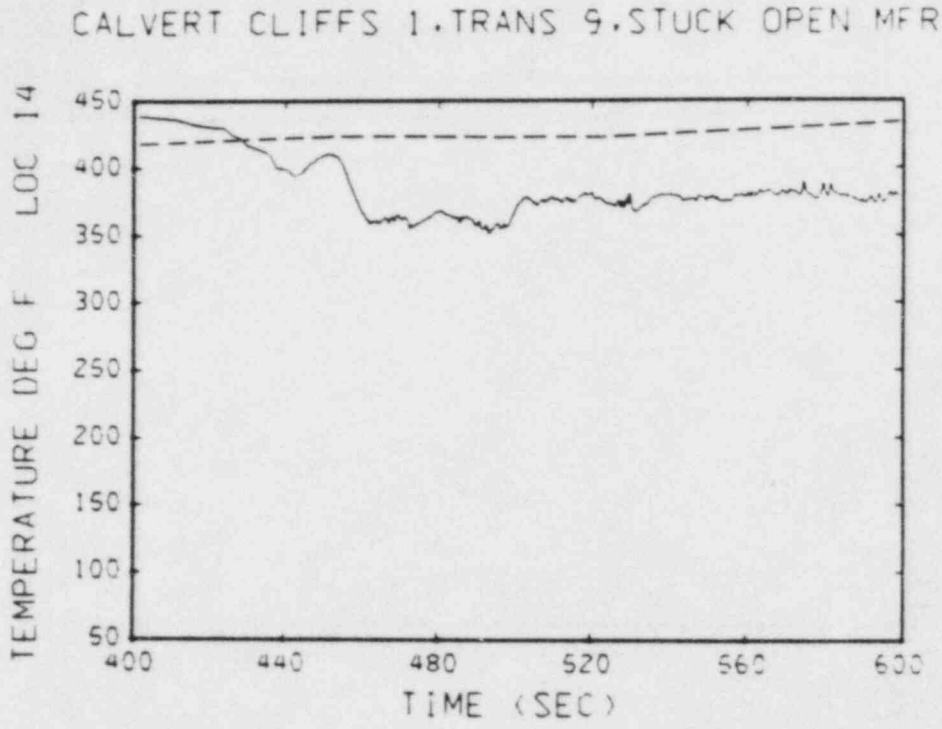

Fig. 81. Transient temperature plot at location 14, Fig. 4. The dashed line shows the TRAC downcomer temperatures (Ref. 3) at approximately the same location.

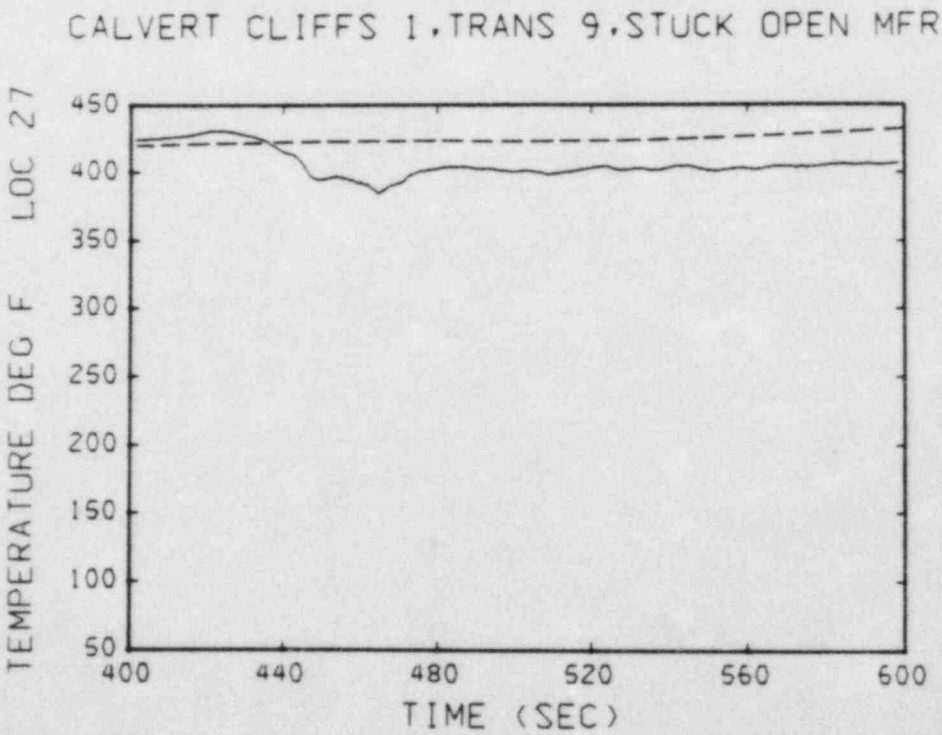

Fig. 82. Transient temperature plot at location 27, Fig. 4. The dashed line shows the TRAC downcomer temperatures (Ref. 3) at approximately the same location.

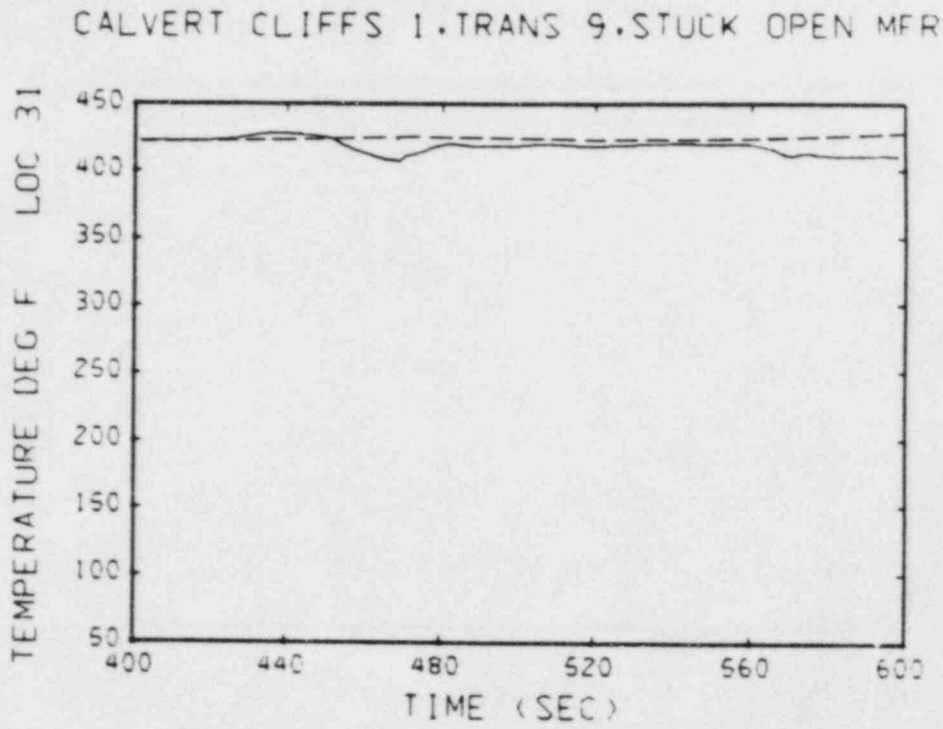

Fig. 83. Transient temperature plot at location 31, Fig. 4. The dashed line shows the TRAC downcomer temperatures (Ref. 3) at approximately the same location.

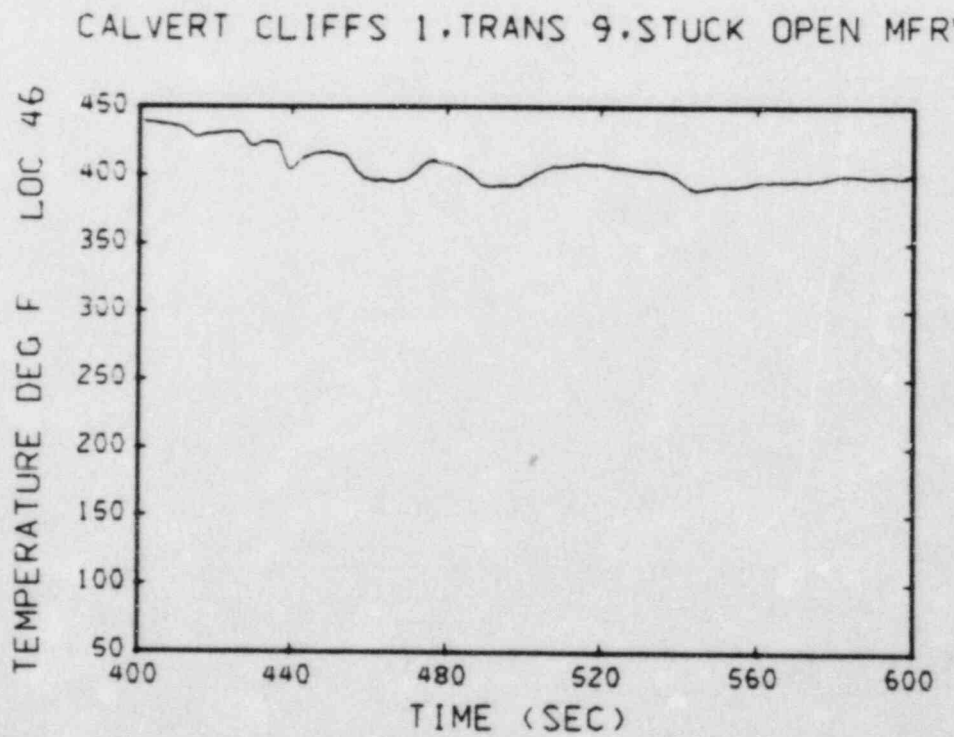

Fig. 84. Transient temperature plot at location 46, Fig. 5.

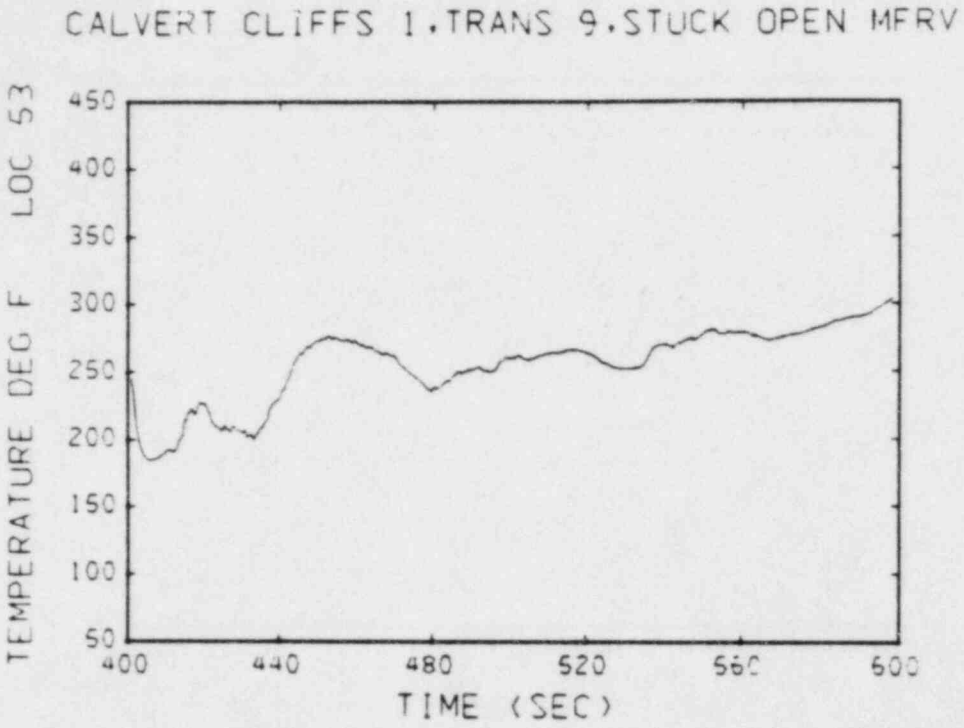

Fig. 85. Transient temperature plot at location 53, Fig. 6.

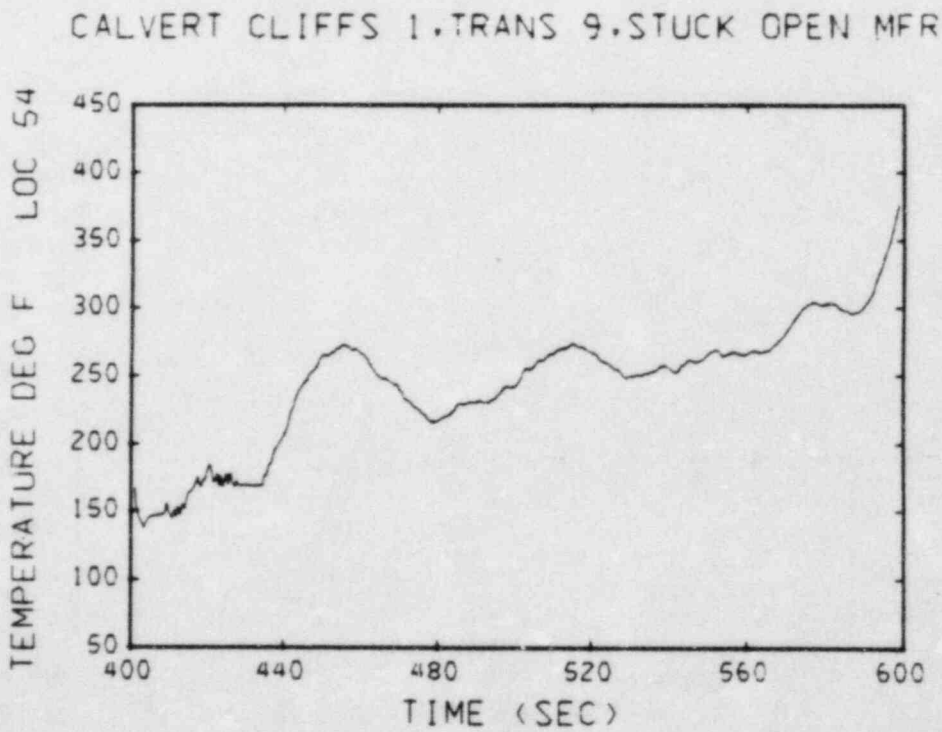

Fig. 86. Transient temperature plot at location 54, Fig. 6.

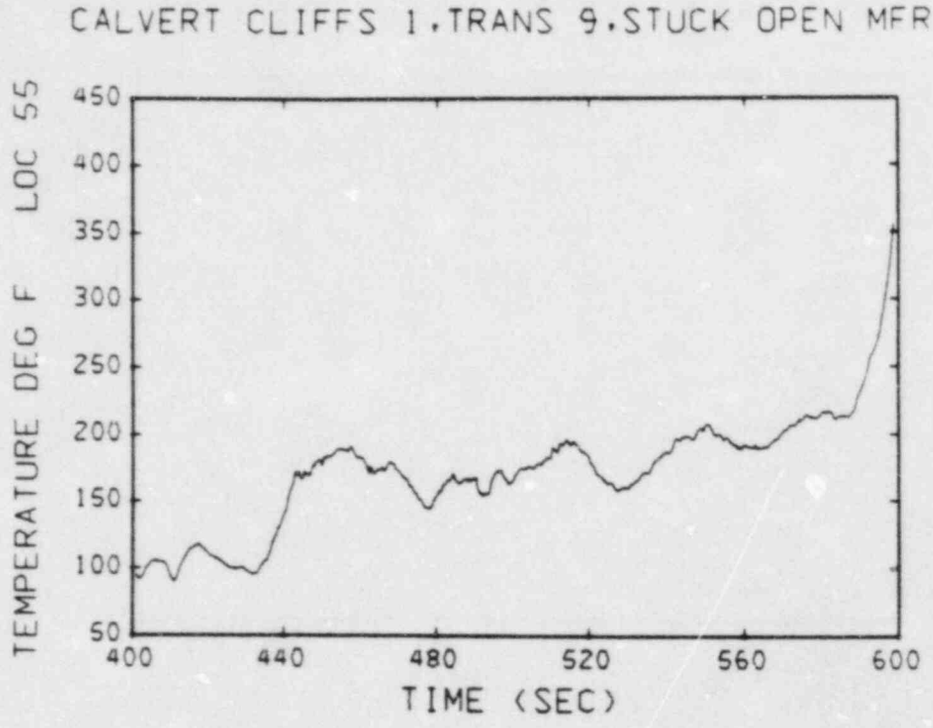

Fig. 87. Transient temperature plot at location 55, Fig. 6.

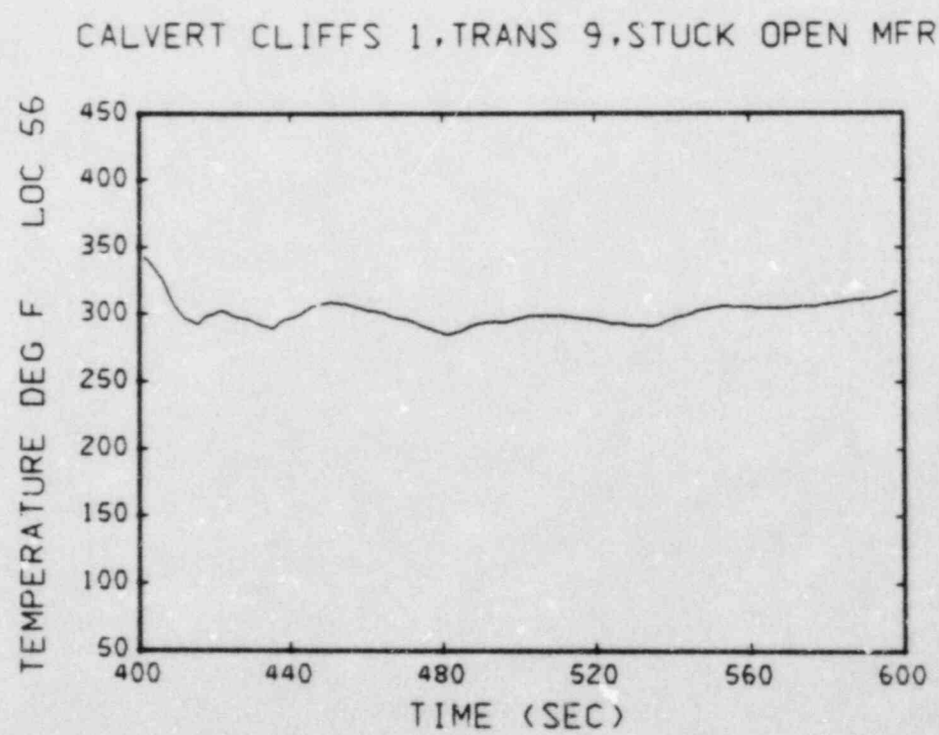

Fig. 88. Transient temperature plot at location 56, Fig. 6.

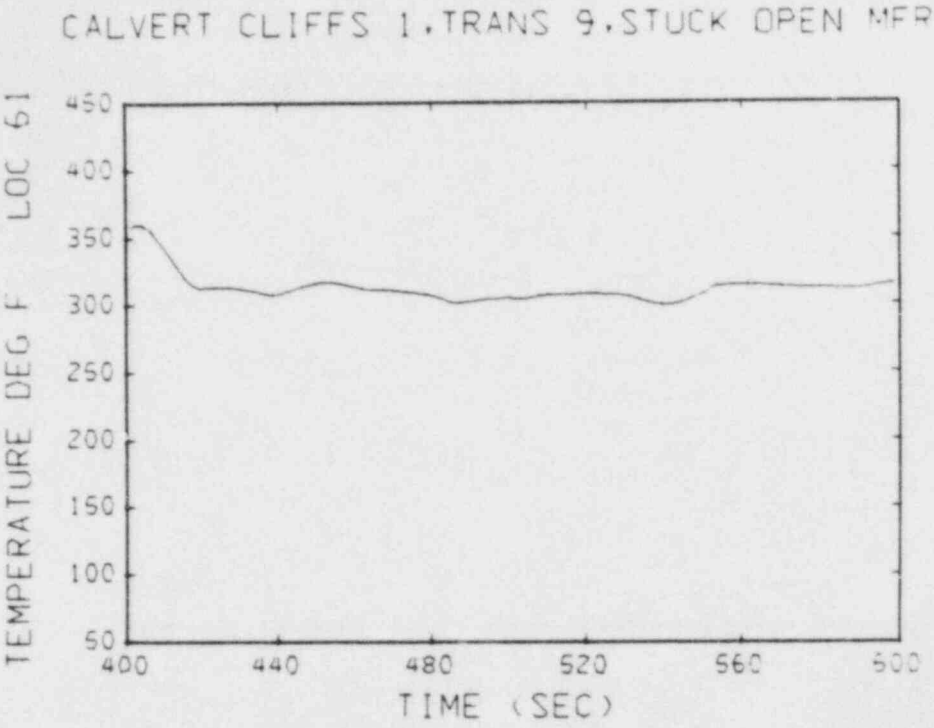

Fig. 89. Transient temperature plot at location 61, Fig. 6.

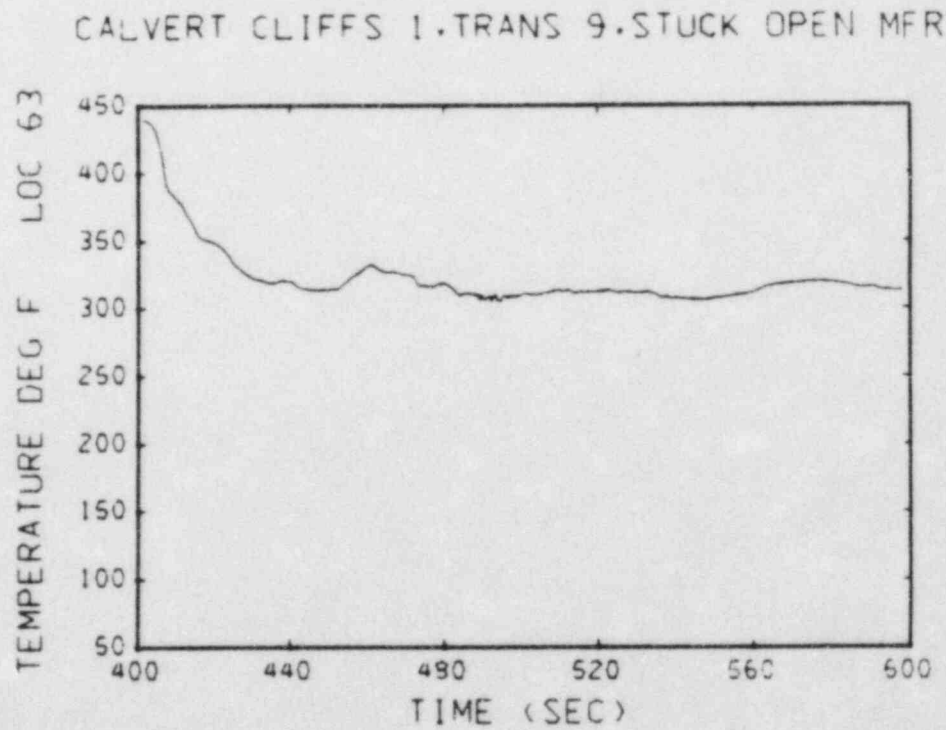

Fig. 90. Transient temperature plot at location 63, Fig. 6.

DISTRIBUTION

	Copies
Nuclear Regulatory Commission, R4 and Supplemental Distribution, Bethesda, Maryland	396
Technical Information Center, Oak Ridge, Tennessee	2
Los Alamos National Laboratory, Los Alamos, New Mexico	50
Total	448

NRC FORM 335 (6-83) U.S. NUCLEAR REGULATORY COMMISSION

BIBLIOGRAPHIC DATA SHEET

1 REPORT NUMBER (Assigned by TIDC, add Vol. No., if any)
NUREG/CR-3704
LA-10039-MS

2 Leave blank

3 TITLE AND SUBTITLE
Three-Dimensional Calculations of Transient Fluid-Thermal Mixing in the Downcomer of the Calvert Cliffs-1 Plant Using SOLA-PTS

4 RECIPIENT'S ACCESSION NUMBER

5 DATE REPORT COMPLETED
MONTH: February YEAR: 1984

6 AUTHOR(S)
Bart J. Daly

7 DATE REPORT ISSUED
MONTH: April YEAR: 1984

8 PERFORMING ORGANIZATION NAME AND MAILING ADDRESS (Include Zip Code)
Los Alamos National Laboratory
Los Alamos, New Mexico 87545

9 PROJECT/TASK/WORK UNIT NUMBER

10 FIN NUMBER
A7306

11 SPONSORING ORGANIZATION NAME AND MAILING ADDRESS (Include Zip Code)
Division of Accident Evaluation
Office of Nuclear Regulatory Research
United States Nuclear Regulatory Commission
Washington, DC 20555

12a TYPE OF REPORT
Informal

12b PERIOD COVERED (Inclusive dates)

13 SUPPLEMENTARY NOTES

14 ABSTRACT (200 words or less)

The SOLA-PTS code has been used to analyze transient fluid-thermal mixing in a 180° sector of the downcomer and a cold leg of the Calvert Cliffs-1 plant for three assumed accident scenarios. The inlet boundary conditions for these calculations were obtained from mass flow rates and temperatures that were computed in systems code studies. The results of the three-dimensional SOLA-PTS calculations indicated that a pressurized thermal shock risk was mitigated for these accident scenarios as the result of the particular circulation patterns that developed in the downcomer.

15a KEY WORDS AND DOCUMENT ANALYSIS

15b DESCRIPTORS

16 AVAILABILITY STATEMENT
Unlimited

17 SECURITY CLASSIFICATION (This report)
Unclassified

18 NUMBER OF PAGES

19 SECURITY CLASSIFICATION (This page)
Unclassified

20 PRICE
$

☆ U.S. GOVERNMENT PRINTING OFFICE: 1984—776-026 / 4059

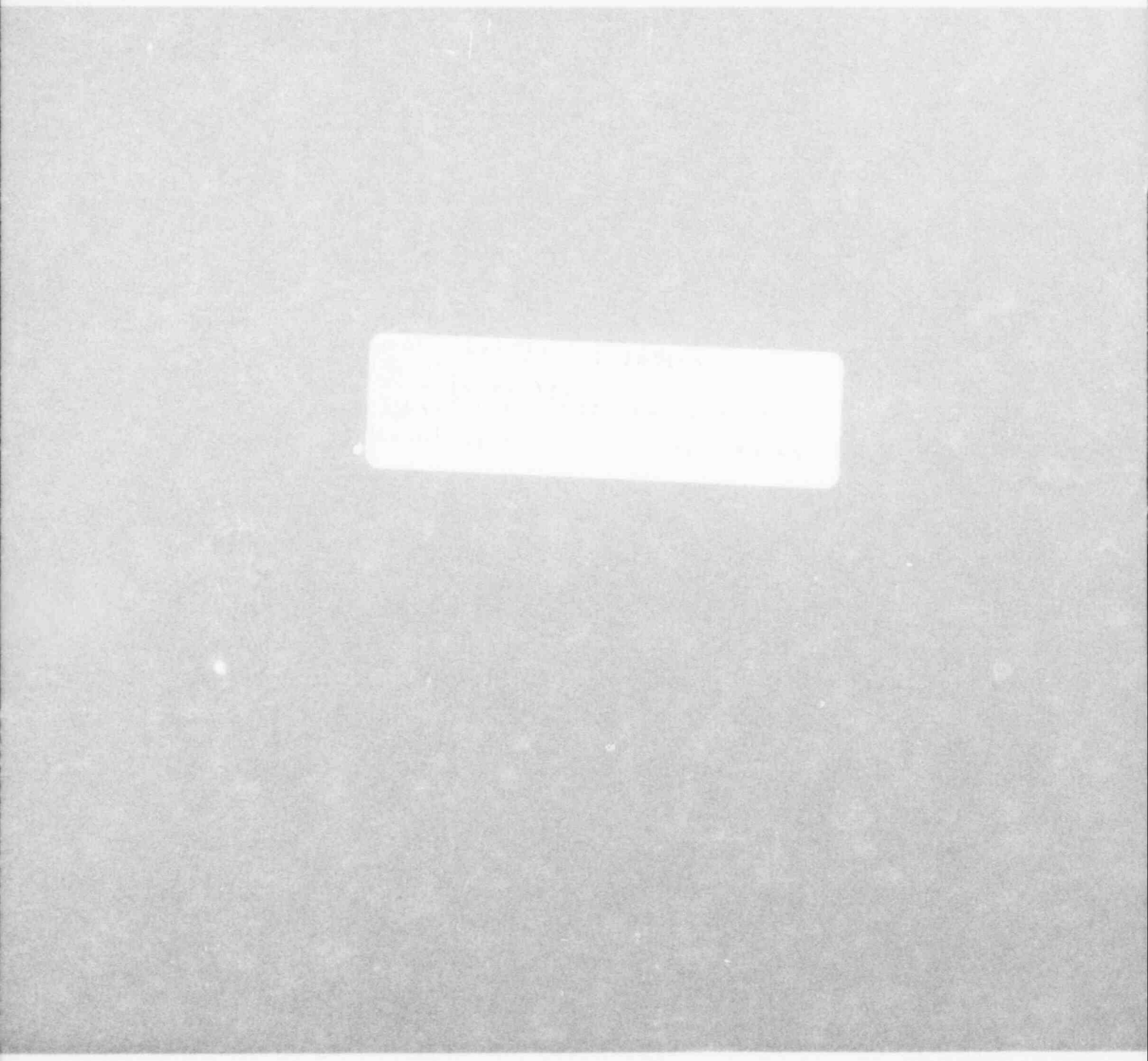

Los Alamos